

Proceedings of Anticancer Research

Editor-in-Chief

MP Balasubramanian

University of Madras

BIO-BYWORD SCIENTIFIC PUBLISHING PTY LTD

(619 649 400)

Level 10

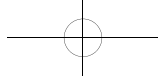
50 Clarence Street

SYDNEY NSW 2000

Copyright © 2022. Bio-Byword Scientific Publishing Pty Ltd.

Complimentary Copy





ISSN (ONLINE): 2208-3553

ISSN (PRINT): 2208-3545

BIQ-BYWORD
SCIENTIFIC PUBLISHING PTY LTD

Proceedings of Anticancer Research

Focus and Scope

Proceedings of Anticancer Research is an international peer-reviewed and open access journal, which is devoted to the rapid publication of high quality original articles, reviews, case reports, short communication and letters on all aspects of experimental and clinical oncology.

- Cellular research and bio-markers
- Identification of bio-targets and agents with novel mechanisms of action
- Preventative and integrated treatment for cancer patients
- Radiation and surgery
- Palliative care
- Patient adherence, quality of life, satisfaction
- Anticancer medicine

About Publisher

Bio-Byword Scientific Publishing is a fast-growing, peer-reviewed and open access journal publisher, which is located in Sydney, Australia. As a dependable and credible corporation, it promotes and serves a broad range of subject areas for the benefit of humanity. By informing and educating a global community of scholars, practitioners, researchers and students, it endeavors to be the world's leading independent academic and professional publisher. To realize it, it keeps creative and innovative to meet the range of the authors' needs and publish the best of their work.

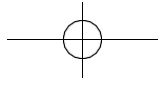
By cooperating with University of Sydney, University of New South Wales and other world-famous universities, Bio-Byword Scientific Publishing has established a huge publishing system based on hundreds of academic programs, and with a variety of journals in the subjects of medicine, construction, education and electronics.

Publisher Headquarter

BIO-BYWORD SCIENTIFIC PUBLISHING PTY LTD Level 10
50 Clarence Street
Sydney NSW 2000
Website: www.bbwpublisher.com Email: info@bbwpublisher.com

Table of Contents

- 1** **Pregnancy and Childbirth After Sertoli-Leydig Cell Tumor Resection: A Case Study and Literature Review**
Lijun Mu, Lihong Zhu
- 5** **An Evaluation of the Clinical Efficacy and Safety of Ixazomib for Relapsed/Refractory Multiple Myeloma**
Lan Li, Weihua Zhang
- 11** **A Novel Analytical Model of Brain Tumor Based on Swarm Robotics**
Mohamed Abbas
- 21** **Using Pegaspargase in Combination with Chemotherapy in the Treatment of Lymphoma**
Yudi Miao
- 26** **A Discussion on TCM Treatment and the Pathogenesis of Membranous Nephropathy in Primary Nephrotic Syndrome**
Xin Li, Genping Lei
- 31** **A Comprehensive Analysis of a Case of Internal Carotid Artery Stenting**
Meng Sun, Jun Wang, Yamei Wang
- 41** **A Correlation Analysis of Postoperative Hypercoagulability and Peripheral Circulating Tumor Cells in Patients with Lung Cancer**
Xuguang Zhang, Duo Zhang, Hefei Li
- 47** **The Level of Circulating Tumor Cells in Patients with Non-Small Cell Lung Cancer and Its Relationship with Tumor Markers**
Rongfang Liu, Ben Li, Xuguang Zhang
- 53** **Analyzing the CT Features of Primary Spontaneous Pneumothorax and Its Application Value**
Duo Zhang, Kuo Xiao
- 59** **Diagnostic Value of Serum TSH, Ultrasound, and Enhanced CT in Papillary Thyroid Carcinoma with Lymph Node Metastasis**
Meiqing He, Xixi Zhang, Hui Li, Tian Wang
- 65** **Effects of Different Doses of BDNF on Postoperative Cognitive Function in Aged Rats Undergoing Abdominal Surgery**
Yuming Zhang, Hui Wang, Kai Lu, Jun Wang, Ning Bai



Call for papers–Proceedings of Anticancer Research

ISSN (Online): 2208-3553

ISSN (Print): 2208-3545

Submission open for September 2022

Dear Researchers,

Proceedings of Anticancer Research is an international peer-reviewed and open access journal, which is devoted to the rapid publication of high quality original articles, reviews, case reports, short communication and letters on all aspects of experimental and clinical oncology.

- Cellular research and bio-markers
- Identification of bio-targets and agents with novel mechanisms of action
- Preventative and integrated treatment for cancer patients
- Radiation and surgery
- Palliative care
- Patient adherence, quality of life, satisfaction
- Anticancer medicine

Proceedings of Anticancer Research is published by Bio-Byword Scientific Publishing Company, it is a fast growing peer-reviewed and open access journal publisher, which is located in Sydney, Australia. As a dependable and credible corporation, it promotes and serves a broad range of subject areas such as medicine, construction, education and electronics for the benefit of humanity. By informing and educating a global community of scholars, practitioners, researchers and students, it endeavours to be the world's leading independent academic and professional publisher.

All Bio-Byword journals are free from all access barriers, allowing for the widest possible global dissemination of their manuscripts and highest possible citations. Bio-Byword publisher online submission will go through a rapid peer review and production, making the process of publishing simpler and more efficient, which benefit from its user friendly online submission system that reduces the overall time from submission to publication.

Acceptance Notification: Within 21 days from the date of manuscript submission

Send your manuscript to the editor at: info@bbwpublisher.com

With Warm Regards,

Editor-in-Chief

MP Balasubramanian

Proceedings of Anticancer Research

Pregnancy and Childbirth After Sertoli-Leydig Cell Tumor Resection: A Case Study and Literature Review

Lijun Mu¹, Lihong Zhu^{2*}

¹Shaanxi University of Traditional Chinese Medicine, Xianyang 712046, Shaanxi Province, China

²The Second Affiliated Hospital of Shaanxi University of Traditional Chinese Medicine, Xianyang 712000, Shaanxi Province, China

*Corresponding author: Lihong Zhu, 1839169171@qq.com

Copyright: © 2022 Author(s). This is an open-access article distributed under the terms of the Creative Commons Attribution License (CC BY 4.0), permitting distribution and reproduction in any medium, provided the original work is cited.

Abstract: *Objectives:* To explore the clinical manifestations and pathological features in the biopsy of ovarian Sertoli-Leydig cell tumor, as well as to improve the clinical understanding of the disease. *Methods:* A case of pregnancy and childbirth after Sertoli-Leydig cell tumor resection was retrospectively analyzed. The patients' clinical data were collected, including the clinical manifestations, postoperative biopsy results, auxiliary examination results, immunohistochemical results, treatment, and prognosis of the patient. *Results:* (1) SLCT occurred unilaterally; (2) according to the International Federation of Obstetrics and Gynecology (FIGO), the clinical staging was stage IA; according to the pathological classification of malignant tumors, it was grade II (moderately differentiated); (3) a healthy female live baby was delivered. *Conclusion:* Such tumors are rare low-grade malignancies and are even rarer in pregnancy. An increase in preoperative testosterone levels with positive ultrasonography results can be used to assist diagnosis; however, postoperative biopsy pathology remains the "gold standard" for the diagnosis of SLCTs. The definite diagnosis of SLCTs is of great significance for surgical planning and prognostic evaluation.

Keywords: Ovarian tumor; Sertoli-Leydig cell tumor; Pathology; Diagnosis; Testosterone; Women

Online publication: July 27, 2022

1. Introduction

Ovarian Sertoli-Leydig cell tumor, also known as androblastoma or male blastoma, occurs mainly in young women and is usually presented as a unilateral solid or cystic-solid mass [1]. Having endocrine functions, its clinical manifestations include defeminized features, and later masculinized signs. The incidence of this disease is low, and there are limited literature reports on this disease at present. This paper discusses a case of natural pregnancy and delivery of a healthy female live baby after the removal of an androblastoma in the right ovary. Based on literature, data were reviewed and summarized for the diagnosis, treatment, and prognosis of the disease.

2. Case report

The patient is a 23-year old lady, married, and not pregnant. The main reason is that there was a cystic-solid mass in her right ovary for more than one month upon physical examination. She had amenorrhea for 5 years, with irregular menstruation in the past. Intermittent oral administration of Diane-35 (cyproterone

acetate and ethinylestradiol) was ineffective. On admission, the patient was obese, with a hoarse, deep voice. On physical examination, thick, black hair was noted all over her body (2 cm × 1.5 cm × 1.5 cm); her abdomen was distended, and a mass of about 5 cm × 5 cm in size, rubbery in nature, with clear boundaries, was palpable at her right adnexal area; there was mild tenderness upon palpation; the left adnexal area was normal.

Investigations for sex hormone determination: testosterone (T) 6.53 nmol/L, estradiol (E2) 42 pg/mL, progesterone (P) 0.4 ng/mL, prolactin (PRL) 610.14 ng/mL, luteinizing hormone (LH) 3.41 mIU/mL, follicle stimulating hormone (FSH) 4.51 mIU/mL, and dehydroepiandrosterone sulfate (DHEAS) 217.5 µg/dL. There were no obvious abnormalities in tumor markers and thyroid function. Gynecological ultrasound showed a cystic-solid mass of 5.3 cm × 4.9 cm × 4.8 cm in the right ovary. In January 2020, a laparoscopic right ovarian cystectomy was performed in a hospital in Shaanxi Province. The right ovarian tumor specimen was round, smooth, and rubbery, and the cut surface was uniformly yellow. Intraoperative quick freezing pathological results: no tumor cells were found in the peritoneal washings, normal ovarian tissue on the left, sex cord stromal tumor on the right, and testicular cells were seen; the specific type could not be determined. Postoperative pathology showed right ovarian androblastoma, with low-grade malignancy. Postoperative chemotherapy was recommended, but the patient refused. One month after the surgery, her menstruation returned, and subsequently, she was found pregnant. Her last menstrual period (LMP) was on February 17, 2020, and she was diagnosed with intrauterine pregnancy five weeks later. In the first trimester, she was treated for “threatened abortion” for half a month, and her thyroid function test about two months in pregnancy indicated subclinical hypothyroidism, which eventually resolved. On November 17, 2020, a 3,300 g female live baby was delivered via cesarean section, and the baby’s development was normal. Peritoneal lavage fluid was collected during the surgery; right adnexectomy, left ovary biopsy, omentum biopsy, peritoneal biopsy (left and right paracolic peritoneal tissues, as well as rectum uterine lacuna peritoneal tissue), pelvic cavity sampling biopsy, pelvic diaphragm, liver, and spleen exploration, as well as tumor cytoreduction were done. On postoperative review, testosterone was more than 60 ng/mL, human chorionic gonadotropin was more than 10,000 mIU/mL, alpha-fetoprotein was 121 ng/mL, carbohydrate antigen 125 (CA-125) was 14.30 U/mL, human epididymis protein was 52.81 pmol/L. The pathological diagnosis was as follows: the frozen section showed no evidence of malignancy, and the paraffin section (right side) showed no obvious abnormalities in the ovary; (greater omentum) there were fat liquefaction and necrosis with foreign body granuloma inflammation; there was no tumor tissue involvement in the left ovarian tissue, bilateral paracolic inguinal peritoneal tissue, uterine-rectal lacuna, and right pelvic lymph node; no tumor metastasis was found in the left pelvic lymph node (0/2); (peritoneal lavage fluid) no cancer cells; (peritoneal washing fluid cell mass) no cancer cells were found. One month after being discharged from the hospital, the patient received chemotherapy as prescribed by the doctor and is still being followed up.

3. Discussion

3.1. Clinical features of ovarian stromal cell tumors

Ovarian Sertoli-Leydig cell tumor ^[2] originates from the sex cord and stromal tissues in the primordial gonad and consists of a mixture of different cells. The main symptoms are endocrine disorders, such as amenorrhea, acne, abnormal menstruation, and so on. With high androgen performance ^[3], more than 30% of patients have amenorrhea, increased acne, hirsutism, Adam’s apple, deeper voice, and enlarged clitoris. Abnormal uterine bleeding or postmenopausal vaginal bleeding occurs in about 50% of patients. In this case, the patient felt a mass in her lower abdomen, which was rubbery, well-demarcated, and non-tender. A small number of patients will experience abdominal discomfort, such as bloating and abdominal pain. When the tumor ruptures or undergoes torsion, the abdominal pain will be aggravated, characterized by a tear-like or knife-like pain, radiating to the anus ^[4]. As the disease progresses, ovarian tumors may rupture, bleed, or undergo torsion, resulting in acute abdomen, or even life-threatening conditions. This patient presented with endocrine disorders; she had prominent hyperandrogenism, amenorrhea for five years,

obesity, thick, black hair over her body, thick vulvar, male distribution of pubic hair, clitoral hypertrophy, as well as high testosterone level.

3.2. Pathological features of ovarian stromal cell tumors

Microscopically, the tumor cells are mainly composed of two cellular components [5]: one is well-differentiated Sertoli-type cells, which are arranged in solid or hollow tubules; they are columnar cells, with sparse or lightly stained cytoplasm; they have small, oval or spherical nuclei, in which mitotic figures are rare; the other is Leydig-type cells, which are distributed in the interstitium singly or in sheets, especially around tubules; they are round granular cells, with abundant eosinophilic cytoplasm, having round nuclei; in the center or on one side, the fibrous mesenchymal tissue is relatively abundant, composed of closely arranged spindle cells, accompanied by varying amounts of collagen fibers. According to the degree of tubular differentiation of Sertoli cells and the proportion of primitive gonads, ovarian Sertoli-Leydig cell tumors can be divided into three pathological grades (Grade I, II, and III): well-differentiated, moderately differentiated, and poorly differentiated reticular type with heterologous elements [6]. Imaging examinations are mostly suggestive of solid, cystic-solid, or cystic masses. In this case, only the right ovarian androblastoma was excised. Rapid intraoperative pathological results revealed normal ovarian tissue on the left side and sex cord-stromal tumor on the right side. Testicular cells were seen, but the specific type could not be determined. Postoperative pathology revealed a right ovarian androblastoma, with low-grade malignancy. After explaining the condition to the patient's family, they refused to remove the affected ovary. Considering the patient's age and reproductive requirements, the bilateral appendages were retained following the patient's requirements; hence, only the tumor was removed. On re-examination after cesarean section, there was no recurrence, and the patient is currently receiving chemotherapy.

3.3. Treatment and prognosis of ovarian stromal cell tumors

Surgery is the mainstay of treatment for stromal cell tumors [7]. The purpose of surgery is to completely remove the tumor and achieve radical treatment. The resected ipsilateral appendage will be sent for pathological examination; if it is benign, the scope is sufficient [8], but if malignant germ cell components are reported, pelvic lymph node dissection, omentectomy, and para-aortic lymph node biopsy are required, in order to remove the diseased tissue to the maximum extent, so as to reduce recurrence and metastases. If the patient has fertility requirements, the contralateral appendage and its reproductive function can be preserved. The majority of patients with stromal cell tumors are curable with standard care; the recurrence rate is extremely low, and patients' quality of life is rarely affected [9], with the majority of cases having no impact on life expectancy. In this case, the patient had no recurrence after tumor resection, and she conceived naturally and gave birth to a healthy female live baby. Therefore, for young patients who desire to have children, if the uterus and contralateral appendages are normal, their reproductive function can be preserved.

Disclosure statement

The authors declare no conflict of interest.

References

- [1] Xie X, Kong B, Duan T, 2018, *Obstetrics and Gynecology Ninth Edition*, People's Health Publishing House, Beijing, 320–321.
- [2] Du X, Lin X, 2018, *Ovarian Support – Clinicopathological Analysis of 12 Cases of Stromal Cell Tumor*. *Chinese Medicine Guide*, 16(34): 108–109.

- [3] Guo L, Chen H, 2018, A Case Report of Ovarian Support-Stromal Cell Tumor and Literature Review. *China Family Planning and Obstetrics*, 10(11): 92–94.
- [4] Ding C, Li Z, Yuan Y, et al., 2019, Clinicopathological Analysis of 6 Cases of Ovarian Support-Stromal Cell Tumor. *Modern Oncology*, 27(23): 4264–4268.
- [5] Yang N, 2018, Ovarian Support – Analysis of Clinical Features and Prognostic Factors of Stromal Cell Tumors. Peking Union Medical College.
- [6] Liu X, Zhao Q, Liu H, 2018, Clinical Analysis of Ovarian Sertoli Cell-Stromal Cell Tumor. *Chinese Journal of Clinical Medicine for Women and Children*, 14(05): 508–514.
- [7] Chen J, Wang Y, Chen H, et al., 2020, CT Diagnosis and Clinicopathological Features of Ovarian Support-Stromal Cell Tumors. *Chinese Journal of Integrative Medicine Imaging*, 18(06): 609–611.
- [8] DiSaia PJ, Creasman WT, 1997, Germ Cell, Stromal and Other Ovarian Tumor, in *Clinical Gynecologic Oncology*, Mosby-Yearbook, 351.
- [9] Wang Y, Jiang H, Wang X, 2008, A Case of Spontaneous Pregnancy and Childbirth After Excision of Ovarian Orchioblastoma. *Chinese Journal of Perinatal Medicine*, 3(2): 143–144.

Publisher's note

Bio-Byword Scientific Publishing remains neutral with regard to jurisdictional claims in published maps and institutional affiliations.

An Evaluation of the Clinical Efficacy and Safety of Ixazomib for Relapsed/Refractory Multiple Myeloma

Lan Li*, Weihua Zhang

Department of Hematology, Shaanxi Provincial People's Hospital, Xi'an 710068, Shaanxi Province, China

*Corresponding author: Lan Li, lilanlanxin@163.com

Copyright: © 2022 Author(s). This is an open-access article distributed under the terms of the Creative Commons Attribution License (CC BY 4.0), permitting distribution and reproduction in any medium, provided the original work is cited.

Abstract: *Objective:* To investigate the clinical efficacy and safety of ixazomib in the treatment of relapsed/refractory multiple myeloma (RRMM). *Methods:* The clinical data of 20 patients with RRMM admitted to the hospital from January 2020 to January 2022 were analyzed retrospectively. All patients were treated with ixazomib-based chemotherapy regimen (IRD regimen 13 cases; ID regimen 7 cases). The objective response rate (ORR) and adverse events (AEs) were observed. *Results:* All 20 patients received two to seven courses of treatment, in which the median was three courses. One patient had CR, four patients had VGPR, seven patients had PR, two patients had SD, and six patients had PD. The ORR was 60.00% (12/20), and 25.00% (5/20) of them had VGPR or more. The ORR of patients with previous treatment lines ≥ 3 , ISS stage III, and high-risk cytogenetic was lower than that of patients with previous treatment lines < 3 , ISS stage I/II, and low-risk cytogenetics. The main AEs include anemia, thrombocytopenia, neutropenia, nausea and vomiting, diarrhea, constipation, and respiratory tract infection, most of which are grade I/II. *Conclusion:* Ixazomib is effective in the treatment of RRMM in some patients, and the AEs are controllable. Patients who had received less than 3 lines of treatment in the past, with ISS stage I to II and low-risk cytogenetics had better treatment effect.

Keywords: Ixazomib; Relapsed/refractory multiple myeloma; Clinical efficacy; Adverse event

Online publication: July 27, 2022

1. Introduction

Multiple myeloma (MM) is one of the hematological malignancies. It originates from bone marrow hematopoietic cells and presents as clonal plasma cell dysplasia, resulting in multiple osteolytic lesions, anemia, kidney damage, and other organ or tissue damage^[1]. With the advent of new anti-tumor drugs, the overall prognosis of MM patients has significantly improved, along with the remission rate and progression-free survival (PFS)^[2]. However, hidden lesions and small residual lesions are still problems that cannot be fully resolved, and drug resistance is also a major problem in clinical treatment. Except for a few patients who may be cured by hematopoietic stem cell transplantation, most patients will eventually relapse and progress. The treatment of relapse/refractory multiple myeloma (RRMM) is still a major clinical problem, which needs to be solved urgently. As the first oral proteasome inhibitor, ixazomib has shown satisfactory results in the treatment of primary relapsed/refractory MM^[3] and is in line with the new trend of treatment simplicity. This study retrospectively analyzed the clinical data of patients with RRMM who received ixazomib-based all-oral regimen in Shaanxi Provincial People's Hospital from January 2020 to January 2022 and evaluated its clinical efficacy and safety.

2. Data and methods

2.1. General information

Twenty patients with RRMM were admitted to the hospital from January 2020 to January 2022. Inclusion criteria: (1) patients who met the diagnostic criteria of MM and the definition of “relapsed/refractory” in “The Guidelines for the Diagnosis and Management of Multiple Myeloma in China (2020 Revision)” [4] and whose diagnosis was confirmed by bone marrow examination and imaging examination; (2) all patients were treated with ixazomib-based all-oral regimen and completed more than one course of treatment; (3) complete clinical data, including gender, age, physical fitness score, blood routine examination, blood biochemistry, laboratory examination, pathological examination, imaging examination, number of previous anti-bone marrow treatment lines, previous drug resistance, cytogenetic risk stratification, and revised international staging system. Exclusion criteria: (1) primary amyloidosis and secondary progression to plasma cell leukemia; (2) complicated with renal insufficiency, unstable cardiovascular disease, and other malignant tumors; (3) combined with central nervous system involvement; (4) ECOG score of > 2.

2.2. Treatment methods

The patients received ixazomib-based regimens (ID and IRD). The ID regimen includes oral ixazomib (Takeda Pharma A/S, H20180010) 4 mg, taken on the 1st-, 8th-, and 15th-day; oral dexamethasone 40 mg, taken on the 1st-, 8th-, 15th-, and 22nd-day, with 28 days as the course of treatment. The IRD regimen includes the doses of ixazomib and dexamethasone based on the ID regimen plus oral lenalidomide 25 mg, taken on the 1st- to 21st-day, with 28 days as the course of treatment. During the treatment, the dosages were adjusted accordingly based on the patient’s age, creatinine clearance rate, and adverse reactions.

2.3. Clinical efficacy and safety evaluation

The clinical efficacy of the treatment was evaluated based on the efficacy standard formulated by the International Myeloma Working Group (IMWG) [5], which can be divided into complete remission (CR), very good partial remission (VGPR), partial remission (PR), minimal remission (MR), stable disease (SD), and progressive disease (PD). The best curative effect during the treatment period was taken as the evaluation result. The objective response rate (ORR) is the sum of the ratios, excluding SD and PD. Common Terminology Criteria for Adverse Events (CTCAE) version 5.0 [6] was used to evaluate the adverse events (grade I~IV) and the safety of treatment.

2.4. Statistical analysis

SPSS 23.0 was used for data analysis. The counting data were expressed in (%) and χ^2 test; $p < 0.05$ signifies that the difference is statistically significant.

3. Results

3.1. Clinical characteristics and efficacy of treatment

By the end of the follow-up, the 20 patients had received two to seven courses of treatment, with a median of three courses. Thirteen patients were treated with IRD, while seven patients were treated with ID. One patient had CR, four patients had VGPR, seven patients had PR, two patients had SD, and six patients had PD. The ORR was 60.00% (12/20), and 25.00% (5/20) of them had VGPR or more. Fourteen patients continued to receive ixazomib, five patients received other treatment regimens due to disease progression, and one patient died due to multiple organ failure. The ORR of patients with previous treatment lines ≥ 3 , ISS stage III, and high-risk cytogenetics was lower than that of patients with previous treatment lines < 3 , ISS stage I or II, and low-risk cytogenetics ($p < 0.05$) (see **Table 1**).

Table 1. Correlation analysis between ixazomib efficacy and clinical characteristics

Clinical characteristics		Cases	ORR	<i>p</i>
Age (years)	18-64	11	6 (54.55)	0.784
	≥ 65	9	6 (66.67)	
Gender	Male	12	7 (58.33)	0.926
	Female	8	5 (62.50)	
ISS staging	I/II	14	12 (85.71)	0.035
	III	6	0	
Cytogenetic risk stratification	Low risk	11	11 (100.00)	0.030
	High risk	9	1 (11.11)	
Number of previous treatment lines	1/2 line(s)	13	12 (92.30)	0.020
	≥ 3 lines	7	0	
ECOG	1 point	9	7 (77.78)	0.465
	2 points	11	5 (45.45)	
Previous bortezomib	Yes	12	5 (41.67)	0.314
	No	8	7 (87.50)	
Previous lenalidomide	Yes	7	4 (57.14)	0.923
	No	13	8 (61.54)	
Previous autologous stem cell transplantation	Yes	5	4 (80.00)	0.612
	No	15	8 (53.33)	
Extramedullary focus	Yes	3	1 (33.33)	0.581
	No	17	11 (64.71)	
Treatment regimen	ID	7	4 (57.14)	0.923
	IRD	13	8 (61.54)	

3.2. Safety evaluation

The main adverse events (AEs) included anemia, thrombocytopenia, neutropenia, nausea and vomiting, diarrhea, constipation, and respiratory tract infection, most of which were grade I or II. After symptomatic treatment, they all improved without affecting the continued use of drugs (see **Table 2**).

Table 2. Analysis of hematological and non-hematological AEs after ixazomib treatment

AEs	I/II	III/IV	Overall incidence (%)
<i>Hematological</i>			
Anemia	4	1	25.00
Neutropenia	3	1	20.00
Thrombocytopenia	6	2	40.00
Lymphopenia	3	0	15.00
<i>Non-hematological</i>			
Nausea and vomiting	14	1	75.00
Weakness	15	0	75.00
Diarrhea	5	1	30.00
Constipation	4	0	20.00
Rash	2	0	10.00

(Continued on next page)

(Continued from previous page)

AEs	I/II	III/IV	Overall incidence (%)
<i>Non-hematological</i>			
Zoster	1	0	5.00
Joint pain	2	0	10.00
Peripheral neuropathy	3	0	15.00
Respiratory tract infection	4	1	25.00
Elevated creatinine	1	1	10.00
Elevated transaminase	1	0	5.00
Insomnia	1	0	5.00

4. Discussion

RRMM has low remission rate and short median survival time. Its treatment has always been the focus and issue in clinical practice. Proteasome inhibitors (PIs) are one of the mainstays of treatment for MM [7], but their long-term use is limited by parenteral administration and treatment-related toxicity [8]. Ixazomib is a reversible PI, which acts on the catalytic center of 20S proteasome [9]. With lower drug concentration in the body, it selectively binds and interacts with proteasome $\beta 5$ subunit, thus inhibiting chymotrypsin-like protease activity; with higher drug concentration in the body, it interacts with $\beta 1$ and $\beta 2$ subunits, thus inhibiting glutamyl peptide hydrolase and trypsin-like protease activities and inducing cell apoptosis [10-12]. In terms of the mechanism of action, ixazomib is similar to bortezomib. However, the half-life of ixazomib is short, about one-sixth of bortezomib [13], and there are only a number of factors that affect the pharmacokinetics. Fixed dose medication can be used to ensure the rigor of the treatment [14]. Intolerable peripheral neuropathy is a major limitation in the use of bortezomib. As a new PI, ixazomib has a much lower incidence of peripheral neuropathy than bortezomib [15]. Additionally, patients receiving ixazomib have better compliance than those receiving intravenous injection drugs, and these patients can be treated for a longer time. Mouse studies have also confirmed that ixazomib can better control tumor cells compared to bortezomib; moreover, it has an effect on bortezomib-resistant myeloma cells.

The use of ixazomib in combination with lenalidomide and dexamethasone is approved for the treatment of MM patients who have received treatment at least once. A number of clinical trials and real-world studies at home and abroad have confirmed that ixazomib-based regimens have good efficacy and safety for RRMM patients. In a study [16], Avet-Loiseau confirmed that IRD is beneficial to RRMM patients with high-risk and standard risk cytogenetics, and it can prolong the progression free survival of patients compared with placebo RD. In another study [17], 90 RRMM patients who received eight cycles of IRD were observed; the results showed that the total effective rate was 51.1%; 23.3% reached CR or VGPR, 10% reached MR, and the clinical benefit rate was 61.1%; the effective rate, PFS, and overall survival (OS) were similar in patients with or without t(4;14) and/or del(17p); however, the PFS and OS were significantly shortened in patients with 1q21 gain; multiple regression analysis showed that the gain of 1q21 is the most critical factor related to OS [17]. A multicenter retrospective analysis showed that the PFS and OS of IgG patients were significantly better than those of non-IgG patients [18]. In this study, among the 20 patients, one patient achieved CR, four patients achieved VGPR, and seven patients achieved PR; the ORR was 60.00%, and 25.00% achieved VGPR or more; 14 patients continued to receive ixazomib treatment, five patients received other treatment regimen due to disease progression, and one patient died due to multiple organ failure. This shows that ixazomib has good curative effect on some patients. The correlation analysis between the clinical characteristics and drug efficacy showed that the ORR of patients with previous treatment lines ≥ 3 , ISS stage III, and high-risk cytogenetics was lower than that of patients with previous treatment lines < 3 , ISS stage I/II, and low-risk cytogenetics.

Drug-related peripheral neuropathy is a common AE with first generation PIs. It has a reported incidence of about 40%, which may seriously affect the quality of life and treatment compliance of patients [19,20]. In this study, the incidence of peripheral neuropathy with ixazomib treatment was only 15.00%, which confirmed that ixazomib has significantly lower neurotoxicity compared to bortezomib. The main AEs in this study included anemia, thrombocytopenia, neutropenia, nausea, vomiting, diarrhea, constipation, and respiratory tract infection, most of which were grade I/II. After symptomatic treatment, they all improved and did not affect the continued use of drugs.

In conclusion, ixazomib is effective in the treatment of RRMM in some patients, and its AEs are controllable. Patients who had received less than three lines of treatment in the past with ISS stage I/II and low-risk cytogenetics achieved better treatment effect. However, compared with large clinical studies, the sample size of this study is small. The effectiveness and safety of ixazomib still require further confirmation by expanding the sample size, extending the follow-up time, and conducting more thorough clinical studies.

Disclosure statement

The authors declare no conflict of interest.

References

- [1] Brigle K, Rogers B, 2017, Pathobiology and Diagnosis of Multiple Myeloma. *Semin Oncol Nurs*, 33(3): 225–236.
- [2] Kazandjian D, 2016, Multiple Myeloma Epidemiology and Survival: A Unique Malignancy. *Semin Oncol*, 43(6): 676–681.
- [3] Moreau P, Masszi T, Grzasko N, et al., 2016, Oral Ixazomib, Lenalidomide, and Dexamethasone for Multiple Myeloma. *N Engl J Med*, 374(17): 1621–1634.
- [4] Chinese Hematology Association, Chinese Society of Hematology, Chinese Myeloma Committee-Chinese Hematology Association, 2020, The Guidelines for the Diagnosis and Management of Multiple Myeloma in China (2020 Revision). *Chin J Intern Med*, 59(5): 341–346.
- [5] Kumar S, Paiva B, Anderson KC, et al., 2016, International Myeloma Working Group Consensus Criteria for Response and Minimal Residual Disease Assessment in Multiple Myeloma. *Lancet Oncol*, 17(8): e328–e346.
- [6] Freites-Martinez A, Santana N, Arias-Santiago S, et al., 2021, Using the Common Terminology Criteria for Adverse Events (CTCAE – Version 5.0) to Evaluate the Severity of Adverse Events of Anticancer Therapies. *Actas Dermosifiliogr (Engl Ed)*, 112(1): 90–92.
- [7] Dimopoulos MA, Lonial S, White D, et al., 2020, Elotuzumab, Lenalidomide, and Dexamethasone in RRMM: Final Overall Survival Results from the Phase 3 Randomized ELOQUENT-2 Study. *Blood Cancer J*, 10(9): 91.
- [8] Tabayashi T, 2019, Management of Multiple Myeloma in the Relapsed/Refractory Patient. *Rinsho Ketsueki*, 60(9): 1257–1264.
- [9] Gentile M, Offidani M, Vigna E, et al., 2015, Ixazomib for the Treatment of Multiple Myeloma. *Expert Opin Investig Drugs*, 24(9): 1287–1298.
- [10] Yang Y, Li Y, Gu H, et al., 2020, Emerging Agents and Regimens for Multiple Myeloma. *J Hematol Oncol*, 13(1): 150.
- [11] Hinsley S, Walker K, Sherratt D, et al., 2020, Myeloma UK Clinical Trials Network. The MUK Eight Protocol: A Randomised Phase II Trial of Cyclophosphamide and Dexamethasone in Combination with

Ixazomib, in Relapsed or Refractory Multiple Myeloma (RRMM) Patients Who Have Relapsed After Treatment with Thalidomide, Lenalidomide and a Proteasome Inhibitor. *Trials*, 21(1): 826.

- [12] Xie J, Wan N, Liang Z, et al., 2019, Ixazomib – The First Oral Proteasome Inhibitor. *Leuk Lymphoma*, 60(3): 610–618.
- [13] He Y, Zhang K, Zou L, et al., 2020, Clinical Study on Ixazomib in the Treatment of Multiple Myeloma. *Zhong Nan Da Xue Xue Bao Yi Xue Ban*, 45(3): 322–327.
- [14] Cohen YC, Magen H, Lavi N, et al., 2020, Ixazomib-Based Regimens for Relapsed/Refractory Multiple Myeloma: Are Real-World Data Compatible with Clinical Trial Outcomes? A Multi-Site Israeli Registry Study. *Ann Hematol*, 99(6): 1273–1281.
- [15] Terpos E, Ramasamy K, Maouche N, et al., 2020, Real-World Effectiveness and Safety of Ixazomib-Lenalidomide-Dexamethasone in Relapsed/Refractory Multiple Myeloma. *Ann Hematol*, 99(5): 1049–1061.
- [16] Avet-Loiseau H, Bahlis NJ, Chng WJ, et al., 2017, Ixazomib Significantly Prolongs Progression-Free Survival in High-Risk Relapsed/Refractory Myeloma Patients. *Blood*, 130(24): 2610–2618.
- [17] Ludwig H, Poenisch W, Knop S, et al., 2019, Ixazomib-Thalidomide-Dexamethasone for Induction Therapy Followed by Ixazomib Maintenance Treatment in Patients with Relapsed/Refractory Multiple Myeloma. *Br J Cancer*, 121(9): 751–757.
- [18] Takakuwa T, Yamamura R, Ohta K, et al., 2021, Outcomes of Ixazomib/Lenalidomide/Dexamethasone for Multiple Myeloma: A Multicenter Retrospective Analysis. *Eur J Haematol*, 106(4): 555–562.
- [19] Siegel DS, Schiller GJ, Song KW, et al., 2020, Pomalidomide Plus Low-Dose Dexamethasone in Relapsed Refractory Multiple Myeloma After Lenalidomide Treatment Failure. *Br J Haematol*, 188(4): 501–510.
- [20] Davies F, Rifkin R, Costello C, et al., 2021, Real-World Comparative Effectiveness of Triplets Containing Bortezomib (B), Carfilzomib (C), Daratumumab (D), or Ixazomib (I) in Relapsed/Refractory Multiple Myeloma (RRMM) in the US. *Ann Hematol*, 100(9): 2325–2337.

Publisher's note

Bio-Byword Scientific Publishing remains neutral with regard to jurisdictional claims in published maps and institutional affiliations.

A Novel Analytical Model of Brain Tumor Based on Swarm Robotics

Mohamed Abbas*

Computers and Communications Department, College of Engineering, Delta University for Science and Technology, Gamasa 35712, Egypt

**Corresponding author:* Mohamed Abbas, mohamed2abbas@gmail.com

Copyright: © 2022 Author(s). This is an open-access article distributed under the terms of the Creative Commons Attribution License (CC BY 4.0), permitting distribution and reproduction in any medium, provided the original work is cited.

Abstract: A tumor is referred to as “intracranial hard neoplasm” if it grows near the brain or central spinal vessel (neoplasm). In certain cases, it is possible that the responsible cells are neurons situated deep inside the brain’s structure. This article discusses a strategy for halting the progression of brain tumor. A precise and accurate analytical model of brain tumors is the foundation of this strategy. It is based on an algorithm known as kill chain interior point (KCIP), which is the result of a merger of kill chain and interior point algorithms, as well as a precise and accurate analytical model of brain tumors. The inability to obtain a clear picture of tumor cell activity is the biggest challenge in this endeavor. Based on the motion of swarm robots, which are considered a subset of artificial intelligence, this article proposes a new notion of this kind of behavior, which may be used in various situations. The KCIP algorithm that follows is used in the analytical model to limit the development of certain cell types. According to the findings, it seems that different KCIP speed ratios are beneficial in preventing the development of brain tumors. It is hoped that this study will help researchers better understand the behavior of brain tumors, so as to develop a new drug that is effective in eliminating the tumor cells.

Keywords: Swarm robots; Brain tumor; Analytical computation; Kill chain; Interior point algorithm

Online publication: July 27, 2022

1. Introduction

The neurological symptoms and indications of brain tumors have no clear connection with the type of tumor; instead, they are related to the tumor’s location within the central nervous system (CNS). Compression or invasion by a tumor may damage or shift neural tissues, resulting in localized pain. Edema increases the mass effect, which further compresses the brain in the surrounding region ^[1]. Patients with brain tumors are unable to make use of brain segmentation software tools. Three-dimensional (3D) imagery and augmented reality are now being utilized in healthcare settings where augmented reality and virtual reality are present ^[2]. **Figure 1** shows how brain tumors compress and displace normal brain tissues.

Aberrant mechanical stresses in the brain must be considered due to the physical limitations of the skull. Intravital imaging studies in mice use conventional transparent cranial windows with an adjustable screw for controlled acute or chronic compression and decompression in the brain ^[3]. Magnetic resonance imaging (MRI) was used to gather textural characteristics from the brains of patients with tumors. Following that, the feature space was processed using the correlation-based feature selection (CFS) technique and the partial least squares regression (PLSR) method ^[4]. The convolutional neural network (CNN) is a machine-learning technique that has shown impressive results in image segmentation and classification. Three different types of brain tumors may be classified using the novel CNN architecture. As compared to current

pre-trained networks, the newly created network is simpler. It was evaluated using T1-weighted contrast-enhanced MRI images [5]. Since the system utilizes a cubic model to minimize vascular input error, it is superior to existing best practices when it comes to treating brain tumors [6]. Dynamic contrast-enhanced magnetic resonance imaging (DCE-MRI) for brain tumor analysis is now possible with a fully automated system that handles everything from beginning to end. Using five different selection methods and six different classification algorithms, thirty diagnostic models were created; several criteria, including sensitivity, specificity, accuracy, and area under the curve (AUC), were considered in determining which model was the most effective area under curve [7].

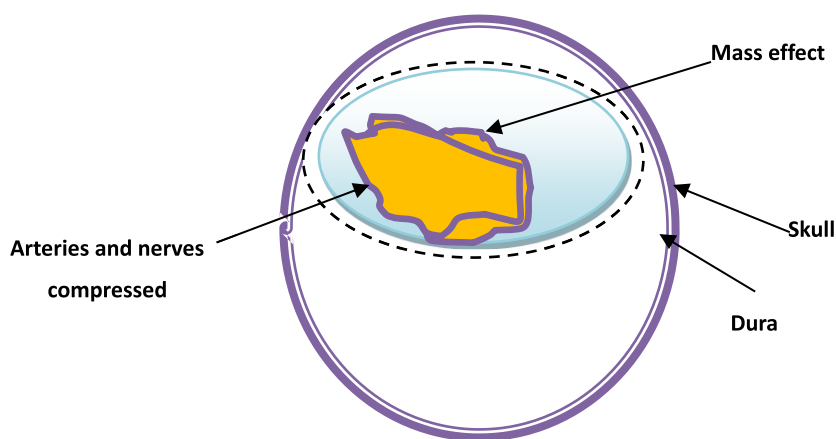


Figure 1. Compression and displacement of normal brain tissues by brain tumor

Preprocessing procedures, image segmentation, feature extraction, and image classification using neural network methods are all part of a computer-based approach for identifying tumors in the brain [8]. For medical image segmentation and classification, the fuzzy brain-storm optimization method combines fuzzy and brain-storm optimization techniques. The study's findings show that it outperforms its competition [9]. Radiologists use genetic algorithms because it is a simple idea and is well-understood by them. Omitted brain tumors can be displayed as segmented regions of interests (SROIs) using a content-based active contour (CBAC) model with content-based segmentation. Intensity and texture-based features for feature extraction genetic algorithms are used to reduce the number of available features [10]. Artificial intelligence has been used in attempt to gauge the severity of brain tumor malignancy. Fuzzy c-means clustering was used to isolate the brain areas suspected of having abnormal growths by radiologists. When it comes to precisely identifying the tumor's boundaries, Fourier descriptors come in handy. There are many Fourier descriptors that introduce a problem with overlearning and the possibility of misclassifications. The proposed diagnosis system efficiently searches for significant boundary features by genetic algorithm and feeds them to an adaptive neuro-fuzzy classifier that is built on these features [11]. An algorithm developed to automatically identify tumor segmentation and outline threshold was applied to MRI brain scans to segment tumor images in a study. MRI brain images and radiology records were used to create two databases for the experiment [12]. Healthcare practitioners may benefit from a MRI method that detects brain tumors shared via the internet. While other techniques sacrifice some visual information to take smaller images, this one does not. In another study, a modified K-means clustering method was utilized to identify the tumor's position before conducting the initial segmentation using mean shift segmentation. Following that, a threshold setting was used to transform the image to black and white, and an erode process was carried out to eliminate noise. The tumors in the images were then located using a watershed technique [13]. A patch-based technique and an inception module were used to extract two concentric patches of different sizes from the input images before training the deep network, which employed dropout regularization to

address the over-fitting problem caused by a lack of data [14]. The MR slices from three distinct axes of the brain include heterogeneous tumor kinds and tissue features that may be accurately segregated for improved visibility by oncologists [15]. Using another method, aberrant and normal brain tissues may be better detected with less gray-level intensity separation, and human brain malignancies may be detected much faster than with previous algorithms, in seconds as opposed to minutes [16].

The aim of this paper is to investigate the relationship between brain tumors and delimited cells to better understand the behaviors of these cells during the invasion process. This information is useful in early-stage cancers because it gives an idea of the degree of risk. The study of brain tumors was modeled in this paper using swarm robots. Following that, KCIP, an integrated version of the kill chain and interior point algorithm, was used to slow down tumor growth. Swarm robot behaviors are determined by probabilistic, automata, differential, and dynamical equations. In this model, a swarm of robots attempts to kill individual robots by injecting brain tumors into their bodies. The research on swarm robotics is concerned with the design of robots, their physical bodies, and their calculating behaviors. It is based on swarm intelligence but is not constrained by it. Individual rules that are simple and easy to follow can lead to a highly complex composite swarming behavior. The constant feedback generated by group communication is a critical component. Individuals changing with the group and group actions are described by swarm behaviors.

2. A proposed analytical model of brain tumor behavior

This section introduces an analytical methodology to simulate brain tumors using an equation set of swarm robots describing their behaviors. In addition, this section introduces an analytical model of a drug that can revive the damaged cells in the brain. Swarm robotics is an innovative approach to the harmonization of multi-robot systems, which consist of hefty numbers of regularly undemanding, substantial robots. It is theoretical that a preferred communal performance emerges from the relationship linking the robots and the relation between the robots and the environment. The equation set should contain the Langevin equation, transition rate, cohesive swarms, integro-differential, Fokker-Plank equation, dynamics of random walk, and Markov chain process.

In this proposed model, these equations are used to describe the behavior of these swarm robots during their spread as comparable to the spread of a brain tumor. **Figure 2** illustrates the general framework of the proposed analytical model using swarm robots. The swarm robots depend on the equation set in their spread to invade the victim cells. Brain tumors begin, as most cancers do, in some other place within the body and unfold to affect the mind. They form when most cancer cells travel through the bloodstream to the brain.

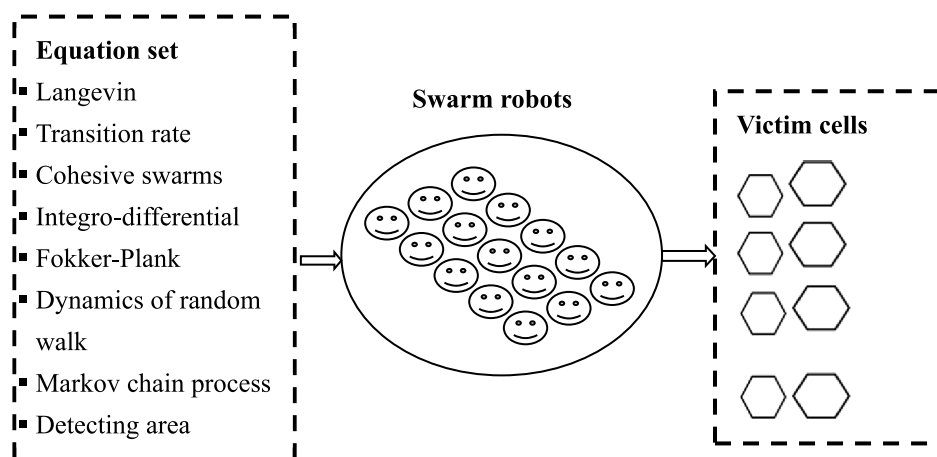


Figure 2. General framework of the planned analytical model using swarm robots

The most common not-unusual cancers that spread to the brain are lung and breast cancers. The brain is unable to make space for an upward accumulation. Some brain tumors may cause a blockage of cerebrospinal fluid, which flows around and through the organ. This blockage will cause an increase in intracranial pressure and enlarge the ventricles. Some brain tumors may also cause edema. A variety of symptoms may occur due to the mass effect produced by pressure, swelling, and even the size of the tumor itself. The following equations describe the glioma type, its conversion, cell migratory response, diffraction, and a model of glioma vessels. Glioma is one of the most prevalent brain tumors that originates from the support cells of the brain, called glial cells. Glial cells are the majority of the brain's universal cellular constituents. There are five to 10 times more glial cells than neurons. Glioma cells migrate more efficiently in the white matter than in the grey matter.

3. Kill chain interior point (KCIP) algorithm for overcoming brain tumor

In order to overcome brain tumors, a proposed algorithm is introduced. It is an integrated version of the kill chain and interior point algorithm. It measures the gap between two superellipsoids. The term kill chain was used as an armed idea linked to the construction of an assault, consisting of target detection, the delivery to the target, the result and arrangement to assault the target, and lastly, the damage to the target. The methodology of this paper depends on measuring the minimum gap between two swarm robots using the interior point algorithm, and then applying the kill chain algorithm to overcome the growth of brain tumor, depending on the analytical analysis of its growth. The proposed methodology assumes that the kill chain algorithm adversaries are familiar with the capabilities and structure of the target system. It employs different methods to deliver loads to their destination. A malware is installed, and the adversaries establish a hidden control channel with compromised entities. Within the victim system, the attack campaign and adversaries now perform actions on their own objectives. The proposed KCIP begins by recognizing an entity of probable concern, while precisely and continuously finding targets, and then compares a call of concern with the preferred entity. The minimum distance between the two swarm robots is calculated.

Suppose r is the first vertex, $n-1$ paths have to leave r . For any other vertex, the number of paths entering the vertex must be exactly one larger than the number of paths leaving the vertex.

The primary problem with using Newton's technique is making sure s zero, which might cause very small step lengths that result in convergence issues. Interior point techniques, in essence, approximately solve a sequence of structures of nonlinear equations.

The center of the concerned objects is the instantaneous preference for the initial bet. The outer loop determines the range of instances μ has to be up to date, that is the number of times needed to be approximately solved for the collection of μ values. At the same time, the inner loop is a version of Newton's method used for approximately solving a set price of μ . Instead of selecting the next node with the lowest price, the selection is based on the cost of the initial node plus an estimate of the immediacy of the destination. The proposed approach would remedy the hassle of finding the most desirable path. Within this context, the cost of node V might be calculated as follows:

$$f(V) = \text{distance from } S \text{ to } V + \text{estimate of the distance to } D$$

$$f(V) = d(V) + h(V,D), \quad f(v) = d(V) + \sqrt{(x(V) - x(D))^2 + (y(V) - y(D))^2};$$

where $x(V)$, $y(D)$ and $x(V)$, $y(D)$ are the coordinates for node V and destination node D . Affirmation employs an extremely complicated broadcasting network. Advanced ability presumably provides support immediately and mechanically; nonetheless, this is a simple estimate of certainty. Stages that were previously sociable perceive the objective, classify it as the preferred objective, and obtain approval to free a bat. A stage may then initiate its sky-to-land arms. It is called the "start" stage. In the "manage" stage,

after a stage starts a bat, the bat may need extra in-journey objective data revision. A few bats do not need maintenance. The management stage ends with bat impact. To conclude the achievement of an assault, responsive stages must execute a fight-harm evaluation. This is known as the “assess” stage. This occasion’s conclusion brings the kill chain for this target to a close. The KCIP algorithm is indicated in algorithm (A), as shown below ^[14].

```

ALGORITHM (A): KILL CHAIN INTERIOR POINT (KCIP)
Start
for each step sp do
for each objective O, compute space(p,t)
calculate speedRatio(p,t)
for each objective O do
task(t,0)=ON , task(t,8)=OFF, completion(t,0)=ON, existinginstance, time_stepCounter=0
total_specified, total_finished=OFF
do while total_finished=OFF
partially_specified=OFF
for each objective O and function f do
if existing_instance=completionTime(t, f) and, existing_instance<>0 then p=laststep(t,f)
if f<>launch then increment step function
for each step p do
calculate closest_objective(p); nearby_specified_objective(p)
if f<=assess then find a nearby
    strictly feasible x0, i
    barrier parameter μ0,
    Output: Closest points solution
        Solve system of linear equations for Newton direction
        Determine step length αk by line search
         $x_{k+1} \leftarrow x_k + \alpha_k \Delta x_k, s_{k+1} \leftarrow s_k + \alpha_k \Delta s_k, \lambda_{k+1} \leftarrow \lambda_k + \alpha_k \Delta \lambda_k$ 
         $k \leftarrow k + 1$ 
if nearby>0 then
    set current task possessions
    add current task to gantt (nearby)
    partially_specified=ON
if nearby=0 then nearby_specified_objective(closest step)=t
    for each objective O and function f, determine total_specified, total_finished
        if total_specified=OFF and total_finished=OFF then
            if partially_specified=ON then nextTime = the earliest completion time of
            the tasks assigned on this iteration
            if secondobjective>1 then nextTime=existing_instance+1
            if partially_specified=OFF then nextTime=existing_instance+0.1
            if total_specified=ON and total_finished=OFF then
                nextTime=the earliest completion time of the tasks that are
            if total_finished=ON then
                for each step p and objective O do
                    compute space from last position; time_step=secondobjective
if time_step>0 then for each step do update step position
for every objective O do
compute space(p, t), calculate speedRatio(p, t); time_stepCounter=time_stepCounter+1
if time_stepCounter>500 then state is infeasible; exit sub
End

```

4. Discussion and results

A network with a limited number of nodes is assumed in the proposed method, which is a reasonable assumption. There are degrees assigned to each of the network's nodes, with the lowest being level 1 and the highest being stage okay. m represents the number of nodes in level 1 of the warned graph, and it represents the number of nodes in level 2 of the cautious graph. As indicated by the symbol n , the entire range of nodes in all degrees of the counseled graph, from the smallest to the biggest, are represented. The number of nodes between stage 1 and level k is equal to the number of stages $(n-m)$. It is possible to use the heuristic method with many nodes that have less than $(n-m)$. The suggested approach is based on the idea of initiating a seek operation from the start node to find the nodes that are closest to the start node and are in stage 1 of the search process. In this phase, any further search operations should begin from each node in order to discover the quickest route to the destination using a brand-new heuristic approach, which is implemented in a brand-new heuristic method, starting from each node in the previous step. Using a mathematical formula, the distance between each node in stage 1 and the target node in the second stage is calculated. While these calculations are taking place, the hints are keeping track of which nodes are on which routes. The shortest distance between two points is calculated, as is the position of the pointer. In this case, the shortest path to the destination node is the one that has the least distance; thus, the route with the shortest distance is chosen. The new heuristic technique is implemented as part of a suggested set of recommendations, which includes other heuristic methods.

The accessibility of glioma cells to their surrounding environment is shown in **Figure 3**. According to the diagram, tumor cells are progressively penetrated until they reach a level of vulnerability, which is apparent from the convergence of points A, B, C, and D. Once they reach this state of vulnerability, the tumor cells are destroyed. In **Figure 4**, the development of neomusculature can be appreciated with the use of swarm robots. The convergence of points A, C, and D shows that evolution is only moving in one direction and accelerating at a specific area inside these cells. A swarm of robots perform the bifurcation process as shown in **Figure 5**. The diagram shows that this process is both, resilient and effective in the case of tumor cell development, as shown by the close convergence of points A, C, and D.

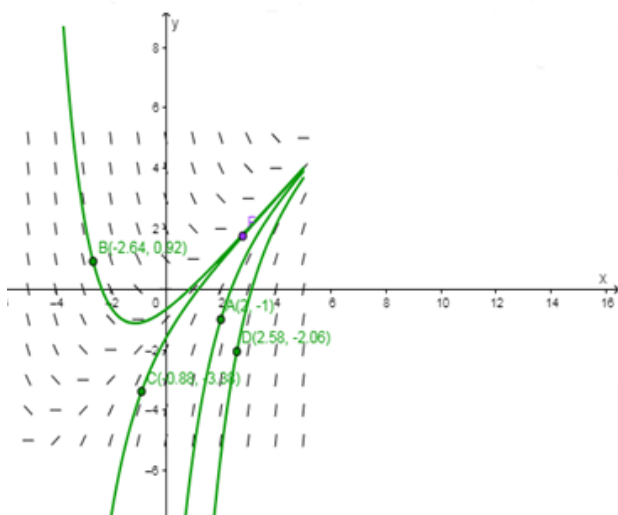


Figure 3. Accessibility of the dissemination of glioma cells

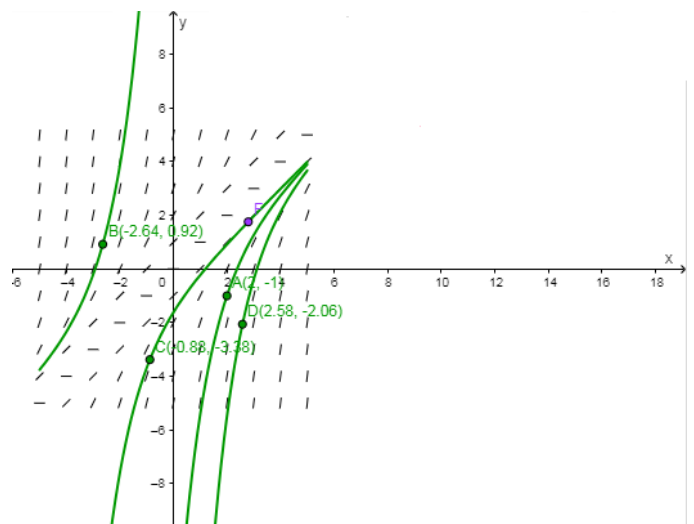


Figure 4. Evolving neomusculature using swarm robots

As demonstrated in **Figure 6**, the rate of cell development is increasing. Based on the diagram, tumor cell proliferation is progressing, but not in a random way; it may be described as a regular growth, as shown by the consistent distances between points A, C, and D. In conducting an examination of the proposed

method, superellipsoids are utilized in this research. This is accomplished by measuring the distance between two superellipsoids in a variety of unique cases.

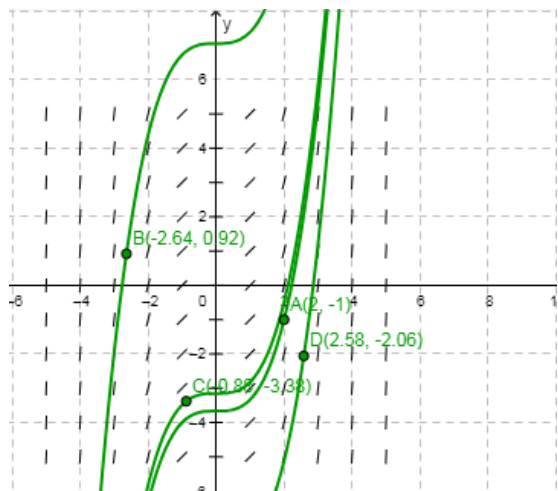


Figure 5. Bifurcation equation using swarm robots

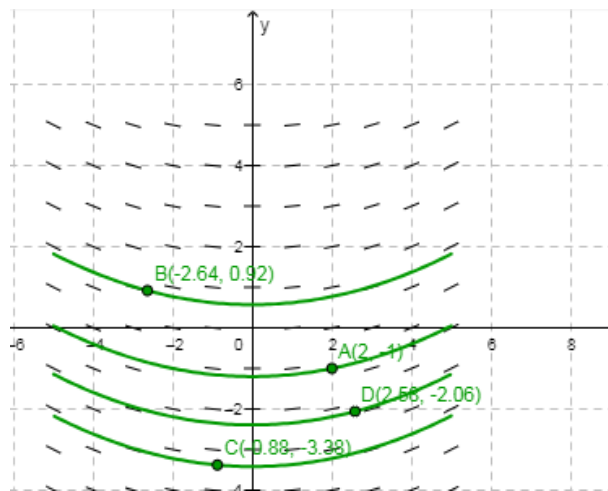


Figure 6. Growth rate of cells

This section includes several case studies, which are denoted by the Roman numerals I to VIII. Taking Case Study I as a reference point, the shortest distance between the two sites is 0.128959 nm, as shown in **Figure 7**. **Figure 8** is an illustration of Case Study II, in which there is a minimum distance of 6.338194 meters between the two sites. **Figure 9** is an illustration of Case Study III with a minimum distance of 3.169937 nm between the two sites. **Figure 10** depicts Case Study IV, which has a minimum distance of 2.490361 nm between the two points in the center of the two-point line.

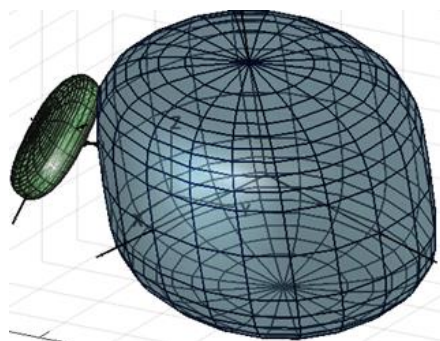


Figure 7. Case Study I (minimum distance 0.128959 nm)

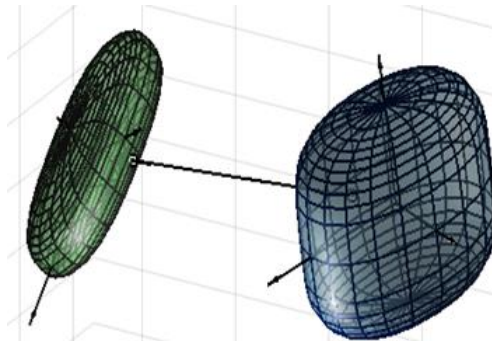


Figure 8. Case Study II (minimum distance 6.338194 nm)

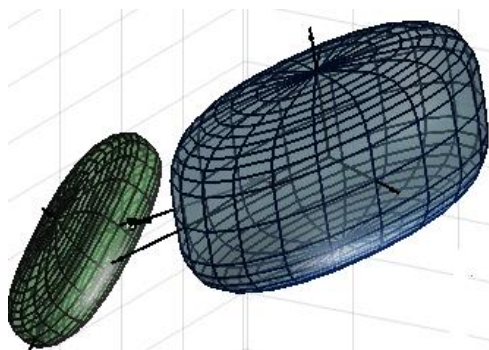


Figure 9. Case Study III (minimum distance 3.169937 nm)

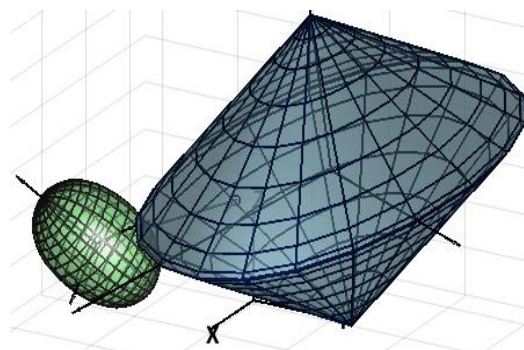


Figure 10. Case Study IV (minimum distance 2.490361 nm)

Figure 11 is an illustration of Case Study V, which has a minimum distance of 1.704994 nm between the two sites. The findings of Case Study VI, which was carried out at a minimum distance of 7.932791 nm and yielded the following results, are shown in **Figure 12**. Case study VII is shown in **Figure 13** with a minimum distance of 1.193461 nm between the two sites, which is the shortest distance feasible. **Figure 14** depicts Case Study VIII, with a minimum distance of 1.464478 nm between the two points. Taking all case studies into consideration, the shortest distance between various characteristic distributions can be estimated based on their shifting locations using the suggested approach.

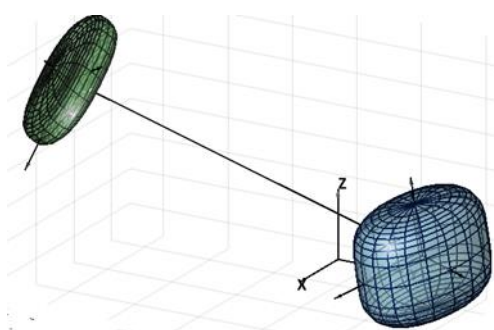


Figure 11. Case study V (minimum distance 1.704994 nm)

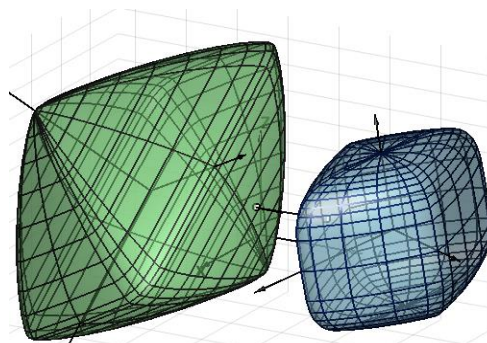


Figure 12. Case study VI (minimum distance 7.932791 nm)

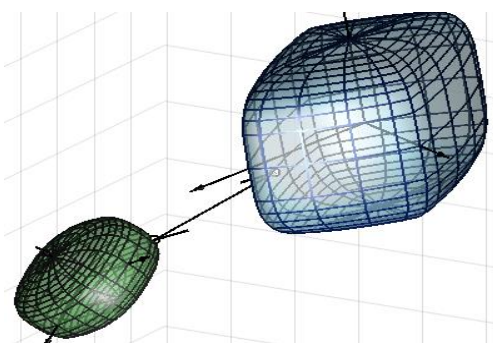


Figure 13. Case Study VII (minimum distance 1.193461 nm)

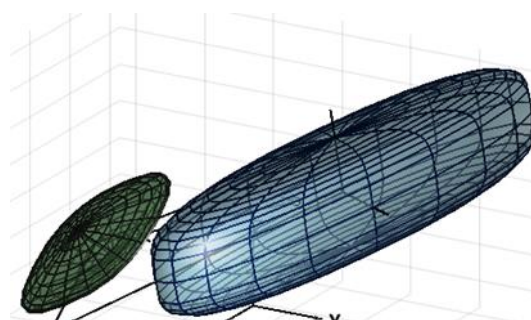


Figure 14. Case Study VIII (minimum distance 1.464478 nm)

5. Conclusion

A brain tumor is a collection, or mass, of abnormal cells in the brain. The skull, which encloses the brain, is very rigid. Any growth inside such a confined space can cause a problem. Brain tumors may be cancerous or non-cancerous. The purpose of this research is to analyze the performance of brain tumors by simulating tumor performance through the motion of swarm robots. The KCIP algorithm, a new logarithm, is proposed by combining the properties of both, the kill chain and the interior point algorithm. This algorithm measures the shortest distance between two robots and then destroys the cancer cells, which are represented by one of these robots. The results have shown how the tumor enters these cells, showing that it does so gradually until the cells reach a stage where they are vulnerable to invasion. The evolving process accelerates at a specific part of these cells, and evolution continues in one direction only. Swarm robots are used in the bifurcation process. In the case of tumor cell proliferation, this process is effective and robust. The tumor cell proliferation process gradually increases but not in a random manner; it may be described as a consistent increase, which is evident from the regular distances.

Disclosure statement

The authors declare no conflict of interest.

References

- [1] Chiavazza C, Franchino F, Ruda R, 2019, Clinical Concepts of Brain Tumors, in *Neurorehabilitation in Neuro-Oncology*, Springer, Cham, 37–51.
- [2] Hou X, Yang D, Li D, et al., 2020, A New Simple Brain Segmentation Method for Extracerebral Intracranial Tumors. *PLoS ONE*, 15(4): e0230754.
- [3] Datta M, Nia HT, Seano G, et al., 2020, TMOD-37. In Vivo Compression and Imaging for Causal Studies of Mechanical Forces in the Brain. *Neuro Oncology*, 22(Suppl 2): ii235–ii236.
- [4] Li M, Shang Z, Dong Y, et al., 2017, Proceeding of the 2017 39th Annual International Conference of the IEEE Engineering in Medicine and Biology Society (EMBC), July 11-15, 2017: Application of MRI Texture Analysis in the Study of the Posterior Fossa Tumors Growing Trend in Children. *IEEE*, Jeju, Korea (South), 620–623.
- [5] Beda MM, Barjaktarovic M, 2020, Classification of Brain Tumors from MRI Images Using a Convolutional Neural Network. *Applied Sciences*, 10(6): 1999.
- [6] Nalepa J, Lorenzo PR, Marcinkiewicz M, et al., 2020, Fully-Automated Deep Learning-Powered System for DCE-MRI Analysis of Brain Tumors. *Artificial Intelligence in Medicine*, 102: 101769.
- [7] Chen C, Ou X, Wang J, et al., 2019, Radiomics-Based Machine Learning in Differentiation Between Glioblastoma and Metastatic Brain Tumors. *Frontiers in Oncology*, 9: 806.
- [8] Badran EF, Mahmoud EG, Hamdy N, 2010, Proceedings of the 2010 International Conference on Computer Engineering & Systems, April 16-18, 2010: An Algorithm for Detecting Brain Tumors in MRI Images. *IEEE*, Chengdu, China, 368–373.
- [9] Narmatha C, Eljack SM, Tuka A, et al., 2020, A Hybrid Fuzzy Brain-Storm Optimization Algorithm for the Classification of Brain Tumor MRI Images. *Journal of Ambient Intelligence and Humanized Computing*, 2020: 1–9.
- [10] Sachdeva J, Kumar V, Gupta I, et al., 2016, A Package-SFERCB-“Segmentation, Feature Extraction, Reduction and Classification Analysis by Both SVM and ANN for Brain Tumors”. *Appl Soft Comput*, 47: 151–167.
- [11] Das A, Bhattacharya M, 2009, Proceedings of the 2009 International Joint Conference on Bioinformatics, Systems Biology and Intelligent Computing, August 3-5, 2009: A Study on Prognosis of Brain Tumors Using Fuzzy Logic and Genetic Algorithm Based Techniques. *IEEE*, Shanghai, 348–351.
- [12] Abdurraqeb A, Al-Haidri W, Sushkova LT, et al., 2017, An Automated Method for Segmenting Brain Tumors on MRI Images. *Biomedical Engineering*, 51: 97–101.
- [13] Kim J, Lee S, Lee G, et al., 2016, Using a Method Based on a Modified K-Means Clustering and Mean Shift Segmentation to Reduce File Sizes and Detect Brain Tumors from Magnetic Resonance (MRI) Images. *Wireless Personal Communications*, 89(3): 993–1008.
- [14] Hussain S, Anwar SM, Majid M, 2018, Segmentation of Glioma Tumors in Brain Using Deep Convolutional Neural Network. *Neurocomputing*, arXiv:1708.00377. <https://doi.org/10.48550/arXiv.1708.00377>
- [15] Alagarsamy S, Kamatchi K, Govindaraj V, et al., 2019, Multi-channelled MR Brain Image Segmentation: A New Automated Approach Combining BAT and Clustering Technique for Better Identification of Heterogeneous Tumors. *Biocybernetics and Biomedical Engineering*, 39(4): 1005–1035.

- [16] Alam MS, Rahman MM, Hossain MA, et al., 2019, Automatic Human Brain Tumor Detection in MRI Image Using Template-Based K Means and Improved Fuzzy C Means Clustering Algorithm. *Big Data Cogn Comput*, 3(2): 27.

Publisher's note

Bio-Byword Scientific Publishing remains neutral with regard to jurisdictional claims in published maps and institutional affiliations.

Using Pegaspargase in Combination with Chemotherapy in the Treatment of Lymphoma

Yudi Miao*

Department of Hematology, Shaanxi Provincial People's Hospital, Xi'an 710068, Shaanxi Province, China

*Corresponding author: Yudi Miao, miaoyudi26@163.com

Copyright: © 2022 Author(s). This is an open-access article distributed under the terms of the Creative Commons Attribution License (CC BY 4.0), permitting distribution and reproduction in any medium, provided the original work is cited.

Abstract: *Objective:* To analyze the clinical effect of pegaspargase combined with chemotherapy on patients with lymphoma. *Methods:* Seventy patients with lymphoma admitted to Shaanxi Provincial People's Hospital between December 2020 and June 2021 were selected as study subjects and were equally divided into the control group and the intervention group using the lottery method, with 35 cases in each group; the control group received conventional treatment, while the intervention group received pegaspargase combined with chemotherapy. The treatment satisfaction, quality of life, psychological status, and incidence of adverse reactions of the patients in the two groups were compared. *Results:* The differences in the indicators between the two groups were statistically significant ($p < 0.05$). *Conclusion:* Pegaspargase combined with chemotherapy can effectively improve the treatment effect and satisfaction of lymphoma patients; hence, it is worthy of promotion in clinical treatment.

Keywords: Pegaspargase combined with chemotherapy; Conventional treatment; Lymphoma

Online publication: July 27, 2022

1. Case study

Lymphoma is a malignant tumor originating from the lymphatic system. Lymphomas can be grouped into Hodgkin's lymphoma or non-Hodgkin's lymphoma. Clinically, painless enlargement of lymph nodes is the main feature, and examination would reveal liver and spleen enlargement, along with symptoms of fever and anemia in the late stage. Chemotherapy is the mainstay of treatment in lymphoma, and it can cure lymphoma in some patients [1-4]. Several studies have shown that the use of pegaspargase in combination with chemotherapy is clinically effective in the treatment of lymphoma [5-8]. In this study, 70 patients with lymphoma admitted to Shaanxi Provincial People's Hospital between December 2020 and June 2021 were used as study subjects. The main objective of the study was to investigate the treatment effect of pegaspargase combined with chemotherapy on patients with lymphoma.

2. Materials and methods

2.1. General information

Seventy patients with lymphoma admitted to Shaanxi Provincial People's Hospital between December 2020 and June 2021 were selected as study subjects and divided into two groups using the lottery method. Thirty-five patients in the control group were treated with conventional treatment, while the other 35 patients in the intervention group were treated with pegaspargase in combination with chemotherapy. There were 19 male patients and 16 female patients in the control group, age ranging from 46 to 78, with a mean age of 58.85 ± 1.84 . In the intervention group, the patients aged 48 to 76, with a mean age of 59.65 ± 1.93 ,

of whom 20 were male and 15 were female. The differences in the general information, including age and gender, between the two groups were not statistically significant ($p > 0.05$) and were comparable. This study was approved by the Ethics Committee of Shaanxi Provincial People's Hospital, and the patients and their families were informed of the study and signed the informed consent form.

2.2. Methods

Both groups were treated with oxaliplatin (Qilu Pharmaceutical [Hainan] Co., Ltd., Guodianshi H20093168) at a dose of 130 mg/m² in 250–500 ml 5% glucose solution for 2–6 hours; gemcitabine (Jiangsu Haosen Pharmaceutical Group Co., Ltd., Guodianshi H20030104) at a dose of 1000 mg/m² intravenously once a week for three weeks, followed by a one-week break, and repeated every four weeks; dexamethasone (Guangdong Nanguo Pharmaceutical Co., Ltd., GMP H44024618) at a dose of 0.75–3.00 mg (1–4 tablets) once for adults, two to four times a day.

- (1) In the control group, L-asparaginase for injection (Kyowa Hakko Kogyo Co., Ltd., H20090520) was administered intravenously at a dose of 50-200 KU per kg body weight on 1 day or every other day. It was increased or decreased as appropriate for age and systemic status.
- (2) The intervention group was treated with pemesterase in combination with chemotherapy: pemesterase (Jiangsu Hengrui Pharmaceutical Co., Ltd., H20153215) 2500 IU/m², administered intramuscularly every 14 days.

2.3. Observed indicators

- (1) The patients were surveyed using a self-made satisfaction questionnaire with a total score of 100, with very satisfied being 80-100, satisfied being 60-79, and unsatisfied being 59 or less; satisfaction = (very satisfied + satisfied)/total*%.
- (2) The Self-Rating Depression Scale (SDS) was used to rate the depression of the two groups, with 20 items in total, 4 points each, and a cut-off score of 53. The Self-Rating Anxiety Scale (SAS) was used to rate the anxiety of patients, with 20 items in total, 4 points each, and a cut-off score of 50, above which anxiety was indicated; the lower the score, the better a patient's psychological state.
- (3) The Generic Quality of Life Inventory-74 (GQOL-74) was used to assess the quality of life of both groups, including physical, psychological, somatic, and social aspects; the total scores were compared.
- (4) The incidence of adverse reactions, including hyperglycemia, gastrointestinal reactions, and granulocytopenia, was compared between the two groups.

2.4. Statistical analysis

SPSS 20.0 was used to process the data; t-test was performed on the data obtained and expressed as *s*, while X² test was performed on the count data and expressed as %. $p < 0.05$ was considered statistically significant.

3. Results

3.1. Patient satisfaction

The difference in patient satisfaction between the intervention and control groups was statistically significant ($p < 0.5$), as shown in **Table 1**.

Table 1. Comparison of patient satisfaction between the two groups (n/%)

Group	Number of cases	Very satisfied	Satisfied	Unsatisfied	Satisfaction
Intervention group	35	34 (97.14)	0 (0.00)	1 (2.86)	34 (97.14)
Control group	35	21 (60.00)	7 (20.00)	7 (20.00)	28 (80.00)
X ²					5.0806
<i>p</i>					0.0242

3.2. Mental state

There was no significant difference in the SAS and SDS scores between the two groups before treatment ($p > 0.05$), and they both improved significantly after treatment ($p < 0.05$). The data comparison between the two groups showed that the SAS and SDS scores of patients in the intervention group were significantly lower than those in the control group ($p < 0.05$), and the difference between the groups was statistically significant (**Table 2**).

Table 2. Comparison of SAS and SDS scores before and after treatment (n = 35, ± s)

Group	Number of cases	SAS		SDS	
		Pre-treatment	Post-treatment	Pre-treatment	Post-treatment
Control group	35	50.55 ± 2.26	43.63 ± 0.57	49.35 ± 2.65	42.26 ± 0.03
Intervention group	35	50.35 ± 1.58	30.42 ± 0.18	49.35 ± 2.52	33.67 ± 0.53
t		0.4291	130.7436	0.0000	95.7319
p		0.6692	0.0000	1.0000	0.0000

3.3. Quality of life

Before treatment, there was no significant difference in the physical, psychological, somatic, and social scores between the two groups ($p > 0.05$); however, after treatment, the physical, psychological, somatic, and social scores of the patients in the intervention group were significantly higher than those of the control group ($p < 0.05$), and the difference was statistically significant (**Table 3**).

Table 3. Comparison of quality-of-life scores before and after treatment (n = 35, ± s)

Group	Number of cases	Physical life		Somatic functions	
		Pre-treatment	Post-treatment	Pre-treatment	Post-treatment
Control group	35	83.55 ± 2.26	87.63 ± 2.57	81.35 ± 3.65	86.26 ± 3.03
Intervention group	35	83.35 ± 2.58	90.42 ± 2.18	80.35 ± 2.52	91.67 ± 2.53
t		0.3450	4.8978	1.3338	8.1082
p		0.7312	0.0000	0.1867	0.0000

Group	Number of cases	Social functions		Psychological functions	
		Pre-treatment	Post-treatment	Pre-treatment	Post-treatment
Control group	35	80.55 ± 3.26	87.63 ± 2.57	79.35 ± 2.65	86.26 ± 2.03
Intervention group	35	81.35 ± 2.58	91.42 ± 2.18	80.35 ± 3.52	91.67 ± 2.53
t		1.1384	6.6533	1.3427	9.8670
p		0.2589	0.0000	0.1838	0.0000

3.4. Incidence of adverse reactions

The incidence of hyperglycemia, gastrointestinal reactions, and granulocytopenia was significantly lower in the intervention group than in the control group ($p < 0.05$), as shown in **Table 4**.

Table 4. Comparison of adverse reactions in the two groups (n, %)

Group	Number of cases	Hyperglycemia	Gastrointestinal reactions	Granulocytopenia	Incidence rate
Intervention group	35	1	0	0	1 (2.86)
Control group	35	3	1	2	6 (17.14)
X^2					3.9683
p					0.0464

4. Discussion

Lymphoma can be caused by a number of factors. Most patients are affected by viral infections, mainly related to EBV infection, which is one of the main causes of Hodgkin's lymphoma [9-14]; others are affected by retroviral infections, which can cause lymphoma as well as t-cell leukemia. There is also a strong relationship between lymphoma and individual immune factors, with a higher incidence of disease in cases of immune deficiencies [15,16]. The systemic symptoms of malignant lymphoma vary widely depending on the type of disease and the time of onset. Some patients may have no systemic symptoms [17-19]. Fever, weight loss (more than 10% weight loss), and night sweats are the most common symptoms, followed by loss of appetite, fatigue, and pruritus. Systemic symptoms are related to age of onset, extent of the tumor, and the body's immunity. Systemic symptoms are significant in elderly patients, those who are immunocompromised, or patients with multiple focal attacks [20]. The survival rate of patients without systemic symptoms is three times higher than that of patients with symptoms. In terms of management, surgery is superior to conventional chemotherapy, as the latter has significant side effects and can be very disruptive or damaging. In the current study, pegaspargase combined with chemotherapy was found effective in treating lymphoma.

In conclusion, by using pegaspargase combined with chemotherapy for lymphoma patients, it can effectively improve the treatment effect and psychological state of patients; thus, it is worthy of promotion in clinical practice.

Disclosure statement

The authors declare no conflict of interest.

References

- [1] Liu CC, Zhang JY, Xiong CL, et al., 2020, Effect of Pemesterase on Coagulation Function and Relapse Rate in Patients with Lymphoma. *Laboratory Medicine and Clinics*, 17(14): 2075–2077.
- [2] Zu L, Zhou J, Zhang GL, et al., 2020, Three Cases of Relapsed/Refractory T-Cell Lymphoma/Leukemia Treated with Decitabine in Combination with Chemotherapy and Review of the Literature. *Journal of Clinical Hematology*, 33(3): 211–214.
- [3] Lu B, 2021, Effectiveness of Dasatinib Combined with Pemantase Chemotherapy Regimen in the Treatment of Patients with Ph-Positive Acute Lymphoblastic Leukemia. *Chinese and Foreign Medical Research*, 19(25): 138–140.
- [4] Yang J, Yan H, Chai L, et al., 2020, Effect of SMILE Regimen on Coagulation Function in Patients with NK/T-Cell Lymphoma. *China Drugs and Clinics*, 20(23): 3931–3933.
- [5] Hu L, Xia M, Li GQ, et al., 2020, Clinical Observation of P-GEMOX Regimen for the First-Line Treatment of Primary Extranasal NK/T-Cell Lymphoma. *Leukemia & Lymphoma*, 29(3): 160–164.

- [6] Chen X, Chen X, Xu G, 2020, Nursing Experience of Sindilizumab Combined with Pemantase, Anrotinib in the Treatment of Primary NK/T-Cell Lymphoma. *Chinese and Western Medicine Nursing*, 6(10): 285–287.
- [7] Han X, 2021, Evaluation of Pemesterase Combined with GEMOX Chemotherapy Regimen in the Treatment of NK/T-Cell Lymphoma. *Contemporary Medicine Series*, 19(17): 69–71.
- [8] Xia C, 2020, Impact of Remission Status After Induction Chemotherapy for Early-Stage Nasal NK/T-Cell Lymphoma on Survival with Combination Therapy. *South China University*.
- [9] Wang S, Pan X, Qi Y, 2020, Meta-Analysis of Pepmonidase and Levomuroidase in the Treatment of Acute Lymphoblastic Leukemia in Chinese Children. *Journal of Shenyang Medical College*, 22(3): 251–255.
- [10] Zhang J, 2021, Analysis of the Effect of Pemesterase Injection on the Chemotherapeutic Effect of NKT Lymphoma. *Clinical Research*, 29(3): 78–79.
- [11] Zhang Z, 2021, Efficacy and Safety Analysis of Pemantase in the Treatment of Extranodal NK/T-Cell Lymphoma. *Chinese Community Physicians*, 37(24): 59–60.
- [12] Sun Y, Lou ZS, 2020, Meta-Analysis of Pemesterase in the Treatment of Extranodal NK/T-Cell Lymphoma. *Journal of Mudanjiang Medical College*, 41(3): 59–65.
- [13] Wang J, Huang G, Cui K, 2020, Effect of Pemesterase on Lipid Levels in Patients with Extranodal NK/T-Cell Lymphoma. *Shaanxi Medical Journal*, 49(4): 481–484.
- [14] Wei Q, Zhang Y, Wang W, et al., 2021, Clinical Characteristics of Patients with Single-Center Extranodal NK/T-Cell Lymphoma and Prognosis Analysis Based on Pemesterase Chemotherapy. *Chinese Journal of Experimental Hematology*, 29(3): 735–740.
- [15] Zhang G, Liu Y, Zhang Y, 2013, The Effect of Pegaspargase on Coagulation Function in Patients with Lymphoma. *China Journal of New Drugs*, 22(19): 2281–2285.
- [16] Lai WP, Zheng RH, Qin PF, et al., 2021, Efficacy of Cetapenem Combined with Chemotherapy in the Treatment of Peripheral T-Cell Lymphoma. *China Practical Medicine*, 16(19): 25–27.
- [17] Liang S, Wen F, 2020, New Advances in the Treatment of Acute Lymphoblastic Leukemia in Children with Silent Inactivation of Pemesterase. *International Journal of Blood Transfusion and Hematology*, 43(5): 418–422.
- [18] Zhou R, Liu W, 2021, Safety Analysis and Management Measures of Pemesterase in the Treatment of Lymphatic System Tumors. *China Prescription Drugs*, 19(8): 90–91.
- [19] Liu YB, Yuan XL, Ma RJ, et al., 2021, Efficacy and Safety of Programmed Death Receptor 1 Inhibitor in Combination with Chemotherapy for Primary Stage III/IV Extranodal NK/T-Cell Lymphoma. *Chinese Medical Journal*, 101(16): 1178–1181.
- [20] He Y, Zhang L, Yu X, et al., 2020, Effectiveness of PEG-ASP Combined with CHOP Regimen Chemotherapy and Sequential Radiotherapy in the Treatment of Stage I-II Nasal NK/T-Cell Lymphoma. *The Great Physician*, 5(1): 23–25.

Publisher's note

Bio-Byword Scientific Publishing remains neutral with regard to jurisdictional claims in published maps and institutional affiliations.

A Discussion on TCM Treatment and the Pathogenesis of Membranous Nephropathy in Primary Nephrotic Syndrome

Xin Li¹, Genping Lei^{2*}

¹Shaanxi University of Traditional Chinese Medicine, Xianyang 712046, Shaanxi Province, China

²Affiliated Hospital of Shaanxi University of Traditional Chinese Medicine, Xianyang 712000, Shaanxi Province, China

*Corresponding author: Genping Lei, 993117092@qq.com

Copyright: © 2022 Author(s). This is an open-access article distributed under the terms of the Creative Commons Attribution License (CC BY 4.0), permitting distribution and reproduction in any medium, provided the original work is cited.

Abstract: *Objective:* To investigate the TCM treatment principle of membranous nephropathy and its effect. *Methods:* A total of 56 patients were selected from the Affiliated Hospital of Shaanxi University of Traditional Chinese Medicine. They were then divided into the control group (western medicine standard therapy) and the study group (Qidi Gushen prescription), with 28 patients in each group. The treatment effect, treatment safety, and patients' satisfaction were observed and compared between the two groups. *Results:* The results showed that the treatment effect of the study group was 96.43%, which was significantly better compared with the control group (75.00%) ($p < 0.05$); in terms of safety, the probability of adverse events was 7.14% in the study group and 32.14% in the control group, in which the difference was statistically significant ($p < 0.05$); in addition, the study group's satisfaction with the treatment measures was significantly higher than that of the control group ($p < 0.05$). *Conclusion:* In treating membranous nephropathy, traditional Chinese medicine can be tailored to its pathogenesis, which is not only beneficial to the treatment effect, but also has a high safety profile.

Keywords: Primary nephrotic syndrome; Membranous nephropathy; Traditional Chinese medicine; Qidi Gushen prescription; Pathogenesis

Online publication: July 27, 2022

1. Introduction

Membranous nephropathy (MN) is a glomerular disease in which immune complexes are deposited beneath the epithelial cells of the diffusely-thickened glomerular basement membrane (GBM) [1]. Several studies have pointed out that MN is a common cause of primary nephrotic syndrome. Its clinical manifestations are proteinuria and edema [2], and its location is mainly in the kidneys, spleen, and lungs. At present, the treatment for MN is mainly based on hormones and immunosuppressants in western medicine, but there are many side effects, which will cause various complications, such as increased risk of infection, immune tolerance, and thromboembolism, which have certain impact on the quality of life of patients and their prognosis [3]. Lei Genping, a chief physician, has been engaged in the clinical work of kidney disease for a long time. He came to realize that the pathogenesis of MN is a combination of deficiency and excess, in which the deficiency lies in the spleen and kidney, where water dampness, damp heat, and blood stasis coexist. Based on this, he established six methods in the treatment of MN, which include cultivating, tonifying, consolidating, promoting, clearing, and dredging, as well as developed Qidi Gushen prescription, which has a significant effect in improving the clinical symptoms of patients with MN and reducing

proteinuria [4]. Since proteinuria is not addressed in traditional Chinese medicine, it belongs to Jingwei substance. It is clear that the majority of patients have insufficient kidney essence, causing a loss in its sealing function. Patients present with symptoms of deficiency and excess. Clinical treatment can benefit the liver and kidney, Qi and blood circulation, as well as dredge the meridians [5]. In this study, 56 patients with membranous nephropathy were recruited as research subjects, in order to investigate the clinical efficacy, adverse reactions, and their satisfaction with different interventions [6].

2. Clinical data and methods

2.1. Clinical data

The subjects were selected from 56 patients with primary membranous nephropathy and divided into two groups (control group and study group), with 28 patients in each group. The basic information of the subjects is shown in **Table 1**.

Table 1. Data comparison among subjects

Group	Number of patients	Average age (years)	Gender	
			Male	Female
Control group	28	40.30 ± 4.12	18	10
Study group	28	40.57 ± 4.01	15	13
<i>p</i>	-	> 0.05	> 0.05	

2.2. Intervention

2.2.1. Control group

Conventional western medicine methods were used to diagnose the disease and treat the patients according to the degree of illness. The treatment measures included reducing sodium intake, controlling protein and calorie intake, consuming detumescence and diuretic drugs, as well as using glucocorticoids and cytotoxic drugs to inhibit immune response [7].

2.2.2. Study group

Traditional Chinese medicine treatment methods were used for the patients in the study group.

(1) Identifying the basic symptoms

According to traditional Chinese medicine theory, the pathogenesis of membranous nephropathy involves the loss of kidney essence, water dampness, blood stasis, and damp heat. The clinical symptoms of the patients were mainly proteinuria and edema.

(2) Qidi Gushen prescription

The methods of tonifying the kidney and spleen, removing blood stasis and swelling, as well as removing dampness and heat were used [8]. Qidi Gushen prescription, which consists of *Astragalus membranaceus*, *Radix rehmanniae*, *Euryale ferox*, *Hedyotis diffusa*, *Schizonepeta tenuifolia*, *Salvia miltiorrhiza*, and other components, were used in this study. Based on the severity of edema, plantain seeds and *Alisma orientalis* were added, accordingly; with proteinuria, cicada slough, perilla, *Ligusticum chuanxiong*, earthworm, and other components were added; in treating damp heat, *Poria cocos* and *Hedyotis diffusa* were added, accordingly; with severe blood stasis, *Angelica sinensis*, *Salvia miltiorrhiza*, red peony root, and motherwort were added to promote blood circulation and remove blood stasis [9]. Water was used for decoction and to remove residues. One dose was divided into three times, and the patients were required to take one dose a day with warm water. The course of the treatment was

one month.

2.3. Observation indicators

The treatment effect, treatment safety, and patients' satisfaction were compared between the two groups.

3. Results

3.1. Treatment effect

According to the research results, the treatment effect of the patients in the study group was 96.43%, which was significantly superior to that of the patients in the reference group (75.00%) ($p < 0.05$), as shown in **Table 2**.

Table 2. Comparison of the treatment effect between the two groups

Group	Number of patients	Very effective	Effective	Ineffective	Effective rate (%)
Control group	28	7	14	7	75.00
Study group	28	15	12	1	96.43
<i>p</i>	-	-	-	-	< 0.05

3.2. Treatment safety

In terms of safety, the probability of adverse events in the study group was 7.14%, while that in the reference group was as high as 32.14%. There was significant difference between the two groups ($p < 0.05$), as shown in **Table 3**.

Table 3. Comparison of the treatment safety between the two groups

Group	Number of patients	Infection	Fever	Nausea and vomiting	Dizziness	Incidence (%)
Control group	28	3	4	1	1	32.14%
Study group	28	0	1	0	1	7.14%
<i>p</i>	-	-	-	-	-	< 0.05

3.3. Patients' satisfaction

In addition, the study group's satisfaction with the intervention was significantly higher than that of the control group ($p < 0.05$), as shown in **Table 4**.

Table 4. Comparison of patients' satisfaction between the two groups

Group	Number of patients	Very satisfied	Satisfied	Dissatisfied	Satisfaction (%)
Control group	28	6	16	6	78.57%
Study group	28	14	12	2	92.86%
<i>p</i>	-	-	-	-	< 0.05

4. Discussion

Membranous nephropathy is an autoimmune glomerular disease that is commonly diagnosed in clinical settings. Patients usually present with edema, hypertension, hematuria, proteinuria, and other symptoms. This disease often affects people aged 40 to 60 [10]. According to research, one of the main pathogenic factors of membranous nephropathy is the deposition of immune complexes on the glomerular epithelial

side, resulting in podocyte damage, a decrease in glomerular filtration rate, and a series of adverse reactions, which seriously affect the quality of life of patients ^[11]. Immunosuppressive therapy or hormonal therapy is often used in western medicine to treat these patients, but the clinical efficacy is debatable due to the influence of various factors, such as the severity of patients' condition and tolerance, and the majority of them will develop adverse effects, resulting in a decline in prognosis and the quality of life of patients.

With the continuous improvement of China's comprehensive national strength, traditional Chinese medicine, as a unique way of curing diseases and saving people, has gained wide recognition. In TCM, syndrome differentiation and treatment are taken as the core, the pathogeneses of diseases are explored through investigations, and medications are prescribed to eliminate diseases ^[12]. Membranous nephropathy belongs to urine turbidity and edema in traditional Chinese medicine. It is primarily caused by kidney and spleen deficiencies. Its treatment is based on tonifying the kidney and strengthening the spleen, clearing away heat and dampness, as well as supplementing qi and activating blood circulation. Qidi Gushen prescription is used for addition and subtraction, and its treatment effect has been found significant ^[13]. Based on the theory of traditional Chinese medicine, the use of conventional western medicine generates heat internally and aggravates the damp heat symptoms of membranous nephropathy, which will further escalate the pathogenesis of membranous nephropathy; thus, it is not conducive to the treatment of the disease. According to traditional Chinese medicine, most patients with membranous nephropathy have coated red tongue, along with symptoms of dry mouth and extreme thirst, burning sensation in the chest, palms, and soles, as well as "limp aching lumbus and knees." However, the fine substances in the body with high demand are 8:30. Once patients have proteinuria, their albumin levels will decrease, resulting in symptoms of spleen deficiency ^[14]. In the treatment of membranous nephropathy, traditional Chinese medicine emphasizes on the principles of diuresis, clearing of heat, removing blood stasis, activating blood circulation, relaxing meridians, and dredging collaterals. In Qidi Gushen prescription, *Astragalus membranaceus* has the effects of consolidating the exterior, supplementing qi, diuresis, and detoxification; *Qidi* has the functions of nourishing yin, generating body fluid, cooling the blood, and clearing away heat; *Euryale ferox* has the functions of supplementing the exterior, qi, kidney, spleen, and dampness; *Hedyotis diffusa* may help in diuresis, dehumidification, detoxification, and heat clearing; *Schizonepeta tenuifolia* may help in "dispersing cold," activating blood circulation, cooling blood, clearing heat, expelling wind, and dehumidification; *Salvia miltiorrhiza* may help in cooling blood, calming nerves, dredging meridians, promoting blood circulation, and removing blood stasis. A multidrug combination can nourish the liver and kidney, strengthen the exterior and spleen, replenish qi, as well as activate blood circulation. Modern pharmacology asserts that the aforementioned prescription can effectively improve proteinuria, inhibit abnormal immune responses, eliminate inflammatory reactions, improve the treatment effect, and enhance the quality of life of patients ^[15].

In conclusion, in treating membranous nephropathy, TCM treatment can be tailored to its pathogenesis to fully ensure the safety of treatment, promote clinical efficacy, and ensure the prognosis and quality of life of patients.

Disclosure statement

The authors declare no conflict of interest.

References

- [1] Qin C, 2018, Discussion on TCM Treatment and Pathogenesis of Membranous Nephropathy in Primary Nephrotic Syndrome. *Special Health*, 2018(22): 45.

- [2] Lei G, 2016, Discussion on TCM Pathogenesis and Treatment of Membranous Nephropathy in Primary Nephrotic Syndrome. *Chinese Journal of Integrated Traditional and Western Medicine Nephropathy*, 17(5): 443–445.
- [3] Pan Q, Ye Z, Zeng C, et al., 2020, Comparison of Clinical Characteristics Between Idiopathic Membranous Nephropathy and Four Common Nephropathy. *Chinese Journal of Clinical New Medicine*, 13(4): 4.
- [4] Gao Y, Cai C, Wang S, 2020, Therapeutic Effect of Yishen Huashi Granule on Nephrotic Syndrome Patients with Idiopathic Membranous Nephropathy. *Heilongjiang Traditional Chinese Medicine*, 2020(3): 33–34.
- [5] Cai X, Zhang X, Zhong Y, et al., 2020, Correlation Between Clinicopathological Features and Renal Function in Patients with Idiopathic Membranous Nephropathy with Nephrotic Syndrome. *Chinese Journal of Integrated Traditional and Western Medicine Nephropathy*, 21(4): 317–320.
- [6] Zheng J, Yang L, Zhang L, et al., 2022, Expert Investigation, Analysis and Discussion on Common TCM Syndrome Types of Primary Membranous Nephropathy. *Introduction to Traditional Chinese Medicine*, 28(2): 113–117.
- [7] Chang M, Zhang Y, 2021, Treatment of Membranous Nephropathy with Traditional Chinese Medicine. *World Journal of Integrated Traditional Chinese and Western Medicine*, 16(6): 1173–1176.
- [8] Pan Y, Wang K, Dai C, et al., 2020, Chenzhiqiang’s Experience in Treating Idiopathic Membranous Nephropathy with Traditional Chinese Medicine. *Chinese Journal of Traditional Chinese Medicine*, 35(7): 3460–3462.
- [9] Li Q, Ren R, Li Z, et al., 2021, Zhaoyuyong’s Experience in Treating Membranous Nephropathy. *Jiangsu Journal of Traditional Chinese Medicine*, 53(8): 20–22.
- [10] Tong M, 2021, Progress in Diagnosis and Treatment of Primary Membranous Nephropathy. *Zhejiang Medical Journal*, 43(4): 352–357.
- [11] Li F, 2021, Comparative Study on Clinical Efficacy of Different Treatment Schemes for Membranous Nephropathy. *Chinese Journal of Nephrology with Integrated Traditional and Western Medicine*, 22(7): 635–637.
- [12] Dong Z, Dai H, Miao W, et al., 2021, Analysis of Clinical Experience in Treating Idiopathic Membranous Nephropathy by Warming Yang and Resolving Exterior Syndrome. *Beijing Traditional Chinese Medicine*, 40(2): 113–116.
- [13] Luan Z, Dai H, Miao W, et al., 2019, Discussion on TCM Pathogenesis and Treatment of Membranous Nephropathy in Primary Nephrotic Syndrome. *Diet Science*, 2019(12): 58.
- [14] Gao H, 2018, Progress in TCM Treatment of Intractable Nephrotic Syndrome. *Health Care Guide*, 000(020): 271.
- [15] Teng J, Huang F, Meng G, 2019, Curative Effect of Traditional Chinese Medicine on Membranous Nephropathy of Primary Nephrotic Syndrome. *China Health Standard Management*, 10(9): 99–101.

Publisher’s note

Bio-Byword Scientific Publishing remains neutral with regard to jurisdictional claims in published maps and institutional affiliations.

A Comprehensive Analysis of a Case of Internal Carotid Artery Stenting

Meng Sun¹, Jun Wang², Yamei Wang^{1*}

¹Affiliated Hospital of Hebei University, Baoding 071000, Hebei Province, China

²College Hospital of Shijiazhuang University, Shijiazhuang 050000, Hebei Province, China

*Corresponding author: Yamei Wang, wym870428@sina.com

Copyright: © 2022 Author(s). This is an open-access article distributed under the terms of the Creative Commons Attribution License (CC BY 4.0), permitting distribution and reproduction in any medium, provided the original work is cited.

Abstract: With the development of science and technology and the continuous progress of interventional equipment, internal carotid artery stenting has become increasingly popular among patients in view of its advantages, which include high efficiency, minimally invasive, and fast postoperative recovery. It has grown importance as a surgical method for the treatment of severe internal carotid artery stenosis. This paper discusses a rare case of severe internal carotid artery stenosis and its management, where various types of pre-dilatation balloons were not able to be positioned in the stenting process. Relevant solutions have also been proposed in hope to provide a more theoretical and practical basis for clinical work.

Keywords: Severe internal carotid artery stenosis; Carotid artery stenting (CAS); Balloon pre-dilatation; Balloon positioning

Online publication: July 28, 2022

1. Case study

Liang XX, a 68-year-old male, was hospitalized on July 17, 2020, at 0905 hour due to dizziness. The patient developed dizziness two months before admission, accompanied by weak limbs, especially the left upper limb, which lasted for about 20 minutes and resolved spontaneously. He visited the outpatient department of the Affiliated Hospital of Hebei University in February 2020. Head and neck computed tomography angiography (CTA) showed severe stenosis at the right proximal internal carotid artery. In February 2020, he was diagnosed with hypertension, and his highest reading ever since being diagnosed was 150/95 mmHg. He has a smoking history of more than 40 years, in which he smokes 20 cigarettes a day.

His diagnoses were as follows: (1) severe stenosis at the right proximal internal carotid artery; (2) stage 2 hypertension (high risk).

His head and neck CTA showed severe stenosis at the right proximal internal carotid artery and severe calcification at the stenotic segment (**Figure 1**).

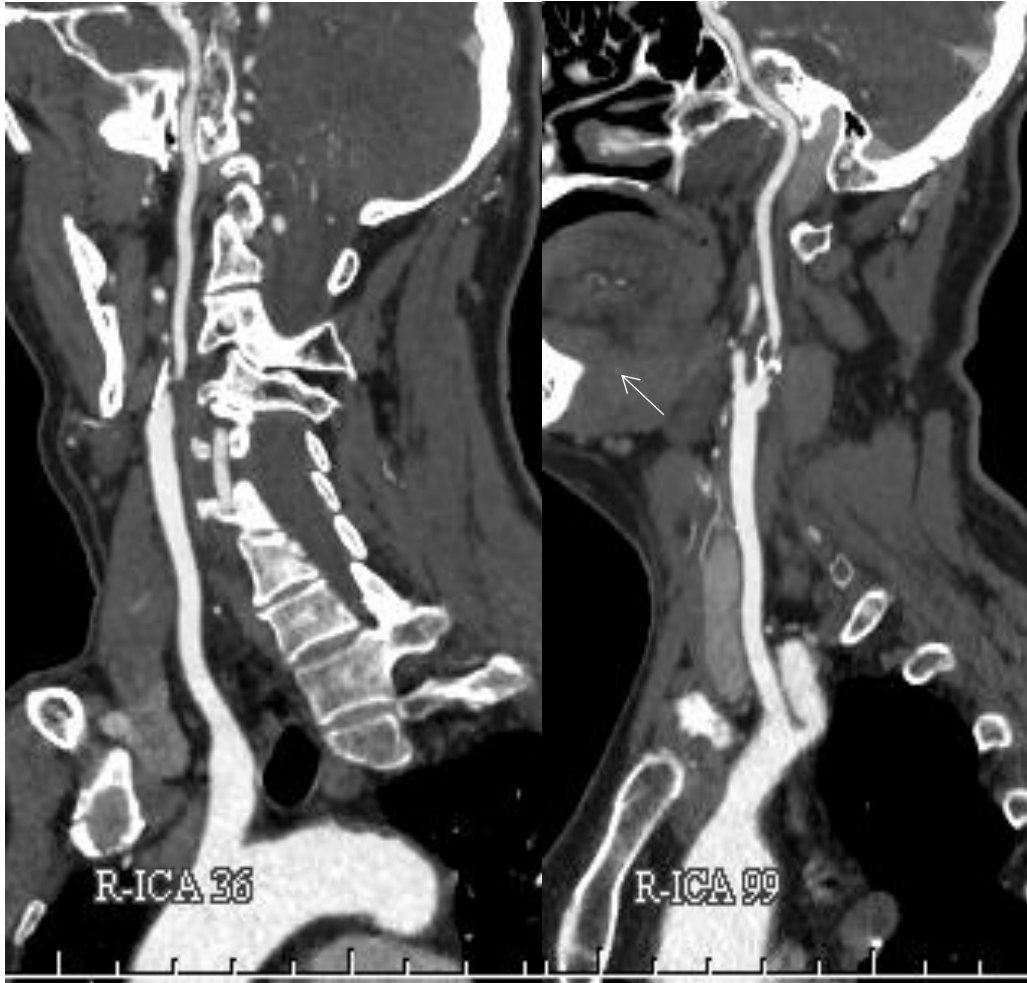


Figure 1. Right carotid CTA

An angiography of the aortic arch and the whole brain was performed on July 21, 2020 (**Figure 2**, **Figure 3**, **Figure 4**, and **Figure 5**).



Figure 2. Aortic arch angiography

Type II aortic arch showed no obvious stenosis, but the occlusion of bilateral common carotid arteries and bilateral vertebral arteries were observed (**Figure 2**).

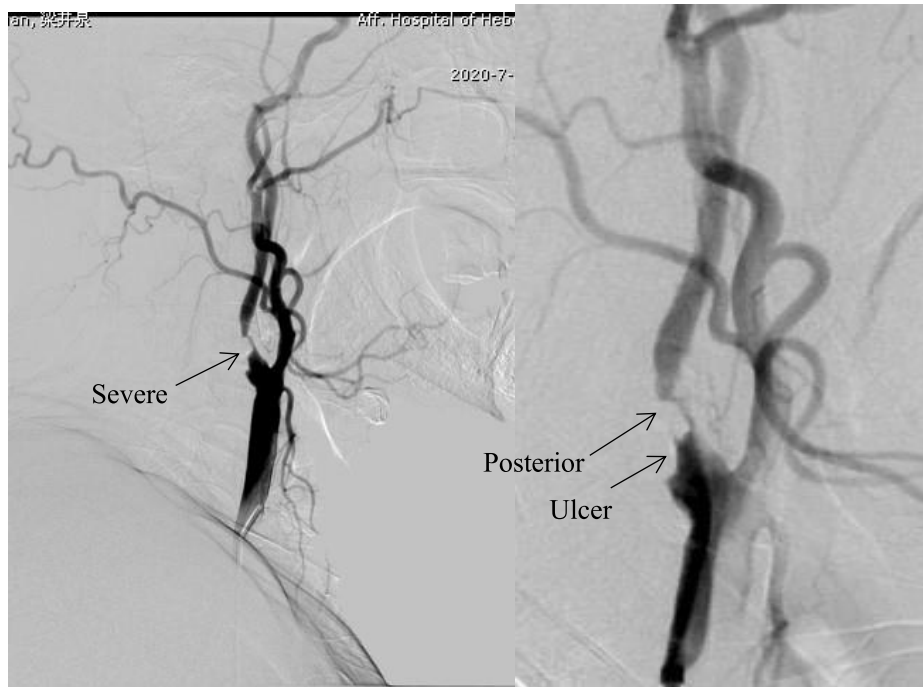


Figure 3. Right common carotid angiography

There was severe stenosis at the right proximal internal carotid artery, and the plaque was located on the posterior wall of the internal carotid artery. Small ulcers had formed on the posterior wall, and the stenosis was tortuous (**Figure 3**).



Figure 4. Left common carotid angiography

There was mild stenosis at the proximal part of the left internal carotid artery, the anterior communicating artery was patent, the bilateral anterior cerebral arteries were well-developed, and no severe stenosis was noted in the trunk or branches (**Figure 4**).

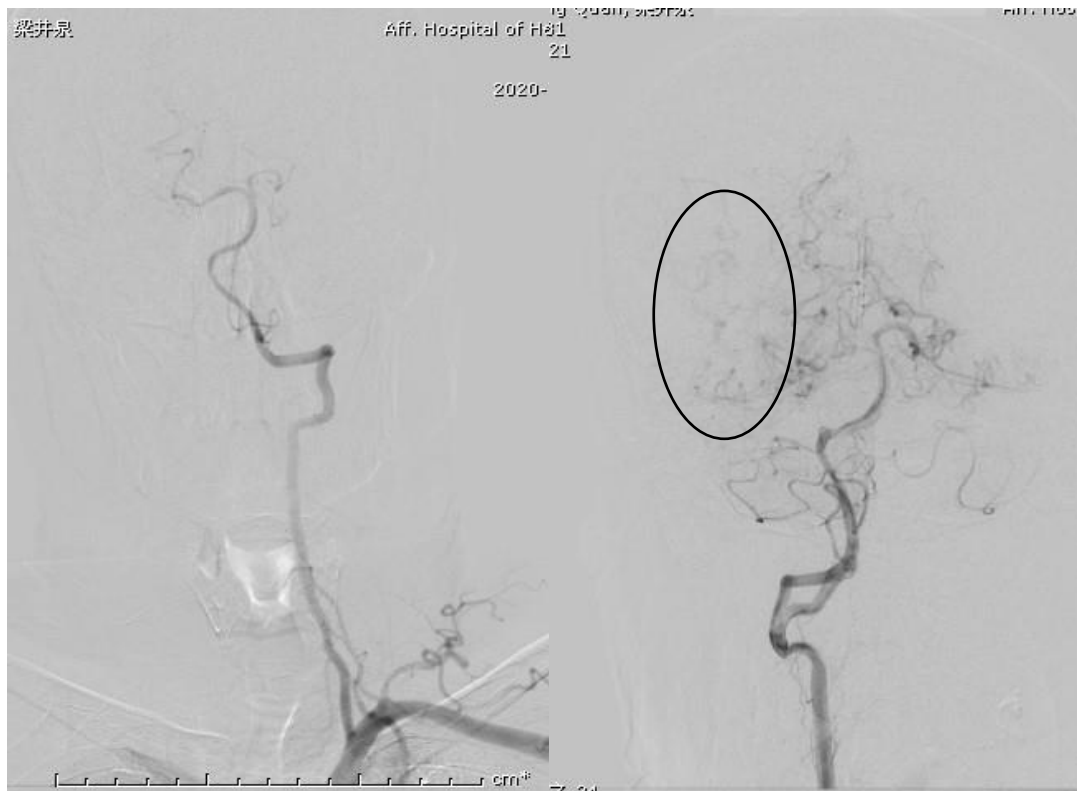


Figure 5. Left vertebral angiography

No severe stenosis was noted in the left vertebral artery and basilar artery as well as their branches. In the late phase of angiogram, the right posterior circulation could compensate for blood supply through the pia mater artery, like the right anterior circulation (**Figure 5**).

2. Interventional surgery

The surgical indication was severe stenosis ($> 70\%$) at the right proximal internal carotid artery with symptoms of cerebral ischemia. The surgical plan for the patient was stenting at the right proximal internal carotid artery. The anesthesia method was local infiltration anesthesia. Stenting of the right internal carotid artery was performed under local anesthesia on July 24, 2020.

The surgical process was as follows: under local infiltration anesthesia, the modified Seldinger technique was performed, in which the right common femoral artery was punctured, and an 8F femoral artery sheath was inserted; through the 8F femoral artery sheath, an 8F guide tube was inserted into the middle and upper segment of the right common carotid artery under the guidance of a loach guidewire and multifunctional catheter; under the guidance of path map, the 0.014-inch guidewire was inserted into the common carotid artery through the 8F guide tube to change the direction of the head end of the guidewire, reaching the distal end through the narrow segment of the internal carotid artery.

The guidewire was kept close to the anterior wall of the blood vessel, reaching the distal end through the narrow part, and avoiding stimulation to the plaque and the posterior wall ulcer as well as damage to the intima and formation of interlayer (**Figure 6**).

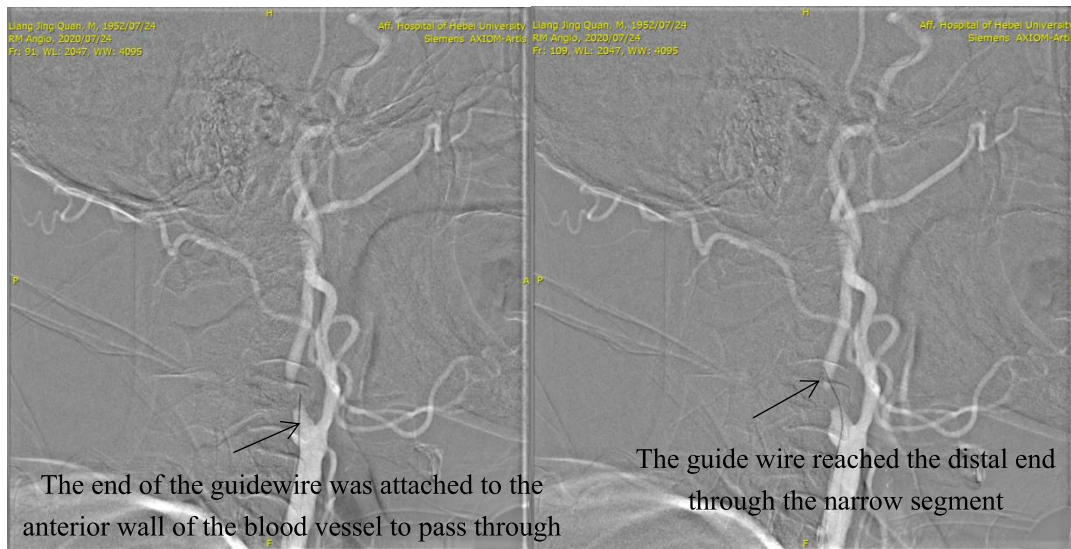


Figure 6. Path map of the right common carotid artery, with a micro-guidewire passing through the stenotic arterial segment

Under the guidance of the micro-guidewire, a carotid protective umbrella (Spider) (4 x 20 mm) was successfully placed. The 0.014-inch guidewire was withdrawn, and the pre-dilatation balloon (5 x 30 mm) was placed along the guidewire of the carotid umbrella, but the balloon could not pass through the narrow part. Although the balloon was replaced with a small-diameter balloon (2 x 15mm), the balloon still could not pass through the narrow part. By adjusting the position of the 8F guide catheter to provide more support to the balloon, the balloon still could not pass through the stenotic part. Even with a smaller diameter balloon (1.5 x 2 mm), it still could not pass through the stenotic part (**Figure 7**).

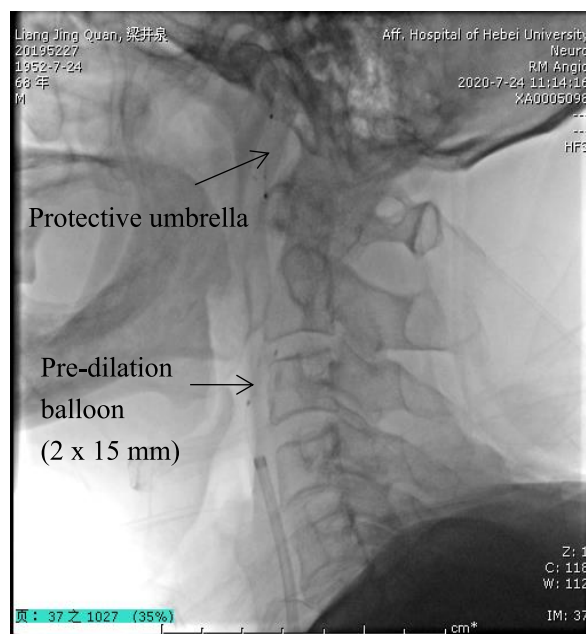


Figure 7. Position of guiding catheter, small balloon, and protective umbrella during the intervention

The following reasons were considered: severe stenosis and calcification at the lesion site, poor vascular compliance, and insufficient guidewire support. Therefore, the combination of the 0.014-inch guidewire and support catheter was inserted through the 8F guide tube, hoping that the support catheter could be inserted into the internal carotid artery to provide better support in place of the V-18 guidewire. However, the support catheter also could not pass through the stenotic part (**Figure 8**).

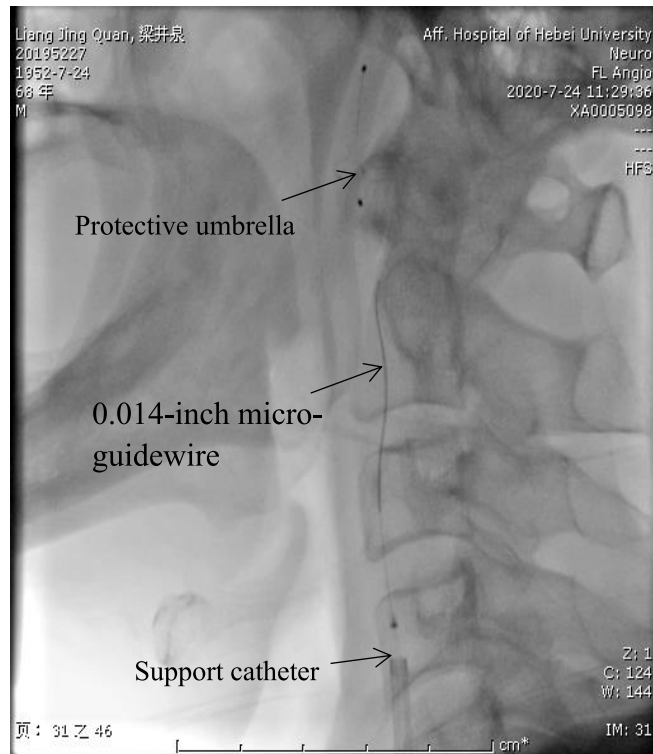


Figure 8. Micro-guidewire, support catheter, and umbrella locations

The balloon and supporting catheter could not pass through the lesion. The intervention was decided to be terminated after recovering the protective umbrella, but the recover catheter of the protective umbrella could not pass through the narrowed part. There was a dilemma during the surgery at that time; if the surgery continues, the pre-dilatation balloon cannot be positioned; if terminated, the protective umbrella cannot be recovered. The reason for the balloon's failure could be the severe stenosis and calcification at the lesion site, as well as the local spasm caused by repeated stimulation by the balloon. Therefore, the operation was suspended for 15 minutes in the hope that the spasm at the stenotic site would be relieved. After dilution with nitroglycerin 1 mg, the pre-dilatation balloon (1.5 x 2 mm) was inserted through the 8F guiding catheter, along the protective umbrella guidewire. After a large resistance, the balloon successfully reached the distal end of the stenotic segment and was then retracted to the stenotic segment; the stenotic segment was pre-dilatated twice (**Figure 9**).

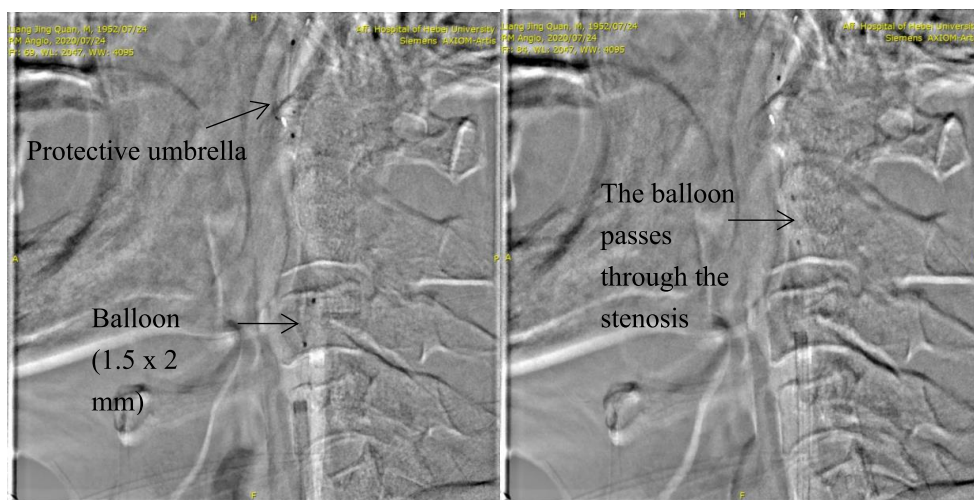


Figure 9. Small balloon passes through the stenosis

Although the small diameter balloon passed through the stenotic site, it still encountered great resistance at the site of the lesion (**Figure 9**).

After that, the 2 x 15 mm, 3 x 10 mm, and 4 x 30 mm balloons were pre-dilatated twice, respectively, while the 5 x 30 mm balloon was pre-dilatated once.

The small diameter balloon (2 x 15 mm) was positioned and pre-dilatated (**Figure 10**).

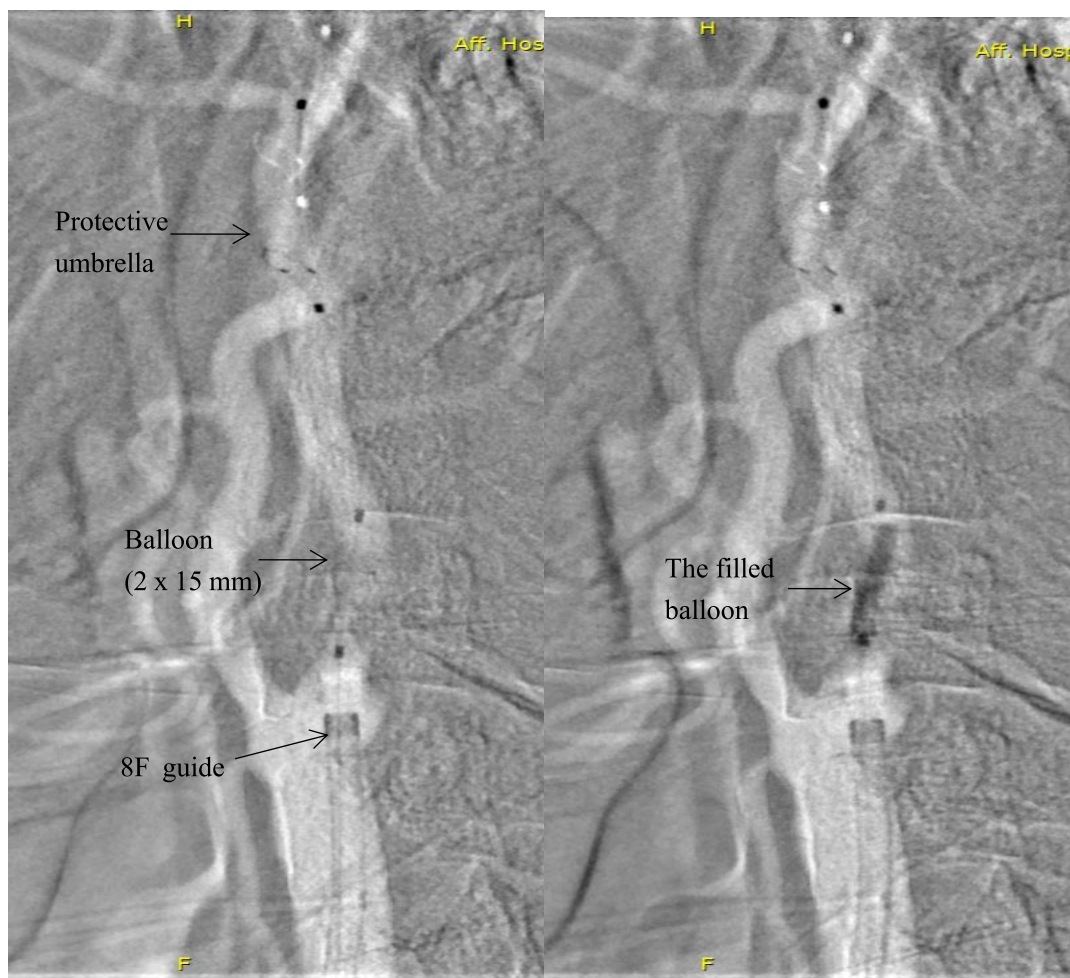


Figure 10. Application of small balloon to dilate stenotic arterial segment

A carotid artery stent (9-7 mm x 40 mm) was successfully implanted, the degree of stenosis improved significantly, and intracranial blood supply also improved (**Figure 11**).

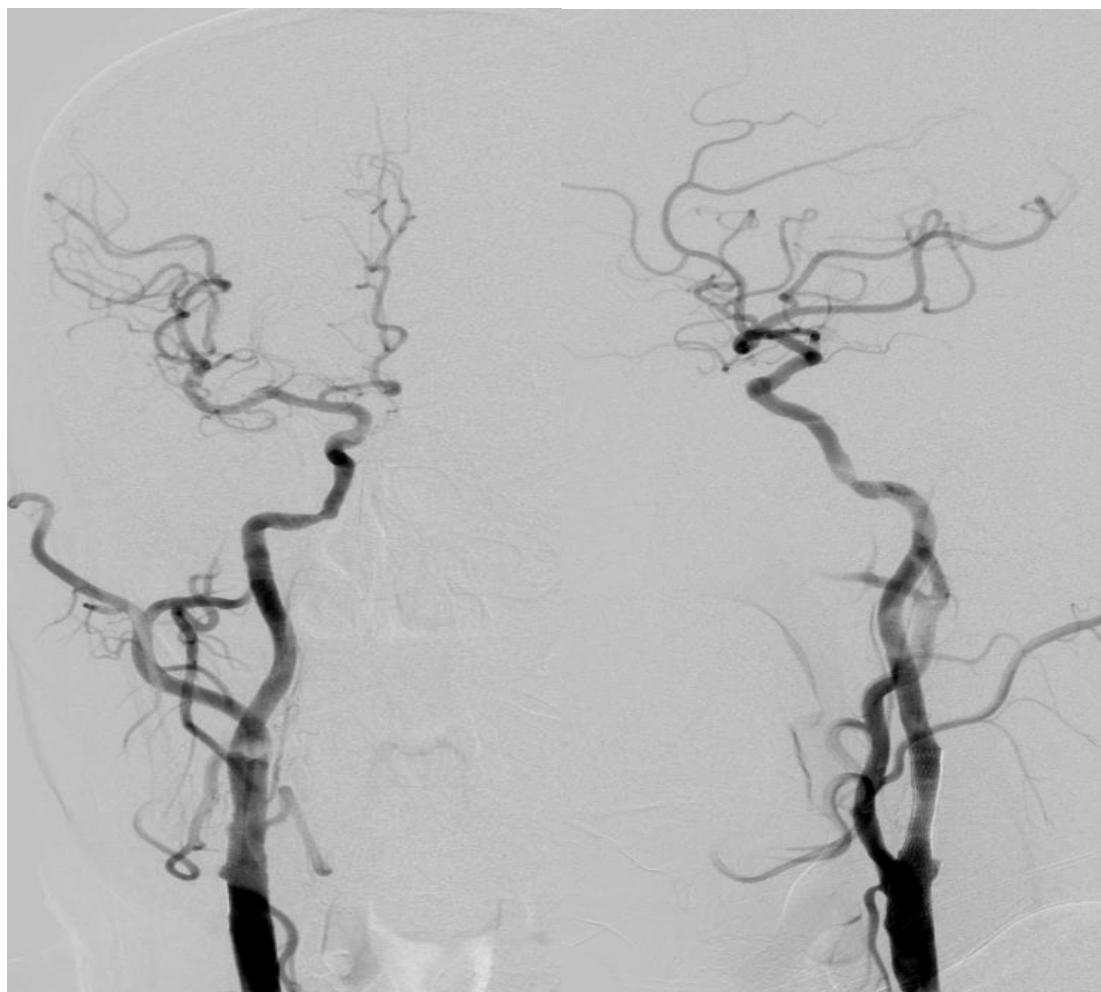


Figure 11. Postoperative right common carotid angiography

The protective umbrella was recovered, the 8F guiding catheter was withdrawn, and a surgical puncture point stapler was used for suture. The surgery was successful.

3. Discussion

Some patients with mild and moderate carotid stenosis may have no clinical symptoms. Patients with stenosis-associated clinical symptoms are categorized under “symptomatic carotid artery stenosis.” Symptomatic carotid bifurcation lesions have a high risk of recurrent ischemic stroke. According to the data of North American Symptomatic Carotid Endarterectomy Trial (NASCET) ^[1], for symptomatic patients treated with drugs, the degree of vascular stenosis was 70% to 99%; after two years of follow-up, the risk of ipsilateral stroke was 26%; on the contrary, the risk of ischemic stroke in patients with asymptomatic carotid bifurcation lesions was significantly lower. In the Asymptomatic Carotid Surgery Trial (ACST) ^[2], carotid ultrasound follow-up showed that patients with asymptomatic carotid stenosis with more than 60% stenosis and receiving drug treatment for more than five years had a stroke risk of 11%. Carotid endarterectomy (CEA) is currently the only method to remove atherosclerotic plaque and restore normal lumen and blood flow. By the 1980s, many centers in Europe and America began to conduct systematic research on CEA. A number of multicenter large sample randomized controlled studies showed that CEA is significantly better than drug treatment for severe carotid stenosis and symptomatic moderate carotid stenosis. The Carotid Revascularization Endarterectomy versus Stenting Trial (CREST) ^[3], published in 2010, is a randomized multicenter trial that compared the effects of CAS and CEA as well as

the incidence of complications in symptomatic and asymptomatic patients. During an average follow-up of 2.5 years in 2,502 patients, there was no significant difference in the incidence of major events between the two groups, which was 7.2% in the CAS group and 6.8% in the CEA group (HR 1.11, 95% CI 0.81-1.51). In 2016, the New England Journal of Medicine published the long-term follow-up results of CREST [4]: 10 years after surgery, CEA (9.9%) was found better than CAS (11.8%) in terms of composite end point of death, stroke, and myocardial infarction, but there was no statistical significance to them; within five years after surgery, the proportion of ipsilateral stroke was very low (0.6% per year), which seemed to be slightly better than CAS (0.7%), but there was no significant difference between the two on the whole. Therefore, with the continuous progress of equipment and instruments, carotid stenting angioplasty (CAS) has been gradually popularized. With it being minimally invasive, having high efficiency and rapid postoperative recovery, along with its equivalent curative effect with CEA, CAS has increasingly favored by patients. CAS has become a method that can replace CEA, especially for those patients with high risk of CEA.

CAS has become a mature surgical method. Although the process is not complex, the risk is still very high. During CAS, difficulty in placing the balloon is common. Generally, it can be solved by changing to a small-diameter balloon. In this case study, balloons with various sizes cannot be successfully placed during the surgery. The reasons may be related to the following factors: (1) the lesion site is severely narrowed, calcified, and tortuous, with a significant decrease in vascular compliance; (2) the first pre-dilatation balloon (5 x 30 mm) was too large, and it stimulated the narrowed part, causing spasm; in that case, when smaller balloons are attempted, they failed to pass through the stenotic part; if the 2 x 15 mm pre-dilatation balloon was selected first, the surgery may have been relatively smooth; (3) the lesion segment is tortuous, and the supporting force of the umbrella guidewire is not enough to change the shape of the narrowed segment; hence, the balloon cannot pass through. For these reasons, the pre-dilatation balloon cannot be in place, and the internal carotid artery protective umbrella cannot be recovered, thus placing the surgery in a difficult situation. The solutions to this include the following: (1) in preoperative evaluation, it is necessary to make an effective evaluation of the lesion site, especially in imaging; (2) adequate surgical plans should be made; (3) it should be expected that the balloon will not be easily placed, therefore a 0.014-inch guidewire should be used to carry a small diameter balloon for pre-dilatation of the lesion site, while direct pre-dilatation via a large diameter balloon should not be used as far as possible; (4) in view of carotid spasm, vasodilator or vasospasm prophylaxis drugs may be given.

In conclusion, CAS has become a mature surgical method for the treatment of carotid stenosis. This case is a rare situation, where the balloon cannot be positioned. Relevant solutions have been proposed, hoping to provide a more theoretical and practical basis for clinical work.

Disclosure statement

The authors declare no conflict of interest.

References

- [1] Barnett HJM, Taylor DW, Eliasziw M, et al., 1998, Benefit of Carotid Endarterectomy in Patients with Symptomatic Moderate or Severe Stenosis. *New England Journal of Medicine*, 339(20): 1415–1425.
- [2] Mayberg MR, Wilson SE, Yatsu F, et al., 1991, Carotid Endarterectomy and Prevention of Cerebral Ischemia in Symptomatic Carotid Stenosis. *JAMA*, 266(23): 3289–3294.
- [3] Brott TG, Hobson RW, Howard G, et al., 2010, Stenting Versus Endarterectomy for Treatment of Carotid-Artery Stenosis. *New England Journal of Medicine*, 363(1): 11–23.

- [4] Brott TG, Howard G, Roubin GS, et al., 2016, Long-Term Results of Stenting Versus Endarterectomy for Carotid-Artery Stenosis. *New England Journal of Medicine*, 374(11): 1021–1031.

Publisher's note

Bio-Byword Scientific Publishing remains neutral with regard to jurisdictional claims in published maps and institutional affiliations.

A Correlation Analysis of Postoperative Hypercoagulability and Peripheral Circulating Tumor Cells in Patients with Lung Cancer

Xuguang Zhang, Duo Zhang, Hefei Li*

Thoracic Surgery Department, Affiliated Hospital of Hebei University, Baoding 071000, Hebei Province, China

*Corresponding author: Hefei Li, 13831275950@163.com

Copyright: © 2022 Author(s). This is an open-access article distributed under the terms of the Creative Commons Attribution License (CC BY 4.0), permitting distribution and reproduction in any medium, provided the original work is cited.

Abstract: *Objective:* To explore the correlation between peripheral circulating tumor cells and hypercoagulability in patients with lung cancer after surgery. *Methods:* From January 2017 to December 2021, 89 patients with lung cancer who were treated in the Affiliated Hospital of Hebei University were selected as the research subjects, and a retrospective analysis was conducted to analyze and observe the D-dimer (DD), fibrinogen (FIB), and platelet (PLT) levels in peripheral blood, as well as detect peripheral CTC. *Results:* There were statistical differences in TMN staging, tumor metastasis, and lymph node metastasis in the clinical data, but there were no statistical differences in gender, smoking history, and pathological classification. After retrospective analysis and comparison of the patients, the DD (mg/ml), FIB (g/L), and PLT ($\times 10^9/L$) levels of the CTC positive group were 3.41 ± 0.58 , 3.98 ± 0.87 , and 367.26 ± 34.98 , respectively; the CTC negative group's DD (mg/ml), FIB (g/L), and PLT ($\times 10^9/L$) levels were 0.89 ± 0.49 , 1.06 ± 0.45 , and 234.69 ± 35.69 , respectively, and the differences were statistically significant. The factors affecting the prognosis of patients included TMN staging and CTC; the number of CTC positives in the death group was significantly higher than that in the survival group, and there was a statistical difference between the groups. Gender, age, smoking history, pathological type, and surgical resection had no effect on the prognosis of patients. Among the enrolled patients, the survival rate was 71.91%. *Conclusion:* CTC-positive patients have a higher probability of hypercoagulability after surgery and are prone to tumor metastasis; thus, CTC can be used as a judgment index for the prognosis of patients.

Keywords: Lung cancer; Hypercoagulable state; Peripheral circulating tumor cells

Online publication: July 28, 2022

1. Case study

Lung cancer is the leading cause of cancer-related death in both, men and women worldwide ^[1]. According to its pathological classification, it can be divided into two categories: small cell lung cancer (SCLC) and non-small-cell lung cancer (NSCLC). Clinically, non-small cell lung cancer patients account for about 85%, and most of them are diagnosed after the cancer has metastasized or at an advanced stage ^[2]. Despite significant advancements in the surgical management of lung cancer in recent years and the potentiality to treat locally advanced or distant metastatic tumors using various methods, such as radiotherapy, chemotherapy, targeted therapy ^[3], and immunotherapy ^[4], the cure rate of patients is still very low, and their prognosis is poor, thus posing a serious threat to human health ^[5-7]. In recent years, with the improvement of people's living standards and health awareness, the concept of regular physical examination has gained recognition, thereby increasing the early detection rate and surgical rate of lung

cancer, but postoperative recurrence and metastasis remain the primary causes of high mortality in non-small cell lung cancer patients.

2. Materials and methods

2.1. General information

From January 2017 to December 2021, 89 patients with lung cancer who were treated in the Affiliated Hospital of Hebei University were selected as the research subjects for retrospective analysis. Among them, 41 were CTC positive patients, and 48 were CTC negative patients, in which 64 of them survived, and 25 of them died. The clinical data of the enrolled patients and their follow-up data were complete.

2.2. Methods

An automatic blood coagulation analyzer and its supporting reagents (STAGO, France) were used to detect D-dimer (DD) and fibrinogen (FIB) levels in patients; another reagent (Minray BC-6088) was used to detect the level of platelets (PLT) in patients. CTC detection was based on CellSearch system, and the related reagents, consumables, as well as its detection methods and judgment standards are based on literature [8,9].

The patients were followed up from the day of the surgery via telephone or outpatient follow-up. The end point was either the death of the patient or the deadline for the follow-up (December 2021). The patients were divided into the death group and the survival group based on the end point to analyze the risk factors affecting the prognosis.

2.3. Observation indicators

The levels of DD, FIB, and PLT in peripheral blood, as well as CTC detection were observed and analyzed.

2.4. Statistical analysis

SPSS 19.0 and GraphPad Prism 6.0 were used for data analysis. The experimental data were expressed as mean \pm standard deviation ($\bar{x} \pm s$); one-way analysis of variance (one-way ANOVA) was used to compare the means of each group, and SNK-q test was used for pairwise comparison analysis. The difference was considered statistically significant when $p < 0.05$.

3. Results

3.1. Comparing the clinical data of the two groups of patients

There were statistical differences in TMN staging, tumor metastasis, and lymph node metastasis in the clinical data, but there were no statistical differences in gender, smoking history, and pathological type, as shown in **Table 1**.

Table 1. Comparison of clinical data of the two groups of patients

Group		CTC positive group (n = 41)	CTC negative group (n = 48)	X ²	p
Gender	Male	21 (51.22)	23 (47.92)	0.0965	0.7561
	Female	20 (48.78)	25 (52.08)		
Age	≥ 60	24 (58.54)	23 (47.92)	1.0007	0.3171
	< 60	17 (41.46)	25 (52.08)		
Smoking history	Yes	21 (51.22)	23 (47.92)	0.0965	0.7561
	No	20 (48.78)	25 (52.08)		
TMN staging	Stage I/II	12 (29.27)	30 (62.50)	9.7988	0.0017
	Stage III	29 (70.73)	18 (37.50)		

(Continued on next page)

(Continued from previous page)

Group		CTC positive group (n = 41)	CTC negative group (n = 48)	X ²	p
Pathological type	Lung adenocarcinoma	14 (34.15)	16 (33.33)	0.2299	0.8914
	Lung squamous cell carcinoma	16 (39.02)	17 (35.42)		
	Small cell lung cancer	11 (26.83)	15 (31.25)		
Tumor metastasis	Yes	28 (68.29)	17 (35.42)	9.5611	0.0020
	No	13 (31.71)	31 (64.58)		
Lymph node metastasis	Yes	27 (65.85)	16 (33.33)	9.3648	0.0022
	No	14 (34.15)	32 (66.67)		

3.2. Comparing the coagulation indices between the two groups of patients

After retrospective analysis and comparison of the enrolled patients, the DD (mg/ml), FIB (g/L), and PLT ($\times 10^9/L$) levels of the CTC positive group were 3.41 ± 0.58 , 3.98 ± 0.87 , and 367.26 ± 34.98 , respectively, whereas the DD (mg/ml), FIB (g/L), and PLT ($\times 10^9/L$) levels of the CTC negative group were 0.89 ± 0.49 , 1.06 ± 0.45 , and 234.69 ± 35.69 , respectively; the differences were statistically significantly, as shown in **Table 2**.

Table 2. Comparison of coagulation indices between the two groups of patients

Group	DD (mg/ml)	FIB (g/L)	PLT ($\times 10^9/L$)
CTC positive group (n = 41)	3.41 ± 0.58	3.98 ± 0.87	367.26 ± 34.98
CTC negative group (n = 48)	0.89 ± 0.49	1.06 ± 0.45	234.69 ± 35.69
t	22.2214	20.3027	17.6273
p	0.0000	0.0000	0.0000

3.3. Analyzing the influencing factors for the prognosis of patients with lung cancer postoperatively

The factors affecting the prognosis of patients in this study were TMN staging and CTC. The number of CTC positives in the death group was significantly higher than that in the survival group, and there was a significant difference between the two groups. Gender, age, smoking history, pathological type, and surgical resection had no effect on the prognosis of patients. Among the enrolled patients, the survival rate was 71.91%, as shown in **Table 3**.

Table 3. Analysis of the influencing factors for the prognosis of lung cancer patients after surgery

Group		Death group (n = 25)	Survival group (n = 64)	X ²	p
Gender	Male	14 (56.00)	30 (46.88)	0.5988	0.4390
	Female	11 (44.00)	34 (53.12)		
Age	≥ 60	12 (48.00)	35 (54.69)	0.3226	0.5700
	< 60	13 (52.00)	29 (45.31)		
Smoking history	Yes	11 (44.00)	33 (51.56)	0.4113	0.5213
	No	14 (56.00)	31 (48.44)		
TMN staging	Stage I/II	6 (24.00)	36 (56.25)	7.5028	0.0062
	Stage III	19 (76.00)	28 (43.75)		

(Continued on next page)

(Continued from previous page)

Group		Death group (n = 25)	Survival group (n = 64)	X ²	p
Pathological type	Lung adenocarcinoma	8 (32.00)	22 (34.38)	0.1334	0.9355
	Lung squamous cell carcinoma	9 (36.00)	24 (37.50)		
	Small cell lung cancer	8 (32.00)	18 (24.12)		
CTC	Positive	18 (72.00)	23 (35.94)	9.4102	0.0022
	Negative	7 (28.00)	41 (64.06)		
Surgical resection	Total lobectomy	11 (44.00)	31 (48.44)	0.1420	0.7063
	Partial lobectomy	14 (56.00)	33 (51.44)		

4. Discussion

In terms of morbidity and mortality, lung cancer ranks first among malignant tumors. Among the cases, 85% of them are non-small cell lung cancer (NSCLC). Although the treatment of NSCLC has made great progress in recent years, the 5-year survival rate of patients is still only about 17%. Surgery is still the preferred treatment for early-stage lung cancer patients. Although postoperative adjuvant chemotherapy can delay tumor recurrence and metastasis, tumor metastasis is still the main cause of death in lung cancer patients. Numerous studies have demonstrated that circulating tumor cells (CTCs) play a key role in the distant metastasis of tumors. CTCs are an independent marker that can predict the survival of patients, and there is a correlation between the number of CTCs and tumor invasion, metastasis, and the time to recurrence [1-7].

Lung cancer is the most common cancer and the leading cause of cancer death in China [2]. According to pathological classification, it can be divided into two categories: SCLC and NSCLC. Clinically, NSCLC patients account for about 85%. Lung cancer is a serious threat to human health as the number of deaths from lung cancer accounts for about 18% of deaths from all cancers each year, and the 5-year survival rate is less than 20%. On the one hand, the early detection and diagnosis of lung cancer pose a challenge. The cure rate of carcinoma in situ is nearly 100%, and the 5-year survival rate of stage I and II lung cancer is about 25% to 73%, but the 5-year survival rate of stage III and IV lung cancer is greatly reduced to 2% to 24%. Traditionally, the diagnosis of lung cancer mainly relies on imaging investigations and histopathological results. However, the former has poor sensitivity for nodules with a diameter of less than 1 cm in the lungs. It is even more difficult to identify CTCs in the blood and micrometastases in other organs, thus often resulting in missed diagnosis of early lung cancer. On the other hand, the recurrence and metastasis of lung cancer after surgery seriously affect the prognosis of patients, which are attributable to minimal residual disease (MRD) [3]. For patients with stage III and above lung cancer, MRD may be derived from residual primary tumor lesions or lymph node metastases after surgery. For patients with early-stage lung cancer recurrence and metastasis after surgery, MRD may be derived from some occult metastases. Most tumor cells are blocked and cleared by the body's immune system, but a small part that is in a static state under the surveillance of the immune system gets activated under the stimulation of certain factors, resulting in the spread and metastasis of malignant tumors [4]. As a non-invasive, real-time, and effective detection method, liquid biopsy is helpful for early diagnosis and prognostic evaluation of patients [6]; it can predict tumor recurrence 1 to 2 years earlier than the progress of radiology [7]. At present, the commonly used CTC detection technology is the FDA-approved CellSearch system, which uses ferromagnetic beads coated with antibodies against epithelial cell surface specific markers, namely epithelial cell adhesion molecule (EpCAM). After initial CTC enrichment, the high expression of CK9, CK18, or CK19 with the low expression of leukocyte surface antigen CD45 based on cell or nuclear morphology, the positive immunofluorescence staining of nuclei, as well as the expression of detectable epithelial cytokeratin (CK)

further promote the identification and enumeration of CTCs [10-15].

Hypercoagulable state is the premise and basis of deep vein thrombosis. DD is the end product of cross-linked fibrin decomposed by plasmin, and its level is an important indicator of hypercoagulable state and abnormal fibrinolytic function. The coagulation factor with the highest content in the plasma is the acute phase reactive protein synthesized by the liver. The level of FIB is closely related to tumor recurrence and metastasis, and it is an important indicator for clinical tumor monitoring. Through the active coagulation factors secreted by tumor cells, platelets will adhere and aggregate. In addition, tumor cells also secrete platelet-derived growth factor, which promotes the rapid growth of tumor cells in the metastatic site. Therefore, the level of PLT is closely related to tumor occurrence, development, and metastasis [16-20].

In conclusion, CTC positive patients have a higher probability of hypercoagulability after surgery and are prone to tumor metastasis; thus, it can be used as a judgment index for the prognosis of patients.

Funding

Baoding Science and Technology Project (Project Number: 18ZF134)

Youth Fund of Affiliated Hospital of Hebei University (Project Number: 2017Q018)

Disclosure statement

The authors declare no conflict of interest.

References

- [1] Wang H, Zhou Z, Shen D, et al., 2021, The Relationship Between Peripheral Blood Circulating Tumor Cells and Coagulation Indexes in Patients with Non-Small Cell Lung Cancer After Surgery. *China Cancer Clinic and Rehabilitation*, 28(03): 335–337.
- [2] Mai C, Tang H, Lin L, 2021, Analysis of the Detection Results of Peripheral Blood Circulating Tumor Cells in Patients with Lung Cancer. *Internal Medicine*, 16(01): 92–94.
- [3] Mei J, 2021, Strict Study on the Levels of Circulating Tumor Cells and NSE, CEA and CYFRA21-1 in Patients with Lung Cancer. *Marker Immunoassay and Clinic*, 28(01): 37–40.
- [4] Sun J, 2020, Correlation Between Peripheral Blood Circulating Tumor Cell Expression and Keratin 19 Fragment and Fibrinogen in Patients with Lung Cancer. *China Health Engineering*, 19(01): 88–89.
- [5] Lin S, Hao Y, Lv Y, et al., 2019, Clinical Correlation of Peripheral Blood Circulating Tumor Cells and Their Chemokine Receptor CCR9 with Non-Small Cell Lung Cancer. *Journal of Postgraduate Medicine*, 32(09): 948–953.
- [6] Nie Q, Liu H, Lu Y, 2019, Study on EP Regimen Regulated by the Mechanism of Epithelial-Mesenchymal Transition of Peripheral Blood Circulating Tumor Cells in the Treatment of Small Cell Lung Cancer. *Chongqing Medicine*, 48(01): 91–93.
- [7] Xiao P, Mei J, Li R, et al., 2018, The Value of Peripheral Blood Circulating Tumor Cells in Different Stages and Different Types of Lung Cancer. *Cancer Progress*, 16(06): 763–765.
- [8] Hu R, Wu Z, 2018, Correlation Between Peripheral Blood Circulating Tumor Cells and Clinical Staging of Patients with Non-Small Cell Lung Cancer. *Journal of Changjiang University (Self-Science Edition)*, 15(08): 29–31.
- [9] Tong B, 2018, Expression and Analysis of PD-L1 in the Primary Tumor of Non-Small Cell Lung Cancer and Circulating Tumor Cells in Peripheral Blood. *Peking Union Medical College*.

- [10] Lou D, 2018, The Clinical Significance of Peripheral Blood Circulating Tumor Cell Count in Lung Cancer Patients. Dalian Medical University.
- [11] Ye C, Chen L, Wang J, et al., 2017, Effects of Pemetrexed Combined with Cisplatin on EGFR Expression and Prognosis in Peripheral Blood Circulating Tumor Cells in Patients with Advanced Non-Small Cell Lung Cancer. *China Medical Frontiers (Electronic Edition)*, 9(12): 34–37.
- [12] Chen Z, Hu H, Chen B, 2017, Relationship Between Peripheral Blood Circulating Tumor Cells and Clinicopathological Factors and Prognosis of Non-Small Cell Lung Cancer. *Journal of Practical Medicine*, 33(23): 3894–3898.
- [13] Zhu J, Zhou L, Zhou D, et al., 2017, Expression of Circulating Tumor Cells in Peripheral Blood of Lung Cancer Patients and Their Relationship with Serum CY-FRA21-1 and FG Levels. *China Cancer Clinic and Rehabilitation*, 24(05): 541–544.
- [14] Jiang B, Jin C, Tu C, et al., 2016, Influence of EGFR Expression in Peripheral Blood Circulating Tumor Cells on TKI Treatment Effect and Prognosis in Patients with Advanced Non-Small Cell Lung Cancer. *Shandong Medicine*, 56(40): 86–88 + 115.
- [15] Wan J, Shen H, Huang H, et al., 2015, A Preliminary Study on the Relationship Between Peripheral Blood Circulating Tumor Cells and Clinical Characteristics in Patients with Non-Small Cell Lung Cancer. *Journal of Clinical and Pathology*, 35(01): 43–47.
- [16] Bai L, Xie J, Bai L, et al., 2021, Detection of Circulating Tumor Cells in Peripheral Blood of NSCLC and Its Relationship with TNM Staging and Prognosis. *Modern Oncology*, 29(19): 3380–3385.
- [17] Li W, Li Y, Liang W, et al., 2021, Differences in the Content of Circulating Tumor Cells in Peripheral Arterial Blood and Venous Blood of Patients with Lung Cancer and Its Clinical Significance. *Journal of Clinical Pulmonology*, 26(04): 567–569 + 574.
- [18] Sun J, 2020, The Correlation Between the Expression of Circulating Tumor Cells in Peripheral Blood of Lung Cancer Patients and the Keratin 19 Fragment and Fibrinogen. *China Health Engineering*, 19(01): 88–89.
- [19] He X, Li S, Ma R, et al., 2019, The Relationship Between Blood Hypercoagulability and Peripheral Blood Circulating Tumor Cells After Lung Cancer Surgery. *China Medical Frontiers*, 11(11): 115–119.
- [20] Li C, Yang Y, Yan D, 2016, Clinical Application Value of Peripheral Venous Circulating Tumor Cell Count in Patients with Non-Small Cell Lung Cancer. *China Primary Medicine*, 23(12): 1768–1771.

Publisher's note

Bio-Byword Scientific Publishing remains neutral with regard to jurisdictional claims in published maps and institutional affiliations.

The Level of Circulating Tumor Cells in Patients with Non-Small Cell Lung Cancer and Its Relationship with Tumor Markers

Rongfang Liu¹, Ben Li², Xuguang Zhang^{2*}

¹Anesthesiology Department, Affiliated Hospital of Hebei University, Baoding 071000, Hebei Province, China

²Thoracic Surgery Department, Affiliated Hospital of Hebei University, Baoding 071000, Hebei Province, China

*Corresponding author: Xuguang Zhang, 570079522@qq.com

Copyright: © 2022 Author(s). This is an open-access article distributed under the terms of the Creative Commons Attribution License (CC BY 4.0), permitting distribution and reproduction in any medium, provided the original work is cited.

Abstract: *Objective:* To explore the level of circulating tumor cells in patients with non-small cell lung cancer and its relationship with tumor markers. *Methods:* Fifty patients with NSCLC admitted to a hospital from March 2019 to February 2022 were retrospectively selected as the research subjects; their clinical data were sorted out and analyzed. All patients were examined for CTCs. According to their levels, the patients were divided into a positive group (30 cases, $\geq 4\%$) and a negative group (20 cases, $< 4\%$). The positive rate of peripheral CTCs in patients with different gender, age, and pathological types of NSCLC, the positive rate of peripheral CTCs in patients with different staging of NSCLC, and the relationship between serum CEA, CA125, CYFRA21-1, and peripheral CTCs were analyzed and observed. *Results:* There was no significant difference in gender, age, and pathological type between the positive group and the negative group. There was also no significant difference in the T staging, N staging, and M staging between the positive group and the negative group. However, there was significant difference in the clinical staging of the positive group and the negative group. The CEA, CA125, and CYFRA21-1 of the positive group were 7.45 ± 1.26 , 38.56 ± 4.12 , and 5.01 ± 1.36 , respectively, whereas those of the negative group were 5.12 ± 1.22 , 32.69 ± 4.01 , and 3.87 ± 1.25 , respectively. The comparison between the two groups was statistically significant. *Conclusion:* CTCs provide the possibility of detecting cancer before the use of imaging methods, guide treatment in combination with other tumor markers, monitor postoperative treatment, and predict patients' outcome.

Keywords: Circulating tumor cells; Tumor markers; Lung cancer

Online publication: July 28, 2022

1. Introduction

Lung cancer is the most common malignant tumor of the respiratory system. Its incidence and mortality rates rank first in the world, and its 5-year survival rate is only about 15%^[1]. Local epidemiological studies have found that the incidence rate of lung cancer is increasing year by year, posing a great threat to people's physical and mental health. Among them, non-small cell lung cancer (NSCLC) accounts for more than 80%^[2]. At present, it is generally believed that it originates from lung epithelial cells and encompasses a number of histological subtypes^[3]. Pathological biopsy is still the only gold standard for diagnosing NSCLC at present; however, this procedure may cause trauma to patients and may even result in complications, such as bleeding and pneumothorax. Its clinical application is limited^[4]. Therefore, it is particularly important to look for a non-invasive diagnostic method. Lung cancer has the highest incidence and mortality rates among malignant tumors, and non-small cell lung cancer (NSCLC) accounts for 85% of the cases. Although

there has been significant progress in the treatment of patients with NSCLC in recent years, the 5-year survival rate of patients is still only about 17%. Surgery is still the treatment of choice for patients with early lung cancer. Postoperative adjuvant chemotherapy may delay tumor recurrence and metastasis, but the latter remains the main cause of death in patients with lung cancer. A large number of studies have proved that circulating tumor cells (CTCs) play a key role in distant metastasis. CTCs are independent markers that can predict the survival of patients with tumors, and there is an association between the number of CTCs and tumor invasion, metastasis, as well as the time to disease recurrence. Therefore, the research on CTCs will not only promote further understanding of tumor metastasis, but also develop new clinical diagnostic methods to guide tumor treatment strategies, so that patients may benefit from quality-of-life improvement and survival-time prolongation.

2. Data and methods

2.1. General information

Fifty patients with NSCLC admitted to a hospital from March 2019 to February 2022 were retrospectively selected as the research subjects. Their clinical data were sorted out and analyzed. All the patients were examined for CTCs. According to their levels, the patients were divided into a positive group (30 cases, $\geq 4\%$) and a negative group (20 cases, $< 4\%$). Patient data, including gender, age, pathological type, staging, tumor size, lymph node infiltration, tumor location, and chemotherapy type, were collected. The general data of the patients were not statistically significant.

2.2. Methods

All patients were tested for CTCs upon admission. After taking 5 ml of venous blood from each patient's median cubital vein, the tumor cells were enriched by the immunomagnetic bead negative enrichment method within 24 days; subsequently, the peripheral CTC count was detected by the CTC detection system (Lyell [Beijing] Medical Devices Co., Ltd.).

2.3. Observation indicators

The observation indicators were the positive rate of peripheral CTCs in NSCLC patients of different gender, age, and pathological type; the positive rate of peripheral CTCs in NSCLC patients with different staging; the relationship between serum CEA, CA125, CYFRA21-1, and peripheral CTCs.

2.4. Statistical analysis

SPSS 19.0 and GraphPad Prism 6.0 were used for data analysis. The experimental data were expressed in mean \pm standard deviation ($\bar{x} \pm s$), one-way ANOVA was used to compare the mean of each group, and SNK-q test was used to compare the data. The difference was considered statistically significant when $p < 0.05$.

3. Results

3.1. The positive rate of peripheral CTCs in NSCLC patients of different gender, age, and pathological type

There was no statistical difference in terms of gender, age, and pathological type between the positive group and the negative group, as shown in **Table 1**.

Table 1. The positive rate of peripheral CTCs in NSCLC patients of different gender, age, and pathological type

Group		Positive group (n = 30)	Negative group (n = 20)	X ²	p
Gender	Male	14 (46.67)	11 (55.00)	0.3333	0.5637
	Female	16 (53.33)	9 (45.00)		
Age	< 60	28 (93.33)	17 (75.00)	0.2315	0.6304
	≥ 60	2 (6.67)	3 (15.00)		
Pathological type	Squamous cell carcinoma	13 (43.33)	9 (45.00)	0.0135	0.9075
	Adenocarcinoma	17 (56.67)	11 (55.00)		

3.2. The positive rate of peripheral CTCs in NSCLC patients with different staging

There was no statistical significance between the positive group and the negative group in terms of T staging, N staging, and M staging. In the positive group, the number of cases with clinical staging I, II, III, and IV was 2, 2, 5, and 21, accounting for 6.67%, 6.67%, 16.66%, and 70.00%, respectively. In the negative group, the number of cases with clinical staging I, II, III, and IV was 4, 1, 9, and 6, accounting for 20.00%, 5.00%, 45.00%, and 30.00%, respectively. The clinical stagings of the positive group and the negative group were statistically significant ($p < 0.05$), as shown in **Table 2**.

Table 2. The positive rate of peripheral CTCs in NSCLC patients with different staging

Group		Positive group (n = 30)	Negative group (n = 20)	X ²	p
Clinical staging	I	2 (6.67)	4 (20.00)	8.829	0.032
	II	2 (6.67)	1 (5.00)		
	III	5 (16.66)	9 (45.00)		
	IV	21 (70.00)	6 (30.00)		
T	T1	4 (13.33)	2 (10.00)	0.195	0.978
	T2	12 (40.00)	9 (45.00)		
	T3	6 (20.00)	4 (20.00)		
	T4	8 (26.67)	5 (25.00)		
N	N0	7 (23.33)	4 (20.00)	0.907	0.824
	N1	6 (20.00)	4 (20.00)		
	N2	10 (33.33)	9 (45.00)		
	N3	7 (23.33)	3 (15.00)		
M	M0	13 (43.33)	6 (30.00)	0.905	0.341
	M1	17 (56.77)	14 (70.00)		

3.3. The relationship between serum CEA, CA125, CYFRA21-1 and peripheral CTCs

The CEA, CA125, and CYFRA21-1 levels of the positive group were 7.45 ± 1.26 , 38.56 ± 4.12 , and 5.01 ± 1.36 , respectively, whereas those of the negative group were 5.12 ± 1.22 , 32.69 ± 4.01 , and 3.87 ± 1.25 , respectively. The comparison between the two groups was statistically significant, as shown in **Table 3**.

Table 3. The relationship between serum CEA, CA125, CYFRA21-1, and peripheral CTCs

Group	Positive group (n = 30)	Negative group (n = 20)	t	p
CEA (µg/L)	7.45±1.26	5.12±1.22	6.4866	0.0000
CA125 (U/ml)	38.56±4.12	32.69±4.01	4.9878	0.0000
CYFRA21-1 (µg/L)	5.01±1.36	3.87±1.25	2.9973	0.0043

4. Discussion

Liquid biopsy is a non-invasive, dynamic monitoring and analysis of body health and disease status through the detection of molecular or cellular markers in body fluid. Therefore, it has great potential in diagnosis, prognosis, monitoring of disease progress and efficacy, understanding disease mechanism, and drug target research [5-9]. Tumor liquid biopsy mainly refers to the analysis of cellular or non-cellular nucleic acids and proteins in the blood to provide timely and accurate dynamic progress information for cancer diagnosis and treatment, including early tumor diagnosis, risk assessment and staging, curative effect, prognosis, recurrence detection, and monitoring [10]. The main components of detection include CTCs (clusters) in the form of cells, circulating tumor DNA (ctDNA), microRNA and RNA in the form of non-cells, as well as extracellular vesicles or platelets assimilated by tumors [11]. Among them, CTCs, ctDNA, and extracellular vesicles represent the most developed and significant advancements of tumor liquid biopsy, and they show increasing value in tumor diagnosis and prognosis [12]. Although the separation of ctDNA and extracellular vesicles is simpler than that of CTCs, the applicable analysis of ctDNA and extracellular vesicles is relatively limited. For instance, ctDNA is mainly used for analyzing genomic mutations [13], whereas CTCs can be used to carry out various analyses, including cell morphology, immunophenotype, and important epitope analysis, tumor cell clone heterogeneity and evolution analysis, as well as epigenetic group, transcriptome, proteome, and metabolome analysis [6,14]. Additionally, patients suffer a great deal of discomfort and anguish with the existing puncture sampling method that is commonly used in clinical practice; even then, the required tumor cells may not be able to be collected. This invasive sampling process also increases the potential risk of cancer metastasis.

There have been a large number of studies on the clinical application value of CTCs, and the United States Food and Drug Administration has already approved the application of CTC detection in the diagnosis of breast cancer [8]. In recent years, it has been found that CTC is of great significance as a new marker in the diagnosis of liver cancer [9]. Therefore, CTC detection can be used for early diagnosis and screening of tumors. CTC PD-L1 expression detection, which is mainly used in disease monitoring and prognosis of metastatic tumors, has not been properly applied to early diagnosis. Therefore, PD-L1 expression in circulating tumor cells has a limited role in early diagnosis and screening [15-20].

Due to the limitations of tissue detection of PD-L1 expression, PD-L1(+) CTC can be used as a potential biomarker for patients with high risk of metastasis and poor prognosis. It can help to screen out the beneficiaries of immunotherapy and more accurately evaluate the prognosis and trend of disease change in patients.

In clinical examination, the aforementioned in vitro methods for detecting CTCs in blood samples are based on a basic assumption, that is, the count of CTCs in peripheral blood will not change significantly over time; however, recent studies have challenged this assumption [15]. They claimed that the distribution of CTCs from recirculation may not be uniform, and patients whom CTCs could not be detected at a given point of time may not be without CTCs [11]. However, it is unrealistic to repeatedly draw patients' blood to determine the distribution of CTCs in accordance with time. Therefore, a feasible strategy is to monitor CTCs by in vivo detection. In vivo flow cytometry (IVFC) enables direct detection of mobile cells in animal models in a non-invasive, continuous manner. Based on different principles, IVFC can be divided into

fluorescent IVFC and photoacoustic flow cytometry (PAFC).

In conclusion, CTCs provide the possibility of detecting cancer before the use of imaging methods, guide treatment in combination with other tumor markers, monitor the postoperative management of patients, and predict patients' outcome.

Funding

Baoding Science and Technology Program Project (Project Number: 18ZF134)

In-Hospital Youth Fund of Hebei University Affiliated Hospital (Project Number: 2017Q018)

Disclosure statement

The authors declare no conflict of interest.

References

- [1] Zhang Y, Zhang Z, Yin X, et al., 2022, The Role and Research Progress of Self Implantation of Circulating Tumor Cells in the Progression of Malignant Tumors. *Modern Oncology*, 30(06): 1113–1117.
- [2] Qin Y, 2022, Research Progress of Circulating Tumor Cells in Early Screening of Hepatocellular Carcinoma. *Modern Oncology Medicine*, 30(06): 1133–1137.
- [3] Shen S, Huang J, Li X, 2022, Research Progress of Circulating Tumor Cell Enrichment Technology. *Laboratory Medicine*, 37(01): 91–96.
- [4] Luo N, Zhong P, Zhang J, et al., 2022, Efficacy of Endu Combined with Concurrent Radiotherapy and Chemotherapy in the Treatment of Non-Small Cell Lung Cancer and Its Effect on Peripheral Blood CTC, VEGF and 3-Year Survival. *Western Medicine*, 34(01): 84–87 + 93.
- [5] Chen P, Jiang P, Yang M, 2022, Research Progress on Invasion and Metastasis of Circulating Tumor Cells in Lung Cancer. *Cancer Progression*, 20(01): 5–7.
- [6] Che K, Cha G, 2021, Clinical Application of Circulating Tumor Cells in the Evaluation of Chemotherapy Efficacy of Advanced Non-Small Cell Lung Cancer. *Jiangxi Medicine*, 56(12): 2351–2353 + 2369.
- [7] Wen S, Zhou D, Xu Y, et al., 2021, The Value of Folic Acid Receptor Positive Circulating Tumor Cell Detection in Early Diagnosis of Lung Adenocarcinoma and Evaluation of Surgical Efficacy. *Chinese Journal of Clinical Laboratory Management*, 9(04): 193–199.
- [8] Wu H, Shen M, Sun Y, et al., 2021, Differential Expression of Four Tumor Stem Cell Markers in Hepatocellular Carcinoma and Peripheral Blood Circulating Tumor Cells and Their Prognostic Value. *Chinese Journal of Laboratory Medicine*, 44(11): 1043–1050.
- [9] Luo Y, Cheng S, Chen W, 2021, Expression of High Mobility Group Protein A2 Glycochain Protein 125 in Circulating Tumor Cells and Its Relationship with Cellular Immune Function in Patients with Non-Small Cell Lung Cancer. *Journal of Practical Medical Technology*, 28(08): 1001–1004.
- [10] Zhou Z, Meng F, Zhao D, et al., 2021, Circulating Tumor Cell Typing and Its Clinical Application in Advanced Lung Cancer. *International Journal of Laboratory Medicine*, 42(15): 1874–1879.
- [11] Cai R, A X, Qi H, et al., 2021, Study on the Relationship Between Circulating Tumor Cells and Serum SCC Ag and Cy-Fra21-1 Levels in Patients with Non-Small Cell Lung Cancer. *Progress in Modern Biomedicine*, 21(14): 2778–2781.

- [12] Zhao Y, Li Y, Ding H, et al., 2021, Value Analysis of Circulating Tumor Cell Count in Evaluating Prognosis of Elderly Patients with Advanced Non-Small Cell Lung Cancer. *Chinese Journal of Modern Medicine*, 23(07): 6–10.
- [13] Deng K, Li Y, Liu G, et al., 2021, Clinical Study on the Use of Circulating Tumor Cells to Distinguish Benign and Malignant Lesions of Pulmonary Nodules. *Journal of Wuhan University (Medical Edition)*, 42(06): 966–970.
- [14] Yu P, Zhu L, Que Z, et al., 2021, Research Progress in Circulating Tumor Cells of Lung Cancer. *Cancer Prevention and Treatment Research*, 48(05): 519–523.
- [15] Lu X, 2021, Application of Circulating Tumor Cells in Diagnosis and Treatment of Small Cell Lung Cancer. *Beijing University of Traditional Chinese Medicine*.
- [16] Wang Y, Guo S, Wang X, et al., 2021, Effect of Kangai Injection Combined with Bevacizumab on Circulating Tumor Cells and CA21-1 Level in Patients with Advanced Non-Small Cell Lung Cancer. *Journal of Difficult Diseases*, 20(09): 914–917 + 923.
- [17] Bo L, Wang X, Yu Z, et al., 2021, Research Progress of CPS1 Regulating the Occurrence and Development of Malignant Tumors. *Modern Oncology*, 29(20): 3654–3657.
- [18] Li H, Wang H, Sun Z, et al., 2021, Consistency of ctDNA Mutation Spectrum Between Tissues and Serum of Patients with Non-Small Cell Lung Cancer and Analysis of Related Factors. *Modern Oncology*, 29(17): 3023–3026.
- [19] Liu W, 2021, Analysis of the Consistency Between the Results of Preoperative Circulating Tumor DNA and Tumor Tissue DNA Detection in Non-Small Cell Lung Cancer. *Zunyi Medical University*.
- [20] Yan F, Ma Y, Song Y, et al., 2021, Value of Combined Detection of Multiple Tumor Markers in the Diagnosis of Non-Small Cell Lung Cancer. *Journal of Practical Clinical Medicine*, 25(09): 14–17.

Publisher's note

Bio-Byword Scientific Publishing remains neutral with regard to jurisdictional claims in published maps and institutional affiliations.

Analyzing the CT Features of Primary Spontaneous Pneumothorax and Its Application Value

Duo Zhang, Kuo Xiao*

Thoracic Surgery Department, Affiliated Hospital of Hebei University, Baoding 071000, Hebei Province, China

*Corresponding author: Kuo Xiao, xkdaoying@163.com

Copyright: © 2022 Author(s). This is an open-access article distributed under the terms of the Creative Commons Attribution License (CC BY 4.0), permitting distribution and reproduction in any medium, provided the original work is cited.

Abstract: *Objective:* To explore the performance characteristics of CT examination in primary spontaneous pneumothorax (PSP) and the effect of pleurodesis on patients with PSP. *Methods:* Sixty-four patients with PSP, who received medical care in the Affiliated Hospital of Hebei University from January 2017 to December 2021, were selected as the research subjects, of which 40 were male and 24 were female patients. All 64 patients were examined by X-ray and CT; the density, enhancement, and morphology of the pneumothorax were observed and analyzed, and the classification of pneumothorax was done. *Results:* The clinical analysis of 64 patients with PSP showed that the number of cases with unilateral pneumothorax was 42, accounting for 65.63%, whereas the number of cases with bilateral pneumothorax was 22, accounting for 34.37%. Among the cases of unilateral pneumothorax, the number of cases with left pneumothorax was 26, accounting for 61.90%, whereas the proportion of cases with right pneumothorax was 38.10%. When examined by CT, the diagnostic coincidence rate of 64 patients with PSP was 73.44%; using X-ray examination, the diagnostic coincidence rate of 64 patients with PSP was 92.19%. *Conclusion:* The detection accuracy of CT is higher than that of X-ray examination, which may improve the treatment effect in PSP, ensure the accuracy of findings, and facilitate follow-up treatment as well as the effect of postoperative analysis.

Keywords: Primary spontaneous pneumothorax; CT; X-ray

Online publication: July 28, 2022

1. Introduction

Primary spontaneous pneumothorax (PSP) can be examined by computed tomography (CT) or X-ray. The cost of CT examination is higher than that of X-ray. According to several reports, the diagnostic accuracy of CT is higher than that of X-ray. Primary spontaneous pneumothorax is usually caused by the rupture of subpleural blebs or pulmonary bullae. These patients generally do not have any underlying lung disease. It often affects young, thin, and tall men. Studies have found that smoking is closely related to primary spontaneous pneumothorax [1-3]. The risk of pneumothorax increases with smoking. Other risk factors include cocaine use, family history of pneumothorax, and surrounding environment [4-6]. Secondary spontaneous pneumothorax (SSP) often occurs in patients with underlying lung diseases, such as chronic obstructive pulmonary disease, cystic fibrosis, lung cancer (primary or metastatic), pulmonary tuberculosis, pneumoconiosis, and intrathoracic endometriosis [7,8]. Among them, chronic obstructive pulmonary disease is the most common, accounting for about 70% of the cases. The clinical symptoms of primary spontaneous pneumothorax are typical, most of which occur at rest. Its symptoms include sudden chest pain with or without dyspnea. Different from the symptoms of primary spontaneous pneumothorax, patients with secondary spontaneous pneumothorax usually have more serious symptoms, especially in elderly patients with chronic obstructive pulmonary disease; even if the lung compression is low, there is obvious dyspnea

[9,10]. Secondary spontaneous pneumothorax often has high mortality and recurrence rate, especially in elderly patients. Regardless of the cause, spontaneous pneumothorax is still a serious condition affecting global health. At present, there are many treatment methods for spontaneous pneumothorax, such as conservative oxygen therapy, thoracic puncture and aspiration, closed thoracic drainage, bullae resection and repair, pleural fixation, and other methods [12-16]. The treatment plan differs depending on the volume of the pneumothorax, which is one of the important bases for deciding whether to carry out closed drainage or surgery. In this study, CT and X-ray examinations are taken as examples to analyze their application effects.

2. Data and methods

2.1. General information

Sixty-four patients with PSP, who received medical care from the Affiliated Hospital of Hebei University from January 2017 to December 2021, were selected as the research subjects. Among the patients, 40 were male, with an average age of 35.69 ± 3.69 , while 24 were female, with an average age of 36.98 ± 4.12 . The clinical data of the enrolled patients were complete and in line with the symptoms of primary spontaneous pneumothorax. The patients were self-aware and met the requirements of the ethics committee; the study excluded cases with incomplete clinical data and patients with allergies, disorders of consciousness, and communication barriers; the patients and their families had given consent to participate in the study.

2.2. Methods

Sixty-four patients were examined by X-ray and CT.

(1) X-ray examination

An X-ray machine (XG501A, Shanghai Medical Instrument Factory) was used to examine the patients with primary spontaneous pneumothorax.

(2) CT examination

The SOMATOM Definition Flash CT was used. The average effective dose required for thoracic CT scanning was 8 mSv to 40 mSv. The scanning parameters were set as follows: 5 mm spacing, 35 cm field of view, and 5 mm scanning layer thickness.

2.3. Observation indicators

X-ray and CT examinations were performed by specially trained personnel. The classification of pneumothorax was based on the films, in which those with a ratio of 1:4 were categorized under small pneumothorax, 1:4 to 1:2 were categorized under moderate pneumothorax, and those less than 1:3 were categorized under massive pneumothorax; the lesion density, enhancement, and morphology of the pneumothorax on the X-ray and CT films were observed.

2.4. Statistical analysis

SPSS 25.0 was used for data analysis. The count and measurement data were expressed in n/% and $\bar{x} \pm s$, respectively. χ^2 and t tests were performed, and the difference was considered statistically significant with $p < 0.05$.

3. Results

3.1. Clinical data analysis

The clinical analysis of 64 patients with PSP showed that the number of cases with unilateral pneumothorax was 42, accounting for 65.63%, whereas the number of cases with bilateral pneumothorax was 22, accounting for 34.37%. Among the cases with unilateral pneumothorax, the number of cases with left pneumothorax was 26, accounting for 61.90%, whereas the number of cases with right pneumothorax was 38.10%.

3.2. CT and X-ray features of primary spontaneous pneumothorax

In clinical diagnostic analysis, the diagnostic coincidence rate of 64 patients with primary spontaneous pneumothorax was 73.44% when examined by CT, of which the number of cases with small pneumothorax, moderate pneumothorax, and massive pneumothorax was 12, 24, and 28, respectively; using x-ray examination, the diagnostic coincidence rate of 64 patients with primary spontaneous pneumothorax was 92.19%, of which the number of cases with small pneumothorax, moderate pneumothorax, and massive pneumothorax was 16, 26, and 22, respectively (**Table 1**). The most common form of primary spontaneous pneumothorax involves the alveoli, with small penetrating shadows under the pleura, and some lesions having high density and irregular shape.

Table 1. CT and x-ray manifestations of 64 patients with primary spontaneous pneumothorax (n/%)

Group	Clinical diagnosis	Diagnostic coincidence rate	Small pneumothorax	Moderate pneumothorax	Massive pneumothorax
CT examination	64	47 (73.44)	12	24	28
X-ray examination	64	59 (92.19)	16	26	22
χ^2		6.8927			
p		0.0087			

4. Discussion

Primary spontaneous pneumothorax is a common clinical thoracic surgery condition that usually affects adolescent males. Studies have shown that PSP can be cured with conservative treatment, but the risk of recurrence is high. Hence, surgical treatment is recommended in clinical practice. With the rapid development of video-assisted thoracoscopic surgery, its efficacy and safety in the treatment of patients with PSP have been affirmed. At present, simple bullectomy and bullectomy combined with pleural fixation are the main thoracoscopic surgical methods in the treatment of patients with PSP. In view of the potential risk of bleeding and tissue damage from pleural fixation, employing pleural fixation to reduce postoperative recurrence rate remains a controversy [4]. However, numerous studies have reported that pleural fixation has been used in the treatment of patients with PSP, resulting in good prognosis [5].

CT is widely used in the qualitative and quantitative diagnoses of pneumothorax because at high-density resolution, there is no tissue overlap. In a study [15], CT was used to scan a lung model, in which the overall shape of the lung model was described using the axial images of each layer, and the functional lung area of the measured layer was calculated based on the area of the computer. The area of each layer was obtained, and the sum of the areas of all layers was calculated and multiplied by a fixed layer thickness to obtain the lung volume measured by CT. The actual volume of the lung model was measured by injecting a required amount of water into the lung model in the experiment. The injected amount of water reflected the actual lung volume. The results of the correlation analysis between CT measurement and actual lung volume revealed a high correlation between them. Hence, this method is considered a reliable method for measuring lung compression in patients with pneumothorax. In another study [16], several researchers approximated the degree of lung compression in pneumothorax to a fixed cross-section and used the ratio of chest area to gas area on the same plane. The arterial trunk plane was selected. When the degree of compression is weak, the median plane can be selected. In the study, the affected chest cavity and pneumothorax were obtained separately, and the total area of the affected chest cavity and the gas area were obtained.

Spontaneous pneumothorax is caused by a lung or pleural lesion, in which the lung pleura ruptures, causing gas to enter and accumulate in the pleural cavity through the ruptured lung pleura. Human lungs

are like elastic air bags, which can expand and contract. There are two layers of pleura covering the lungs: the visceral layer and the parietal layer. They form a closed chamber called the pleural cavity. When pneumothorax occurs, the pressure in the chest cavity rises, impairing the lungs' ability to expand, pressurizing the hilar, and even displacing the trachea and heart, thus eventually causing respiratory and circulatory failure.

4.1. Causes of spontaneous pneumothorax

The first is congenital developmental defects. This kind of pneumothorax is commonly seen in young adults aged 15 to 35, and most of them are male patients.

The second is lung diseases, such as pulmonary tuberculosis, chronic bronchitis with emphysema, bronchial asthma, bronchiectasis, pneumoconiosis, extensive pulmonary fibrosis, and lung cancer, which may cause pleural cavity cracks and eventually lead to pneumothorax. There are three types of spontaneous pneumothorax. The first is closed pneumothorax, which is characterized by small tear, rapid closure, and rapid lung recruitment. The second is open pneumothorax, in which air can enter and leave freely, and the pressure in the pleural cavity is equal to the atmospheric pressure. The third is tension pneumothorax, where a valve-like effect is created at the rupture. When inhaling, air enters the pleural cavity, but when exhaling, the valve closes, thus trapping the air. Hence, the intrathoracic pressure is higher than the atmospheric pressure.

4.2. Approaches to diagnosing spontaneous pneumothorax

Patients with spontaneous pneumothorax often present with shortness of breath, dry cough, and varying degrees of chest pain. Elderly patients may also have cyanosis, sweating, respiratory failure, and other symptoms. Patients with infection may have fever and an increase in leukocyte count. If blood vessels are damaged, hemothorax or even shock may occur. The following approaches can be used to identify whether the patient has spontaneous pneumothorax or not.

First, patients who develop spontaneous pneumothorax tend to experience sudden sharp or stinging chest pain. Coughing or deep inhalation may aggravate the pain. This can be explained by the pulling and tearing of the adhered pleura.

Second, patients with spontaneous pneumothorax tend to have dry cough, which is caused by the reflex stimulation of the pleura. With concurrent infection and bronchopleural fistula will worsen the cough and cause expectorated purulent sputum.

Third, if tension pneumothorax is not treated in time, shock may occur. In addition to dyspnea, patients may present with cyanosis, sweating, restlessness, unconsciousness, cold limbs, weakened pulse, decreased blood pressure, and other signs and symptoms.

Fourth, if cyanosis worsened after oxygen administration, or symptoms cannot be relieved by bronchodilator or hormonal therapy, shock or coma develops, and breath sounds are reduced on the affected side, spontaneous pneumothorax should be considered. Especially in elderly patients with respiratory diseases, if they are not treated in time, spontaneous pneumothorax may occur, but the symptoms may be occult. If there is a delay in diagnosis or treatment, their lives may be in danger. In addition, the primary condition may mask the signs and symptoms of spontaneous pneumothorax, resulting in delayed diagnosis. In order to identify potential risk factors, X-ray and CT examinations should be performed in time, the degree of lung compression should be evaluated, and tracheal deviation should be examined for.

4.3. Precautions for elderly patients with pneumothorax

In order to prevent the occurrence of spontaneous pneumothorax, elderly patients with lung diseases should take some precautions. First, it is necessary to control the underlying lung disease and strengthen the

treatment of chronic lung diseases, in order to prevent the occurrence of spontaneous pneumothorax from the root. Second, they should avoid breath holding activities, exertion, intense physical activity, and severe coughing, all which could induce spontaneous pneumothorax. Third, pneumothorax in elderly patients is often complicated with heart disease. Their clinical manifestations are similar to other cardiopulmonary emergencies, and the risk is high. These patients should consult their doctors as soon as symptoms appear to avoid delaying treatment.

5. Conclusion

In conclusion, the detection accuracy of CT is higher than that of X-ray examination, which may improve the treatment effect in primary spontaneous pneumothorax, ensure the accuracy of findings, and facilitate follow-up treatment as well as postoperative effect analysis.

Funding

Baoding Science and Technology Planning Project (Project Number: 1941ZF088)

Disclosure statement

The authors declare no conflict of interest.

References

- [1] Yang J, Hu X, Li J, et al., 2022, Correlative Analysis of lung CT Findings in Patients with Birt-Hogg-Dube Syndrome and the Occurrence Of Spontaneous Pneumothorax: A Preliminary Study. *BMC Medical Imaging*, 22(1): 1–8.
- [2] Lee SH, Lee SG, Cho SH, et al., 2022, Outcomes of Single-Incision Thoracoscopic Surgery Using the Spinal Needle Anchoring Technique for Primary Spontaneous Pneumothorax. *Journal of Chest Surgery*, 55(1): 44.
- [3] Wu W, 2021, Comparative Study on the Effect of VATS and VAMT on the Clinical Efficacy of Patients with Spontaneous Pneumothorax. *Gansu Science and Technology*, 37(20): 126–128.
- [4] Duffy A, Ward J, Malvika B, et al., 2021, Ambulatory Management of Primary Spontaneous Pneumothorax. *Breathe*, 17: 200342. <https://doi.org/10.1183/20734735.0342-2020>
- [5] Huang Y, Ma R, Li G, et al., 2021, Thoracoscopic Bullectomy Combined with Pleural Fixation in the Treatment of Spontaneous Pneumothorax in Adolescents. *Clinical Medical Engineering*, 28(05): 561–562.
- [6] Xu T, 2020, Clinical Diagnostic Value of Observing Chest CT in Chest Radiograph Negative Spontaneous Pneumothorax. *China Medical Device Information*, 26(04): 148–149.
- [7] Gong L, Luo W, Wang Y, 2016, Clinical Summary of Spontaneous Pneumothoracic Surgery in 34 Young Adults. *Shenzhen Journal of Integrated Traditional Chinese and Western Medicine*, 26(11): 86–88.
- [8] Luo X, 2016, Clinical Experience of Patients with Spontaneous Pneumothorax. *World Latest Medical Information Abstracts*, 16(47): 120 + 125.
- [9] Wang C, 2016, Clinical Characteristics of Spontaneous Pneumothorax in Women. Southeast University.
- [10] Gong L, Luo W, Wang W, et al., 2016, Clinical Analysis of 22 Cases of Concealed Spontaneous Pneumothorax. *Chinese Primary Medicine*, 23(09): 1387–1389.

- [11] Liu X, 2016, Electrocardiogram Analysis of Patients with Spontaneous Pneumothorax. *Gansu Medicine*, 35(03): 209–211.
- [12] Feng W, Bai X, 2016, Research Progress of Spontaneous Pneumothorax. *Journal of Practical Medical Technology*, 23(01): 48–51.
- [13] Hou X, 2015, X-ray Manifestations and Clinical Analysis of Spontaneous Pneumothorax. *Everyone Health (Academic Edition)*, 9(21): 60.
- [14] Jiang D, 2015, The Diagnostic Value of X-ray and CT in Spontaneous Pneumothorax. *Chinese Medical Guide*, 13(20): 122–123.
- [15] Bu X, 2013, CT Measurement of Trachea and Thoracic Diameter Line in Young Patients with Spontaneous Pneumothorax and Its Related Factors Analysis. Dalian Medical University.
- [16] Huang D, Lu Y, Li Q, et al., 2009, CT Diagnostic Value Analysis of a Small Amount of Spontaneous Pneumothorax. *Journal of Youjiang Medical College for Nationalities*, 31(03): 457–458.

Publisher's note

Bio-Byword Scientific Publishing remains neutral with regard to jurisdictional claims in published maps and institutional affiliations.

Diagnostic Value of Serum TSH, Ultrasound, and Enhanced CT in Papillary Thyroid Carcinoma with Lymph Node Metastasis

Meiqing He*, Xixi Zhang, Hui Li, Tian Wang

Ultrasonic Diagnosis Center of Shaanxi Provincial People's Hospital, Xi'an 710068, Shaanxi Province, China

*Corresponding author: Meiqing He, hmq359340106@sina.com

Copyright: © 2022 Author(s). This is an open-access article distributed under the terms of the Creative Commons Attribution License (CC BY 4.0), permitting distribution and reproduction in any medium, provided the original work is cited.

Abstract: *Objective:* To explore the diagnostic value of serum TSH, ultrasound, and enhanced CT in papillary thyroid carcinoma with lymph node metastasis. *Methods:* 168 patients who underwent thyroidectomy in Shaanxi Provincial People's Hospital from January 2020 to December 2021 were selected as the research subjects. Based on the pathological nature (benign or malignant), they were divided into two groups, with 86 patients in the control group and 82 patients in the study group. Based on whether the pathology was accompanied with lymph node metastasis, the PTC group was divided into a lymph node metastasis group and a non-lymph node metastasis group, with 51 and 31 patients in the respective groups. Retrospective analysis was conducted to observe and analyze the pathological results of the thyroid nodules' thyroid ultrasound results, neck enhanced CT results, and thyroid function test serology results. *Results:* Compared with the PTC group, there were significant differences in TR classification, ultrasonic lymph nodes, and enhanced CT lymph nodes, but no significant differences in the course of disease, nodule distribution, and the number of nodules between the benign nodule group and PTC group; in the comparison of lymph node metastasis using ultrasound and enhanced CT, the number of patients with ultrasound lymph nodes without abnormal metastasis in the non-metastasis group was 28, while that of the metastasis group was 21; the number of patients with abnormal metastasis in the non-metastasis group was 3, while that of the metastasis group was 30. The number of patients with a single node without metastasis and metastasis was 14 and 8, respectively, whereas the number of patients with multiple nodes without metastasis and metastasis was 17 and 43, respectively. There were statistically significant differences in the number of ultrasound lymph nodes and nodules, but no statistically significant differences in TR classification, enhanced CT lymph nodes, nodules distribution, and disease course. *Conclusion:* Serum TSH can be used to identify the nature (benign and malignant) of thyroid nodules, and enhanced CT is better than ultrasound when evaluating complex lesions. It can be used as a supplement to ultrasound based on clinical context.

Keywords: Serum TSH; Ultrasound; CT; Thyroid papillary carcinoma; Lymph node

Online publication: July 28, 2022

1. Introduction

Papillary thyroid carcinoma is a differentiated thyroid carcinoma with high incidence rate, and 30% to 80% of patients will have cervical lymph node involvement. Lymph node metastasis is an important risk factor for the recurrence of thyroid cancer. The presence of cervical lymph node metastasis is an important basis for determining the clinical stage and treatment options ^[1]. Cervical lymph node tuberculosis is a common extrapulmonary tuberculosis, mainly manifested by cervical lymph node enlargement. In late stages, it may develop into a fistula, which requires a substantial amount of time to heal ^[2]. Before surgery, ultrasound

can precisely locate lymph nodes and provide a qualitative diagnosis. It is possible to detect lymph node metastases in 33% to 39% of cases with negative clinical palpation. The outline and enhancement pattern of lymph nodes can be appreciated in contrast-enhanced ultrasound, thus providing reference in clinical practice. With the continuous development of CT, there is a close relationship between the morphological features of primary thyroid cancer and lymph node metastasis, especially the texture features, such as microvessel density, new lymphatic vessel density, and elastic fiber distribution, which are all closely related to the degree of CT enhancement in primary thyroid cancer and can be used as an evaluation index of tumor malignancy as well as metastatic potential [3]. Serum thyroid markers are commonly detected by clinical immunological methods, among which calcitonin is useful in detecting medullary thyroid cancer [4], while other commonly used traditional serological tumor markers, such as carcinoembryonic antigen, have little reference significance for thyroid cancer. Studies have shown that the levels of thyroid stimulating hormone (TSH) [5], thyroglobulin [6], and thyroid autoantibody are all related to the occurrence of thyroid cancer [7].

2. Data and methods

2.1. General information

Hundred-and-sixty-eight patients who underwent thyroidectomy in Shaanxi Provincial People's Hospital from January 2020 to December 2021 were selected as the research subjects. According to the pathological nature (benign or malignant), they were divided into two groups, namely, with 86 cases in the control group and 82 cases in the study group. The average age of the patients was 49.63 ± 2.96 years. According to whether the pathology was accompanied by lymph node metastasis, the PTC group was divided into a lymph node metastasis group and a non-lymph node metastasis group, with 51 and 31 patients, respectively. Retrospective analysis was carried out, indicating no statistical difference in the general data of the patients. Moreover, the clinical data of all the patients were complete, and all patients underwent thyroidectomy.

2.2. Methods

(1) Contrast enhanced ultrasound

Toshiba Aplio 400, a color doppler ultrasound, with probe frequency of 7.5~13.0 MHz was used. SonoVue, produced by the Italian Bracco Group, was used as the contrast agent, and 5 ml of normal saline was added to form a suspension. The patients assumed a horizontal or lateral position and exposed their necks fully. The largest lymph node was selected as the subject of observation. Routine ultrasound was used to observe its zoning, the ratio of long to short diameter, lymph hilus, internal necrosis, calcification, blood flow distribution (lymph hilus type, peripheral type, mixed type, and no blood flow type), and resistance index. Then, contrast-enhanced ultrasound was performed. The patients were instructed to breathe quietly and avoid swallowing as much as possible; 2 ml of contrast agent was rapidly injected through the vein located at the elbow, and 5 ml of normal saline was then used to flush the tube. At the same time, the start timing key and dynamic storage key were pressed, and the perfusion process of the contrast agent in the enlarged lymph nodes was recorded. According to the echo changes of lymph nodes before and after contrast-enhanced ultrasound, the lymph node enhancement modes were divided into homogeneous enhancement, heterogeneous enhancement, and non-enhancement. Non-uniform enhanced lymph nodes were divided into non-ring (no ring enhancement after enhancement), thin ring (enhanced ring thickness ≤ 2.0 mm), and thick ring (enhanced ring thickness > 2.0 mm) according to the thickness of circular enhancement [8-10], which refers to the circular hyperecho around the lymph nodes, where the degree of echo enhancement is greater than that in the inner and peripheral parenchyma of the lymph nodes; the reinforced ring was measured at the thickest point.

(2) Serum TSH

Each patient's venous blood was drawn from the anterior elbow on an empty stomach in the morning, and serum TSH level was detected by double-antibody sandwich method. All procedures were carried out in strict accordance with the instructions given on the kit.

(3) CT quantitative parameter determination

All patients underwent PTC resection and received CLNM (central lymph node metastasis) pathological examination. Routine plain CT scan and dual-phase, dual-energy enhanced CT scan of the neck were done before surgery. The dual-source CT machine and data processing workstation were used for plain neck CT and dual-phase arteriovenous scan. The scanning parameters were set as follows: the voltage was 100 kV, the pitch was 0.8, the layer thickness was 1.0 mm, and the layer spacing was 0.7 mm. The patients assumed the supine position with their shoulders relaxed. Their lower jaws were raised as much as possible, and the patients were requested to refrain from swallowing during the examination. The scanning range was from the skull base to the aortic arch, and the moving direction of the probe scanning was from the foot to the head. The conventional scanning mode was set for plain scanning, and the dual energy mode was used for enhanced scanning. Iohexol and ioversol (300 mg I/ml) were used as contrast agents; the dose was 1.5 to 2.0 ml/kg, and the total amount was 95 to 100 ml. During scanning, the trigger threshold was set to 100 HU, and arterial phase scanning and venous phase scanning were performed successively.

2.3. Observation indicators

The pathological results of the thyroid nodules, thyroid ultrasound results, neck enhanced CT results, and thyroid function test serology results were observed and analyzed.

2.4. Statistical analysis

SPSS 25.0 was used to analyze the data. The counting and measuring data were expressed in n/% and $\bar{x} \pm s$, respectively, and χ^2 test was carried out. T-test showed that the difference was statistically significant ($p < 0.05$).

3. Results

3.1. Comparison of disease course, ultrasound results, and enhanced CT results between benign nodule group and PTC group

There were significant differences in TR classification, ultrasound lymph nodes, and enhanced CT lymph nodes, but no significant differences in the course of disease, nodule distribution, and number of nodules between the benign nodule group and the PTC group, as shown in **Table 1**.

Table 1. Comparison of disease course, ultrasound results, and enhanced CT results between benign nodule group and PTC group

Group	Benign nodule (n = 86)	PTC group (n = 82)	\bar{x}	p	
Course of disease	< half a year	26	24	0.5709	0.9031
	< 1 year	32	29		
	< 5 years	6	7		
	< 10 years	10	12		
	≥ 10 years	12	10		

(Continued on next page)

(Continued from previous page)

Group		Benign nodule (n = 86)	PTC group (n = 82)	\bar{x}	<i>p</i>
Nodule distribution	Unilateral	45	46	0.2406	0.6238
	Bilateral	41	36		
Number of nodules	Single	39	40	0.1984	0.6560
	Multiple	47	42		
Ultrasound TR classification	TR3	42	4	46.1672	< 0.05
	TR4	26	62		
	TR5	18	16		
Ultrasound lymph nodes	No abnormality	76	21	67.7625	< 0.05
	Abnormal	10	61		
Enhanced CT lymph nodes	No abnormality	50	24	14.1969	< 0.05
	Abnormal	36	58		

3.2. Comparison of lymph node metastasis with ultrasound and enhanced CT

In the comparison of lymph node metastasis with ultrasound and enhanced CT results, the number of patients with ultrasound lymph nodes without abnormality in the non-metastasis group was 28, while that of the metastasis group was 21; the number of patients with abnormal ultrasound lymph nodes in the non-metastasis group was 3, while that of the metastasis group was 30. The number of patients with single node without metastasis and metastasis was 14 and 8, respectively, whereas the number of patients with multiple nodes without metastasis and metastasis was 17 and 43, respectively. There were statistically significant differences in the number of ultrasound lymph nodes and nodules, but no statistically significant differences in TR classification, enhanced CT lymph nodes, nodules distribution, and course of disease as shown in **Table 2**.

Table 2. Comparison of lymph node metastasis with ultrasound and enhanced CT

Group		Non-lymph node metastasis (n = 31)	Lymph node metastasis (n=51)	\bar{x}	<i>p</i>
Ultrasound TR classification	TR3	10	19	0.2399	0.8870
	TR4	11	16		
	TR5	10	16		
Ultrasound lymph nodes	No abnormality	28	21	19.3648	< 0.05
	Abnormal	3	30		
Enhanced CT lymph nodes	No abnormality	22	38	0.1232	0.7256
	Abnormal	9	13		
Nodule distribution	Unilateral	12	24	0.5457	0.4601
	Bilateral	19	27		
Course of disease	< half a year	8	16	1.0866	0.7803
	< 1 year	5	11		
	< 5 years	6	9		
	< 10 years	7	8		
Number of nodules	≥ 10 years	5	7	8.5326	< 0.05
	Single	14	8		
	Multiple	17	43		

4. Discussion

Accurately determining the presence of cervical lymph node metastases in PTC prior to surgery is crucial for determining the extent of neck lymph node dissection. At present, conventional ultrasound is widely used in the evaluation of cervical lymph node status before surgery and has proven to have high sensitivity. However, the qualitative diagnosis of lymph nodes with both benign and malignant characteristics is often challenging. Contrast-enhanced ultrasound (CEUS), as a microvascular imaging technique, can display the distribution of smaller blood vessels in the lymph nodes. Despite the fact that there are several studies on the use of CEUS in studying lymph nodes, there are more qualitative analyses than quantitative analyses, and the majority of earlier literatures have selected whole lymph nodes as the region of interest (ROI). The difference with previous studies is that the central and peripheral regions of lymph nodes were selected as ROI in this study to refine the analysis of the characteristics of lymph node outcomes and their quantitative parameters were analyzed to reduce the impact of subjective factors and individual differences.

Routine tests related to thyroid function include TSH, FT3, FT4, TG, anti-TG, anti-TPO, TSH receptor antibody, and calcitonin. TSH and FT3 are commonly used to evaluate thyroid function. Anti-TPO and anti-TG are commonly used to diagnose and differentiate Hashimoto's thyroiditis and Graves' disease. Calcitonin is an important marker of medullary thyroid carcinoma. Some studies have shown that the serum TSH level of patients with malignant thyroid nodules is higher than that of patients with benign diseases. In more aggressive tumors, TSH increases in proportion ^[11]. This study revealed that preoperative serum TSH concentration could independently predict thyroid nodule malignancy. The reason may be that the combination of TSH and receptors on thyroid cells can activate many growth promoting pathways in normal and malignant thyroid cells. Therefore, high-dose levothyroxine can be used to inhibit TSH after thyroidectomy to prevent recurrence. However, some studies have shown that the effect of inhibiting TSH on differentiated thyroid cancer is poor ^[12], in which its mechanism requires further investigation. The differentiation methods of thyroid nodules recommended by the current guidelines include four components: clinical history and examination, serum TSH, ultrasound examination, and fine needle aspiration examination if necessary. If the serum TSH level is low, thyroid scanning should be performed to distinguish between solitary hot nodules in multiple thyroid nodules, thyrotoxic goiter with multiple nodules, or less common, thyroiditis or Graves' disease. Despite being easy to operate and has few contraindications, ultrasound is highly operator-dependent. Therefore, thyroid ultrasonography should be performed on palpable nodules by professionals with rich experience in this field. Despite the fact that the current high-resolution ultrasound can detect very small lesions, it still can clearly display superficial organs and tissues. However, the guidelines suggest that routine thyroid cancer screening is not recommended except for high-risk groups, because the detection of early thyroid cancer has not been shown to improve the survival rate. Based on the clinical and ultrasound risk factors for thyroid cancer, fine needle aspiration should only be performed for nodules ≥ 1.0 cm ^[13-15].

In conclusion, serum TSH can be used to identify the benign and malignant nature of thyroid nodules, and enhanced CT is better than ultrasound in evaluating complex lesions. It can be used as a supplement to ultrasound based on clinical context.

Disclosure statement

The authors declare no conflict of interest.

References

- [1] Wang M, Wang X, Li L, 2022, Study on the Characteristics of cervical Lymph Node Metastasis and Related Factors in Papillary Thyroid Carcinoma. *Journal of Practical Cancer*, 37(03): 520–522.

- [2] Zhang X, Deng W, Zhang Y, 2022, Progress in the Application of Ultrasonomics in Evaluating the Invasiveness of Thyroid Papillary Carcinoma. *Chinese Journal of Medical Imaging*, 30(03): 287–290.
- [3] Jia X, Zhang Y, 2022, Application of Ultrasound Combined with CT in the Diagnosis of Cervical Lymph Node Metastasis of Thyroid Papillary Carcinoma. *Imaging Research and Medical Applications*, 6(06): 191–193.
- [4] Zuo P, Yang J, 2022, Analysis of Maternal and Fetal Outcomes of Postoperative Pregnancy Patients with Thyroid Papillary Carcinoma. *Chinese Journal of Obstetrics and Gynecology*, 23(02): 157–159.
- [5] Li J, Wang Y, Liu H, Guo Q, et al., 2022, Clinical Application Value of High Frequency Ultrasound Combined with CT in Thyroid Papillary Carcinoma. *Chinese Journal of CT and MRI*, 20(03): 29–31.
- [6] Wang D, Wang D, Liang R, et al., 2021, Ultrasonic Features and Elastographic Diagnosis of Thyroid Papillary Carcinoma. *Chinese Journal of Clinical Health Care*, 24(06): 847–850.
- [7] Sun Y, Wu H, 2021, Relationship Between Serum miRNA-221, miRNA-451 Expression and Pathological Features and Prognosis in Patients with Papillary Thyroid Carcinoma. *Zhejiang Medical Journal*, 43(20): 2190–2193.
- [8] Miao X, Liu P, Kan Y, et al., 2021, Immune Cell Infiltration Pattern and Prognosis of Papillary Thyroid Carcinoma with Cervical Lymph Node Metastasis. *Chinese Journal of Endocrine Surgery*, 15(05): 488–493.
- [9] Xu H, Pan J, Gong X, et al., 2021, Predictive Value of CT Enhancement Combined with Thyroglobulin and Antibody in Cervical Lymph Node Metastasis of Thyroid Papillary Carcinoma. *Medical Information*, 34(20): 119–121 + 128.
- [10] Du K, Dong G, 2021, Clinical Efficacy and Safety of Ultrasound-Guided Radiofrequency Ablation for Thyroid Papillary Carcinoma. *Basic and Clinical Oncology*, 34(05): 378–381.
- [11] Zheng H, Chen W, Cai K, et al., 2021, Ultrasonic Elastography Characteristics of Thyroid Papillary Carcinoma and Its Correlation with Laboratory Detection Indexes. *Journal of Clinical Ultrasound Medicine*, 23(09): 708–710.
- [12] Liang Z, Shao Y, Chen L, et al., 2021, Study on the Influencing Factors of Lymph Node Metastasis in the Central Region of Multifocal Thyroid Micropapillary Carcinoma. *Chinese Journal of Ultrasound Medicine*, 37(09): 971–973.
- [13] Liu Y, Wu X, Li K, et al., 2021, The Value of Ultrasound-Guided Expression of Two Indicators in Predicting Cervical Lymph Node Metastasis in Patients with Thyroid Papillary Carcinoma. *Journal of Practical Clinical Medicine*, 25(17): 105–108 + 113.
- [14] Shu Y, Tian M, Han Z, et al., 2021, The Predictive Value of Lymph Node Size in CT Examination for Ipsilateral Central Group Lymph Node Metastasis of Single Thyroid Papillary Carcinoma. *Chinese Journal of Endocrine Surgery*, 15(04): 373–376.
- [15] Liu N, Xie Y, Huang Z, et al., 2021, Prediction of Cervical Lymph Node Metastasis of Thyroid Papillary Carcinoma Based on CT Enhanced Imaging Model. *Radiology Practice*, 36(08): 971–975.

Publisher's note

Bio-Byword Scientific Publishing remains neutral with regard to jurisdictional claims in published maps and institutional affiliations.

Effects of Different Doses of BDNF on Postoperative Cognitive Function in Aged Rats Undergoing Abdominal Surgery

Yuming Zhang¹, Hui Wang¹, Kai Lu¹, Jun Wang², Ning Bai^{1*}

¹Department of Anesthesiology, Shaanxi Provincial People's Hospital, Xi'an 710068, Shaanxi Province, China

²Department of Anesthesiology, Shaanxi Provincial Cancer Hospital, Xi'an 710061, Shaanxi Province, China

*Corresponding author: Ning Bai, ningbai202207@sina.com

Copyright: © 2022 Author(s). This is an open-access article distributed under the terms of the Creative Commons Attribution License (CC BY 4.0), permitting distribution and reproduction in any medium, provided the original work is cited.

Abstract: *Objective:* To investigate the effects of different doses of BDNF on postoperative cognitive function in aged rats undergoing abdominal surgery. *Methods:* 72 aged healthy male SD rats of SPF grade were selected. According to the random number table method, the rats were randomly divided into the control group, model group, low dose BDNF injection group, and high dose BDNF injection group, with 18 rats in each group. The model group, low dose group, and high dose group underwent abdominal surgery after anesthesia, and 5 μ L/time of BDNF was intranasally administered to the rats in the low dose and high dose groups 6 hours after abdominal surgery, of which the dose of the low dose group was 0.1 g/L, while that of the high dose group was 0.2 g/L. The drug was administered alternately through both nostrils, with an interval of 2 minutes each time, for 5 times. The control group did not undergo surgery after anesthesia. The escape latency and swimming distance of the four groups of rats were compared before surgery, the first day, the third day, and the seventh day after surgery; similarly, the BDNF protein expression level in the hippocampus of the four groups of rats was compared on the first day, the third day, and the seventh day after surgery. *Results:* The escape latency and swimming distance of the control group were not statistically significant on the first day, the third day, and the seventh day after surgery, $p > 0.05$; the escape latency and swimming distance of the model group, low dose group, and high dose group on the first day, the third day, and the seventh day after surgery were statistically significant, $p < 0.05$. Before surgery, the escape latency and swimming distance of the four groups were not statistically significant, $p > 0.05$; on the first day, the third day, and the seventh day after surgery, the escape latency and swimming distance of the model group $>$ low dose group $>$ high dose group $>$ control group, $p < 0.05$. The BDNF protein expression level in the hippocampus of the control group on the first day, the third day, and the seventh day after surgery showed no statistical significance $p > 0.05$; the expression level of BDNF protein in the hippocampus of the model group, low dose group, and high dose group on the first day, the third day, and the seventh day after surgery was statistically significant, $p < 0.05$. On the first day, the third day, and the seventh day after surgery, the expression level of BDNF protein in the hippocampus of the model group $<$ low dose group $<$ high dose group $<$ control group, $p < 0.05$. *Conclusion:* Compared with 0.1 g/L of BDNF, 0.2 g/L of BDNF can improve the postoperative cognitive function of aged rats undergoing abdominal surgery.

Keywords: BDNF; Abdominal surgery; Aged rats; Postoperative cognitive function

Online publication: July 28, 2022

1. Introduction

Studies have found that surgical stimulation can lead to vasoconstriction and cause a rise in blood pressure

[1]. Anesthetics can reduce negative cardiovascular effects and blood pressure, as well as result in an imbalance of oxygen supply to the brain under the dual effects of anesthesia and surgery, thus affecting brain oxygen saturation and increasing the tendency for postoperative cognitive dysfunction. At the same time, age is a major risk factor for postoperative cognitive dysfunction [2]. Studies have found that the incidence of cognitive dysfunction in patients aged 60-69 years is about 23% one week after surgery, while the incidence of cognitive dysfunction in patients over 70 years old is about 29% [3]. The incidence of cognitive dysfunction in the elderly over 70 years old three months after surgery is about 14%, indicating that the incidence of cognitive dysfunction increases with age, which may be attributed to the decrease of brain oxygen saturation with age, resulting in cognitive dysfunction [4]. In recent years, the aging population in China has been increasing, along with the proportion of surgery among the elderly, which in turn increases the incidence of postoperative cognitive dysfunction [5]. Brain-derived neurotrophic factor (BDNF) is a small molecular protein isolated from pig brain. The amino acid coding sequence of BDNF in humans, rats, and pigs is identical. Additionally, its sequence of nerve growth factor is similar, and it is also a member of the nerve growth factor family [6-8]. Laboratory studies have found that BDNF is negatively correlated with the severity of postoperative cognitive function in aged rats. Therefore, this time, aged rats undergoing abdominal surgery were given different doses of BDNF to analyze its effects on postoperative cognitive function, so as to provide a basis for improving the severity of postoperative cognitive dysfunction in elderly patients.

2. Materials and methods

2.1. Study population

A total of 72 SPF-grade healthy aged male SD rats, with age ranging from 18-20 months and weight ranging from 480-600 g, were purchased from the Animal Center of School of Medicine, Xi'an Jiaotong University. After a week of adaptive feeding, the rats were randomly divided into a control group, model group, low dose BDNF injection group, and high dose BDNF injection group, with 18 rats in each group, based on the random number table method.

2.2. Reagents and instruments

BDNF antibody was purchased from Biosharp Company, China, Western blot kit was purchased from Wuhan Seville Biotechnology Co., Ltd., Morris water maze equipment was purchased from Nanjing Calvin Biotechnology Co., Ltd., and BDNF protein was purchased from American Sigma Corporation.

2.3. Study design

All 72 rats were anesthetized, in which the rats in the model group, low dose group, and high dose group were anesthetized via intraperitoneal injection with 10% chloral hydrate at a dose of 0.3 ml/100 g. After the loss of righting reflex, the rats were fixed in a supine position, and their abdominal skin was disinfected. In each rat, a longitudinal incision of about 3 cm was made 0.5 cm below the ribs along the abdominal midline, and then abdominal exploration of the stomach, liver, large intestine, and small intestine was performed every 5 minutes. The operation time was set to 20 minutes, and thereafter, the abdominal cavity was closed. The control group did not undergo surgery after anesthesia.

For the low dose and high dose groups, the rats were anesthetized and placed in a supine position, their heads and necks were raised, and 5 μ L/time of BDNF was administered intranasally using a micro-syringe six hours after abdominal surgery. The low dose group received 0.1 g/L, while the high dose group received 0.2 g/L. The drug was administered alternately through both nostrils, with an interval of 2 minutes each time, for 5 times.

2.4. Observation indicators

- (1) Water maze test [6] was performed before surgery on the first day, the third day, and the seventh day after surgery, and the escape latency and swimming distance of the four groups were recorded.
- (2) After completing the water maze test on the seventh day, the rats in the two groups were killed, and the BDNF protein expression level in the hippocampus of the four groups was detected by Western blot.

2.5. Statistical analysis

SPSS 23.0 was used for analysis; counting data were expressed in frequency and analyzed by Chi-square test; measurement data were expressed as $\bar{x} \pm s$ and tested by one-way ANOVA. $p < 0.05$ was considered statistically significant.

3. Results

3.1. Comparison of escape latency and swimming distance of rats in the four groups before surgery, the first day, the third day, and the seventh day after surgery

The escape latency and swimming distance of the control group were not statistically significant on the first day, the third day, and the seventh day after surgery, $p > 0.05$; the escape latency and swimming distance of the model group, low dose group, and high dose group on the first day, the third day, and the seventh day after surgery were statistically significant, $p < 0.05$. Before surgery, the escape latency and swimming distance of the four groups were not statistically significant, $p > 0.05$; on the first day, the third day, and the seventh day after surgery, the escape latency and swimming distance of the model group $>$ low dose group $>$ high dose group $>$ control group, with $p < 0.05$.

Table 1. Comparison of escape latency and swimming distance of rats in the four groups before surgery, the first day, the third day, and the seventh day after surgery (n = 18, $\bar{x} \pm s$)

Group	Escape latency (s)				F/p	Swimming distance (cm)				F/p
	Pre-operation	Post-operation				Pre-operation	Post-operation			
		1d	3d	7d			1d	3d	7d	
Control	24.71 ± 3.67	24.91 ± 4.67	24.81 ± 3.02	24.82 ± 3.09	0.009/0.999	353.10 ± 78.09	356.02 ± 82.34	360.99 ± 82.36	358.99 ± 77.67	0.033/0.992
Model	24.92 ± 4.02	46.31 ± 5.21	43.31 ± 7.61	34.67 ± 6.03	48.406/ < 0.001	352.89 ± 81.02	729.89 ± 106.56	658.02 ± 105.77	526.56 ± 87.62	52.936/ < 0.001
Low dose	24.78 ± 3.89	36.34 ± 5.23	34.10 ± 4.23	30.78 ± 5.12	21.195/ < 0.001	352.99 ± 84.23	687.92 ± 89.78	624.10 ± 92.13	476.89 ± 76.54	58.372/ < 0.001
High dose	24.78 ± 4.12	28.76 ± 4.99	26.56 ± 3.90	25.34 ± 4.12	3.139/ 0.031	352.89 ± 85.10	644.10 ± 85.23	591.32 ± 87.34	423.13 ± 65.43	51.444/ < 0.001
F	0.009	63.333	34.400	17.818		0.000	61,681	38.228	15.635	
p	9.999	< 0.001	< 0.001	< 0.001		1.000	< 0.001	< 0.001	< 0.001	

3.2. Comparison of BDNF protein expression level in the hippocampus of rats in the four groups on the first day, the third day, and the seventh day after surgery

The comparison of BDNF protein expression level in the hippocampus of the control group on the first day, the third day, and the seventh day after surgery showed no statistical significance, $p > 0.05$; the expression level of BDNF protein in the hippocampus of the model group, low dose group, and high dose group on the first day, the third day, and the seventh day after surgery was statistically significant, $p < 0.05$. On the first day, the third day, and the seventh day after surgery, the expression level of BDNF protein in the

hippocampus of the model group < low dose group < high dose group < control group, with $p < 0.05$.

Table 2. Comparison of BDNF protein expression level in the hippocampus of rats in the four groups on the first day, the third day, and the seventh day after surgery (n = 18, $\bar{x} \pm s$)

Group	Post-operation 1d	Post-operation 3d	Post-operation 7d	F/p
Control	148.02±15.81	149.02±14.88	148.99±15.45	0.025//0.975
Model	89.16±8.25	99.03±10.23	105.76±9.23	14.596/<0.001
Low dose	100.34±11.34	105.45±13.12	120.78±12.13	13.643/<0.001
High dose	123.67±12.45	124.10±15.34	134.13±14.23	3.191//0.049
F	81.690	49.372	36.472	
p	<0.001	<0.001	<0.001	

4. Discussion

Memory and learning are both major cognitive functions. Elderly patients often have cognitive dysfunction after surgery. These patients will show changes in personality, mental activities, cognitive ability, social activities, and other functions. In addition to reduced social ability, their attention, memory, and language ability are also affected. These are caused by the joint action of many factors, which seriously affect the quality of life of elderly patients undergoing surgery [9-11]. BDNF is a neurotrophic factor synthesized by the central nervous system and widely found in various brain tissues. It can improve brain injury. The stress effect of surgery on elderly patients causes certain damage to their brain tissues [12-14]. This paper analyzed the effect of exogenous BDNF on brain injury, a topic that has garnered increasing attention in recent years [15].

The results showed that the escape latency, swimming distance, and BDNF protein expression level in the hippocampus of the control group on the first day, the third day, and the seventh day after surgery were not statistically significant, whereas the escape latency, swimming distance, and BDNF protein expression level in the hippocampus of the model group, low dose group, and high dose group on the first day, the third day, and the seventh day after surgery were statistically significant. The escape latency, swimming distance, and BDNF protein expression level in the hippocampus of the four groups on the first day, the third day, and the seventh day after surgery were statistically significant. The escape latency and swimming distance of the model group > low dose group > high dose group > control group, while the expression level of BDNF protein in the hippocampus of the model group < low dose group < high dose group < control group, with $p < 0.05$. This shows that BDNF can improve the postoperative cognitive function of aged rats undergoing abdominal surgery. The effect of high-dose BDNF was found better than that of low-dose BDNF. BDNF is composed of 120 proteins, which are mainly mediated by two transmembrane proteins: low-affinity neurotrophin receptor and high-affinity receptor TrkB [16]. When BDNF binds to TrkB extracellular ligand binding region, autophosphorylation and substrate phosphorylation occur, thus information is transmitted from cell membrane to nucleus, resulting in cellular response effect, which improves brain injury and reduces postoperative cognitive dysfunction in aged rats [17,18].

In conclusion, compared with 0.1 g/L of BDNF, 0.2 g/L of BDNF can improve the postoperative cognitive function of aged rats undergoing abdominal surgery.

Funding

Key Research and Development Program of Shaanxi Province (2021SF-288)

Natural Science Basic Research Program of Shaanxi Province (2020JQ-950, 2022JM-570)

Health Research Program of Shaanxi Province (2022D002)

Incubation Fund of Shaanxi Provincial People's Hospital (2018YXQ-07)

Disclosure statement

The authors declare no conflict of interest.

References

- [1] Wu X, Zhou Z, Wang H, et al., 2021, Feasibility of Cerebral Blood Flow / Cerebral Oxygen Metabolic Rate in Predicting Postoperative Cognitive Dysfunction in Elderly Patients Undergoing Non Cardiac Surgery. *Zhejiang Medical Journal*, 43(7): 716–720.
- [2] Shi J, He P, Zhao C, et al., 2021, Sedative Effect of Dexmedetomidine Combined with Spinal Anesthesia in Elderly Patients and Analysis of Risk Factors Affecting Postoperative Cognitive Dysfunction. *International Journal of Geriatrics*, 42(3): 158–162.
- [3] Liu D, Wu X, Pu G, et al., 2021, Construction and Validation of a Predictive Model for Postoperative Cognitive Impairment in Elderly Patients Undergoing Abdominal Surgery Under Non General Anesthesia. *Nursing Research*, 35(21): 3780–3784.
- [4] Cai S, Ye L, Zhang P, et al., 2021, Effects of Different Anesthesia Methods on Postoperative Cognitive Function and Peripheral Blood High Mobility Group Protein B1 in Elderly Patients Undergoing Gastrointestinal Surgery. *Journal of Practical Clinical Medicine*, 25(4): 41–44.
- [5] Chen Z, Li Z, Li S, 2021, Effects of Dexmedetomidine on Postoperative Cognitive Function, Brain Oxygen Metabolism and Delirium in Elderly Patients with Hip Fracture Surgery. *Hainan Medical Journal*, 32(21): 2762–2765.
- [6] Turkkahraman D, Sirazi EC, Aykal G, 2022, Serum Alpha-Melanocyte-Stimulating Hormone (A-MSH), Brain-Derived Neurotrophic Factor (BDNF), and Agouti-Related Protein (AGRP) Levels in Children with Prader-Willi or Bardet-Biedl Syndromes. *Journal of Endocrinological Investigation*, 45(5): 1031–1037.
- [7] Guo M, Dong L, Liu X, et al., 2021, Effect of Dexmedetomidine on the Level of Brain-Derived Nerve Growth Factor in Plasma of Patients with Meningioma After Operation. *Stroke and Neurological Diseases*, 28(4): 425–430.
- [8] Yang K, Hu G, Wang Y, et al., 2021, Effect of Acupuncture Point Pressing Method on Brain-Derived Nerve Growth Factor in Cerebral Cortex of Rats After Ischemic Stroke. *Jilin Traditional Chinese Medicine*, 41(6): 701–704.
- [9] Huang Y, Chen S, Huang J, 2021, TLR4/NF- κ Role of B Signal Pathway in Sevoflurane Induced Postoperative Cognitive Dysfunction in Elderly Rats. *Chinese Journal of Gerontology*, 41(13): 2782–2785.
- [10] Zhao G, Shi J, Cheng J, et al., 2021, The Ameliorative Effect of Tangerine Peel on Learning and Memory Impairment in Aged Rats with Cognitive Impairment After Anesthesia. *Journal of Northern Sichuan Medical College*, 36(6): 689–695.
- [11] Fang K, Lu G, Wang X, et al., 2021, Effects of Exercise Training on Learning and Memory Impairment and Hippocampal Histopathological Changes in Mice with Mild Cognitive Impairment. *PLA Journal of Medicine*, 33(2): 5–9.

- [12] Wan H, Tao F, Zhao J, et al., 2021, Analysis of Influencing Factors of Postoperative Cognitive Dysfunction in Elderly Patients with Spinal Tuberculosis. *Chinese Journal of Tuberculosis*, 43(5): 441–445.
- [13] Zhang H, Guo X, Bai X, et al., 2021, Effects of Jianpi Zhidong Decoction on Cognitive Function and Brain-Derived Neurotrophic Factor in Rats with Chronic Stress-Induced Tic. *Chinese Journal of Traditional Chinese Medicine*, 36(8): 4676–4680.
- [14] Li Y, Si X, Niu J, et al., 2021, Research Progress of Brain-Derived Neurotrophic Factor and Its Tyrosine Kinase Receptor B Signaling Pathway in Neurological Diseases. *Chinese Journal of Clinical Pharmacology*, 37(9): 1121–1125.
- [15] Li J, Wang Y, Wen Y, et al., 2022, The Effect of Serum Cysc, BDNF and Vilip-1 Levels on Swallowing Dysfunction in Elderly Patients with Mild Cognitive Impairment and the Predictive Efficacy of Clinical Outcomes. *Shandong Medicine*, 62(14): 71–74.
- [16] Xing W, Zhang J, Wu X, et al., 2022, Research Progress on the Role of Brain-Derived Neurotrophic Factor and Neuroinflammation in Neurodegenerative Diseases. *Chinese Medical Science*, 12(10): 21–24.
- [17] Wang W, Zhuo Y, Hou Y, et al., 2022, Effects of Donepezil Hydrochloride Combined with Comprehensive Rehabilitation Training on Cognitive Function, Event-Related Potential and Serum BDNF and IGF-1 in Patients with Senile Dementia. *Progress in Modern Biomedicine*, 22(1): 99–102 + 112.
- [18] Chen X, Wang Z, 2021, Effects of Dexmedetomidine on Postoperative Cognitive Function and Plasma Mir-206 and BDNF Levels in Elderly Patients with Colorectal Cancer. *Journal of Southeast University: Medical Edition*, 40(4): 442–449.

Publisher's note

Bio-Byword Scientific Publishing remains neutral with regard to jurisdictional claims in published maps and institutional affiliations.

Author Guidelines

Before your submission, please check that your manuscript has been prepared in accordance to the step-by-step instructions for submitting a manuscript to our online submission system. We recommend that you keep this page open for your reference as you move through the submission process.

If there are any differences in author guidelines between the print and online version, it is recommended that authors refer to the online version for use.

Manuscript Format

Proceedings of Anticancer Research accepts manuscript that is in MS Word or LaTeX format. All manuscripts must be written in clear, comprehensible English. Both American and British English are acceptable. Usage of non-English words should be kept to a minimum and all must be italicized (except for e.g. and i.e.) If you have concerns about the level of English in your submission, please ensure that it is proofread before submission by a native English speaker or a scientific editing service.

Cover letter

All submissions for *Proceedings of Anticancer Research* should include a cover letter as a separate file. A cover letter should contain a brief explanation of what was previously known, the conceptual advancement with the findings and its significance to broad readership. The cover letter is confidential and will be read only by the editors. It will not be seen by reviewers.

Title

The title should capture the conceptual significance for a broad audience. The title should not be more than 50 words and should be able to give readers an overall view of the paper's significance. Titles should avoid using uncommon jargons, abbreviations and punctuation.

List of Authors

The names of authors must be spelled out rather than set in initials with their affiliations footnoted. Authors should be listed according to the extent of their contribution, with the major contributor listed first. All corresponding authors (maximum 2) should be identified with an asterisk. Affiliations should contain the following core information: department, institution, city, state, postal code, and country. For contact, email address of only one corresponding author is expected within the manuscript. Please note that all authors must see and approve the final version of the manuscript before submitting.

Abstract

Articles must include an abstract containing a maximum of 200 words. The purpose of abstract is to provide sufficient information for a reader to choose either to proceed to the full text of the article. After the abstract, please give 3-8 key words; please avoid using the same words as those already used in the title.

Section Headings

Please number all section headings, subheadings and sub-subheadings. Use boldface to identify major headings (e.g. **1, 2, 3**, etc.) and subheadings (e.g. **1.1, 1.2, 2.1, 2.2** etc.) For the sub-subheadings, please distinguish it further using non-boldface numbers in parenthesis (e.g. (1), (2), (3), etc.)

Introduction

Introduction should provide a background that gives a broad readership an overall outlook of the field and the research performed. It tackles a problem and states its importance regarding the significance of the study. Introduction can conclude with a brief statement of the aim of the work and a comment about whether that aim was achieved.

Materials and Methods

This section provides the general experimental design and methodologies used. The aim is to provide enough detail for other investigators to fully replicate your results. It is also required to facilitate better understanding of the results obtained. Protocols and procedures for new methods must be included in detail to reproduce the experiments.

Ethics

Ethics information, including IACUC permit numbers and/or IRB name, if applicable. This information should be included in a subheading labelled "Ethics Statement" in the "Methods" section of your manuscript file, in as much detail as possible.

Results

This section can be divided into subheadings. This section focuses on the results of the experiments performed.

Discussion

This section should provide the significance of the results and identify the impact of the research in a broader context. It should not be redundant or similar to the content of the results section.

Conclusion

Please use the conclusion section for interpretation only, and not to summarize information already presented in the text or abstract.

Conflict of Interest

All authors are required to declare all activities that have the potential to be deemed as a source of competing interest in relation to their submitted manuscript. Examples of such activities could include personal or work-related relationships, events, etc. Authors who have nothing to declare are encouraged to add "No conflict of interest was reported by all authors" in this section.

Funding

Authors should declare all financial and non-financial support that have the potential to be deemed as a source of competing interest in relation to their submitted manuscript in this section. Financial supports are generally in the form of grants, royalties, consulting fees and more. Examples of non-financial support could include the following: externally-supplied equipments/biological sources, writing assistance, administrative support, contributions from non-authors etc.

Appendix

This section is optional and is for all materials (e.g. advanced technical details) that has been excluded from the main text but remain essential to readers in understanding the manuscripts. This section is

not for supplementary figures. Authors are advised to refer to the section on ‘Supplementary figures’ for such submissions.

Text

The text of the manuscript should be in Microsoft Word or Latex. The length of the manuscript cannot be more than 50000 characters (inclusive of spaces) or approximately 7000 words.

Nomenclature for genes and proteins

This journal aims to reach researchers all over the globe. Hence, for both reviewers’ and readers’ ease in comprehension, authors are highly encouraged to use the appropriate gene and protein nomenclature. Authors may prefer to utilize resources such as <http://www.ncbi.nlm.nih.gov/gene>

Figures

Authors should include all figures into the manuscript and submit it as 1 file in the OJS system. Reference to the “Instructions for Typesetting manuscript” is strongly encouraged. Figures include photographs, scanned images, graphs, charts and schematic diagrams. Figures submitted should avoid unnecessary decorative effects (e.g. 3D graphs) as well as be minimally processed (e.g. changes in brightness and contrast applied uniformly for the entire figure). It should also be set against a white background. Please remember to label all figures (e.g. axis etc.) and add in captions (below the figure) as required. These captions should be numbered (e.g. **Figure 1**, **Figure 2**, etc.) in boldface. All figures must have a brief title (also known as caption) that describes the entire figure without citing specific panels, followed by a legend defined as description of each panel. Please identify each panel with uppercase letters in parenthesis (e.g. A, B, C, etc.)

The preferred file formats for any separately submitted figure(s) are TIFF or JPEG. All figures should be legible in print form and of optimal resolution. Optimal resolutions preferred are 300 dots per inch for RGB coloured, 600 dots per inch for greyscale and 1200 dots per inch for line art. Although there are no file size limitation imposed, authors are highly encouraged to compress their figures to an ideal size without unduly affecting legibility and resolution of figures. This will also speed up the process of uploading in the submission system if necessary.

The Editor-in-Chief and Publisher reserve the right to request from author(s) the high-resolution files and unprocessed data and metadata files should the need arise at any point after manuscript submission for reasons such as production, evaluation or other purposes. The file name should allow for ease in identifying the associated manuscript submitted.

Tables, lists and equations

Tables, lists and equations must be submitted together with the manuscript. Likewise, lists and equations should be properly aligned and its meaning clear to readers. Tables created using Microsoft Word table function are preferred. Place each table in your manuscript file right after the paragraph in which it is first cited. Do not submit your tables in separate files. The tables should include a concise but sufficiently explanatory title at the top. Vertical lines should not be used to separate columns. Leave some extra space between the columns instead. All tables should be based on three horizontal lines to separate the caption, header and body. A few additional horizontal lines MAY be included as needed (example below). Any explanations essential to the understanding of the table should be given in footnotes at the bottom of the table. SI units should be used.

Supplementary information

This section is optional and contains all materials and figures that have been excluded from the entire manuscript. This information are relevant to the manuscript but remains non-essential to readers' understanding of the manuscript's main content. All supplementary information should be submitted as a separate file in Step 4 during submission. Please ensure the names of such files contain 'suppl. info'.

In-text citations

Reference citations in the text should be numbered consecutively in superscript square brackets. Some examples:

1. Negotiation research spans many disciplines ^[3,4].
2. This result was later contradicted by Becker and Seligman ^[5].
3. This effect has been widely studied ^[1-3,7].

Personal communications and unpublished works can only be used in the main text of the submission and are not to be placed in the Reference section. Authors are advised to limit such usage to the minimum. They should also be easily identifiable by stating the authors and year of such unpublished works or personal communications and the word 'Unpublished' in parenthesis.

E.g. (Smith J, 2000, Unpublished)

References

This section is compulsory and should be placed at the end of all manuscripts. Do not use footnotes or endnotes as a substitute for a reference list. The list of references should only include works that are cited in the text and that have been published or accepted for publication. Personal communications and unpublished works should be excluded from this section.

For references in reference list, all authors must be stated. Authors referenced are listed with their surname followed by their initials. All references should be numbered (e.g. 1. 2. 3. etc.) and sequenced according to the order it appears as an in-text citation. References should follow the following pattern: Author(s) followed by year of publication, title of publication, full journal name in italics, volume number, issue number in parenthesis, page range and lastly the DOI (if applicable). If the referred article has more than three authors, list only the first three authors and abbreviate the remaining authors to italicized 'et al.' (meaning: "and others").

Journal

Journal article (print) with one to three authors

[1] Yao Y., Xia B. Application of Phase Frequency Feature Group Delay Algorithm in Database Differential Access. *Computer Simulation*, 2014, 31(12): 238-241.

Journal article (print) with more than three authors

[2] Gamelin F.X., Baquet G., Berthoin S., et al. Effect of high intensity intermittent training on heart rate variability in prepubescent children. *European Journal of Applied Physiology*, 2009, 105: 731–738.

Journal article (online) with one to three authors

[3] Jackson D., Firtko A., Edenborough M. Personal resilience as a strategy for surviving and thriving in the face of workplace adversity: a literature review. *Journal of Advanced Nursing*, 2009, 60(1): 1–9.

Journal article (online) with more than three authors

[4] Hargreave M., Jensen A., Nielsen T.S.S., et al. Maternal use of fertility drugs and risk of cancer in children—A nationwide population-based cohort study in Denmark. *International Journal of Cancer*, 2015, 136(8): 1931–1939.

Book

Book with one to three authors

[5] Schneider Z., Whitehead D., Elliott D. *Nursing and midwifery research: methods and appraisal for evidence-based practice*. 3rd edn. 2009, Elsevier Australia, Marrickville, NSW.

Book with more than three authors

[6] Davis M., Charles L., Curry M.J., et al. *Challenging spatial norms*. 2013, Routledge, London.

Chapter or Article in Book

[7] Knowles M.S. Independent study. In *Using learning contracts*. 1986, Jossey-Bass, San Francisco, 89–96.

Others

Proceedings of meetings and symposiums, conference papers

[8] Chang S.S., Liaw L. and Ruppenhofer J. (eds). *Proceedings of the twenty-fifth annual meeting of the Berkeley Linguistics Society, February 12–15, 1999: general session and parasession on loan word phenomena*. 2000, Berkeley Linguistics Society, Berkeley.

Conference proceedings (from electronic database)

[9] Bukowski R.M. Prognostic factors for survival in metastatic renal cell carcinoma: update 2008. *Innovations and challenges in renal cancer: proceedings of the third Cambridge conference*. *Cancer*, 2009, 115 (10): 2273, viewed 19 May 2009, Academic OneFile database.

Online Document with author names

[10] Este J., Warren C., Connor L., et al. *Life in the clickstream: the future of journalism*, Media Entertainment and Arts Alliance, 2008. viewed 27 May 2009, http://www.alliance.org.au/documents/foj_report_final.pdf

Online Document without author name

[11] *Developing an argument* n.d., viewed March 30 2009, http://web.princeton.edu/sites/writing/Writing_Center/WCWritingResources.htm

Thesis/Dissertation

[12] Gale L. *The relationship between leadership and employee empowerment for successful total quality management*. 2000, University of Western Sydney.

Standard

[13] Standards Australia Online. Glass in buildings: selection and installation. AS 1288–2006. 2006, SAI Global database.

Government Report

[14] National Commission of Audit. Report to the Commonwealth Government, Australian Government Publishing Service, 1996, Canberra.

Government report (online)

[15] Department of Health and Ageing. Ageing and aged care in Australia, 2008, viewed 10 November 2008, <http://www.health.gov.au/internet/main/publishing.nsf/Content/ageing>

No author

[16] Guide to agricultural meteorological practices. 2nd edn, Secretariat of the World Meteorological Organization, 2010, Geneva.

Note: When referencing an entry from a dictionary or an encyclopedia with no author there is no requirement to include the source in the reference list. In these cases, only cite the title and year of the source in-text. For an authored dictionary/encyclopedia, treat the source as an authored book.

Submission Preparation Checklist

As part of the submission process, authors are required to check off their submission's compliance with all of the following items, and submissions may be returned to authors that do not adhere to these guidelines.

1. The submission has not been previously published, nor is it before another journal for consideration (or an explanation has been provided in Comments to the Editor).
2. The submission file is in OpenOffice, Microsoft Word, RTF, or WordPerfect document file format.
3. Where available, URLs for the references have been provided.
4. The text is single-spaced; uses a 12-point font; employs italics, rather than underlining (except with URL addresses); and all illustrations, figures, and tables are placed within the text at the appropriate points, rather than at the end.
5. The text adheres to the stylistic and bibliographic requirements outlined in the Author Guidelines, which is found in About the Journal.
6. If submitting to a peer-reviewed section of the journal, the instructions in Ensuring a Blind Review have been followed.



Integrated Services Platform of International Scientific Cooperation

Innoscience Research (Malaysia), which is global market oriented, was founded in 2016. Innoscience Research focuses on services based on scientific research. By cooperating with universities and scientific institutes all over the world, it performs medical researches to benefit human beings and promotes the interdisciplinary and international exchanges among researchers.

Innoscience Research covers biology, chemistry, physics and many other disciplines. It mainly focuses on the improvement of human health. It aims to promote the cooperation, exploration and exchange among researchers from different countries. By establishing platforms, Innoscience integrates the demands from different fields to realize the combination of clinical research and basic research and to accelerate and deepen the international scientific cooperation.

Cooperation Mode



Clinical Workers



In-service Doctors



Foreign Researchers



Hospital



University



Scientific institutions

OUR JOURNALS



The *Journal of Architectural Research and Development* is an international peer-reviewed and open access journal which is devoted to establish a bridge between theory and practice in the fields of architectural and design research, urban planning and built environment research.

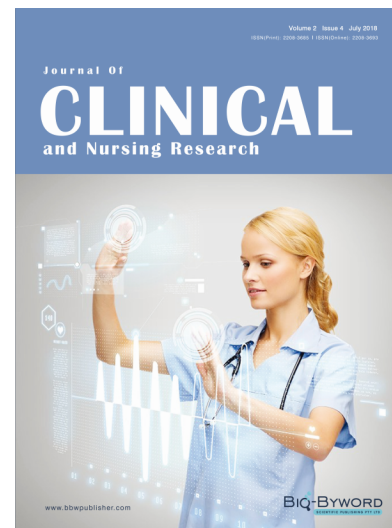
Topics covered but not limited to:

- Architectural design
- Architectural technology, including new technologies and energy saving technologies
- Architectural practice
- Urban planning
- Impacts of architecture on environment

Journal of Clinical and Nursing Research (JCNR) is an international, peer reviewed and open access journal that seeks to promote the development and exchange of knowledge which is directly relevant to all clinical and nursing research and practice. Articles which explore the meaning, prevention, treatment, outcome and impact of a high standard clinical and nursing practice and discipline are encouraged to be submitted as original article, review, case report, short communication and letters.

Topics covered by not limited to:

- Development of clinical and nursing research, evaluation, evidence-based practice and scientific enquiry
- Patients and family experiences of health care
- Clinical and nursing research to enhance patient safety and reduce harm to patients
- Ethics
- Clinical and Nursing history
- Medicine



Journal of Electronic Research and Application is an international, peer-reviewed and open access journal which publishes original articles, reviews, short communications, case studies and letters in the field of electronic research and application.

Topics covered but not limited to:

- Automation
- Circuit Analysis and Application
- Electric and Electronic Measurement Systems
- Electrical Engineering
- Electronic Materials
- Electronics and Communications Engineering
- Power Systems and Power Electronics
- Signal Processing
- Telecommunications Engineering
- Wireless and Mobile Communication

